Development and Application of a Linear Polyamidoamine-SiRNA Delivery System

Zainab Haitham Fathi

Thesis submitted for the Degree of Doctor in Philosophy to
The University of Nottingham, Nottingham, UK

September 2017

Abstract

Spleen tyrosine kinase (Syk) plays a critical role in regulation of immune and inflammatory responses. The important role of Syk in inflammatory signalling cascades has led to the development of therapeutic agents designed to knock down Syk gene as novel therapeutic agents for allergic diseases (1). This thesis investigated the role of siRNA in Syk silencing using the newly developed RBL reporter systems as an *in vitro* model to study degranulation.

Lack of an efficient and safe non-viral delivery systems has hindered the progress of siRNA into clinics. The ideal properties of the siRNA-nanoparticles for efficient delivery would require the following properties, 1. Safe with low toxic effects to the cells (non-toxic polymers and nanoparticle components); 2. Compact and well-condensed nanoparticles (thiol crosslinking and PEG); 3. Small size (20–200 nm) for easy cellular internalization (thiol crosslinking and PEG); 4. Less interaction with the environment to enable access to the target cells (PEG); 5. Neutral surface charged and sterically stable siRNA polyplexes with bio-reducible characteristics essentially required for *in vivo* delivery (Thiol-modified siRNA and PEG). Hence, low-toxicity linear cationic polyamidoamine (PAA) consisting of a mixture of PEGylated copolymer (CP) and non-PEGylated homopolymer (HP) were used for the formulation of the PAA-siRNA nanoparticles. This system has previously been shown to assemble into small sterically stabilised particles with reducible crosslinks.

A cross-linked system of HP and HP-CP blends showed complete incorporation of thiolated siRNA during gel electrophoresis, and produced particle size less than that of non-thiolated siRNA as determined using a dynamic light scattering technique. A degranulation inhibition assay revealed that these cross-linked polyplexes prepared using thiol-modified siRNA efficiently inhibited release of fluorescent granules (NPY-

mRFP) from the genetically modified RBL-2H3 NPY-mRFP cell line. There was no cytotoxicity associated with this delivery system. By using HP/SH-siRNA nanoparticle, a remarkable dose-dependent Syk gene silencing (~80%) was observed on mRNA level using RT-qPCR. Finally, the HP/SH-siRNA polyplexes produced also showed a significant reduction in Syk protein levels using Western blotting.

From the data obtained it is concluded that cross-linked siRNA polyplexes prepared with thiolated siRNA are safe, effective and easy to prepare for future siRNA *in vivo* gene silencing applications to treat allergic diseases.

Acknowledgments

It is difficult for me to express enough in words my heartfelt gratitude towards both of my supervisors, Dr. Martin Garnett and Dr. Franco Falcone, whose office doors were always open to me, and who went far beyond what was required of them to help me. I always admire your patience and scientific rigor. I thank them for believing in me and my abilities even when nothing was working and extending your support in every possible way. It was a great pleasure to be able to work on this project and share your great knowledge in the field of nucleic acid delivery.

I thank Dr. Snow Stolnik, my thesis committee member, for the stimulating discussions, deep insights and different perspectives she had provided for the project.

I thank Shubaash, Fahad, Abdulaziz, Daniel, Waleed, Mohammed, Eman, Aymen, Vincenzo and Nafal for all the wonderful, pleasant and memorable moments that we shared in the lab (D35) and for all your help during my stay at Nottingham.

Finally, I would like to thank my family for their support. I would like to dedicate this thesis to my wonderful mother Manal, my kind sisters Farah and Fatima, and my lovely kids Noor, Mohammed and Mustafa for your encouragement, motivation to pursue research and providing emotional support during all these years and making my PhD a pleasant experience of my life. Words fail to express my appreciation for my husband, Ammar. He was always there cheering me up and stood by me throughout the good times and the bad times.

Table of Contents

List of Figures

List of Tables

List of Abbreviations

A	Adenine
AHR	Airway hyper-responsiveness
ALN	Alnylam
ApoB	apolipoprotein B
ASO	Antisense oligo nucleotides
BCA	Bicinchoninic Acid
Bp	Base pairs
BSA	Bovine serum albumin
C	Cytosine
cDNA	Complementary deoxyribonucleic acid
CDS	Coding sequence
CP	Copolymer [PEG-PAA-PEG]
CP2k	PEG1.7kDa–PAA–PEG1.7kDa
CPP	Cell penetrating peptide
CT	Cycle threshold
Da	Dalton
dATP	Deoxyadenosine triphosphate
dCTP	Deoxycytidine triphosphate
dGTP	Deoxyguanosine triphosphate
DLS	Dynamic light scattering
DMEDA	Dimethyl-ethylene-diamine
DNA	Deoxyribonucleic acid
DNP	Dinitrophenyl
DPBS	Dulbecco’s phosphate buffered saline

DPCs	Dynamic polyconjugates
DTT	1,4-Dithiothreitol
dTTP	Deoxythymidine triphosphate
ECM	Extracellular matrix
EDTA	Ethylenediaminetetraacetic acid
EGF	Epidermal growth factor
ELISA	Enzyme-linked immunosorbent assay
FcεRI	Fc epsilon (IgE) receptor I
G	Generation
G	Guanine
GalNAc	N-acetylgalactosamine
GAPDH	Glyceraldehyde 3-phosphate dehydrogenase
Ggt1	Gamma-glutamyltransferase 1
GSH	Glutathione
HBV	Hepatitis B virus
HCV	Hepatitis C virus
HIV-1	Human immunodeficiency virus type 1
HIV-1 gp41	Human immunodeficiency virus, glycoprotein 41
HP	Homopolymer
HPLC	High-performance liquid chromatography
HPV-16	Human papilloma virus type 16
IC50	Half maximal inhibitory concentration
IgE	Immunoglobulin E (erythema)
IL	Interleukin
INF-7	Interferon

ITAM	Immunoreceptor tyrosine-based activation motif
kDa	Kilodalton
MBA	Methylene bisacrylamide
MEM	Minimum essential medium
miRNA	micro-Ribonucleic acids
Mono (Boc)	N-(tert-butoxycarbonyl)
mRFP	Monomeric red fluorescent protein
Mrna	Messenger ribonucleic acid
NG47	PEGylated PAA copolymer
NG49	Cationic PAA homopolymer
NK	Natural killer
NPY	Neuropeptide Y
ONPs	Oligonucleotide nanoparticles
OVA	Ovalbumin
PAA	Linear polyamidoamine polymers
PAGE	Polyacrylamide gel electrophoresis
PAMAM	Polyamidoamine dendrimer
PBS	Phosphate buffered saline
pDNA	Plasmid deoxyribonucleic acid
PEC	Polyelectrolyte complexes
PEG	Poly(ethylene glycol)
PEI	Polyethylenimine
pH	Potential of hydrogen
PLGA	Polylactide-co-glycolic acid
PLL	Poly-L-lysine

PPARα	peroxisome proliferator-activated receptor alpha
RBCs	Red blood cells
RBL	Rat basophilic leukaemia
RES	Reticuloendothelial System
RIPA	Radioimmunoprecipitation assay
RISC	RNA Induced Silencing Complex
RNA	Ribonucleic acid
RNAi	RNA interference
RT	Reverse transcription
RT-qPCR	Real Time-Quantitative Polymerase Chain Reaction
RU	Repeating units (of the polymer)
RU/Nt	Polymer repeating unit to RNA nucleotide ratios
SCR	Scrambled
SD	Standard deviation
SDS	Sodium dodecyl sulphate
SH	Thiol
SH2	SRC homology 2
shRNA	Short hairpin ribonucleic acid
SiRNA	Small interfering ribonucleic acid
SLP 76	Src homology 2 domain containing leukocyte protein of 76 kDa
SV40	Simian virus 40
SYK	Spleen tyrosine kinase
T	Thymine
TAE	Tris-Acetic Acid-EDTA buffer
TEM	Transmission electron microscopy

TK	Thymidine kinase
TNF-α	Tumour necrosis factor-alpha
U	Uracil
UTR	Un-translated Region
VEGF	Vascular endothelial growth factor

Chapter 1

1 General Introduction

1.1 Nucleic acid therapy

Basically gene therapy is an intracellular delivery of genomic materials (transgene) into specific cells to generate to generate therapeutic effect by correcting the existing abnormality or providing the cells with new functions. The idea of utilizing genetic materials for therapy is not new, and was proposed by Tatum in 1966 (2). The science behind gene therapy was first shown possible in 1977 when the thymidine kinase (TK) gene was transferred into TK- L mammalian cells in 1977 (3). The genetic deficiency of these cells was corrected by the transfer of a single copy of a functional copy of the TK gene in 1980 (4). *In vivo* expression in a mouse was soon obtained using the retroviral vector N2 expressing a Neomycin Resistance (NeoR) marker gene in 1985 (5), which was then used to treat tumour infiltrating lymphocytes in the first human clinical trial in skin cancer patients in 1990 (6).

Gene therapy aims to act on the genetic cause of a pathology by gene inhibition or gene substitution. Gene substitution relies on the introduction, into the cell, of transcriptionally fully competent genes, to augment the production of a specific protein in order to restore its functional expression. Gene silencing inhibiting the gene expression which is responsible for a disease, normally at the messenger RNA (mRNA) level, stopping the expression of proteins at the post-transcriptional level (7, 8). Nucleic acid therapy can be based on DNA [including plasmids, oligonucleotides (antisense and antigene applications), DNA aptamers and DNAzymes] or RNA [including antisense RNA, ribozymes, RNA decoys, RNA aptamers, small interfering

RNA (siRNA) and microRNA] (9).

A variety of approaches have been developed to enable gene therapy to treat complex acquired diseases like cardiovascular diseases and cancers, including the replacement or correction of missing or functionally impaired genes, the addition of a new function to a cell and the inhibition of proteins with undesirable effects. However, to achieve the therapeutic potential of gene therapy as a novel treatment, many barriers must be overcome. The safety and efficiency of gene transfer will determine how successful the gene therapy application will be. This can be considered a major rate limiting step. In all cases, a vector must be used to carry the therapeutic or corrective genetic sequence in order to efficiently deliver it to the patient's target cells or tissue. Difficulties in achieving sustained gene expression has resulted in limited clinical benefits from gene therapy to date.

1.1.1 Discovery and mechanism of RNA interference

The term RNA interference (RNAi) was first used after the discovery that double-stranded RNAs (dsRNAs) can trigger silencing of messenger RNA (mRNA) sequences in the nematode *Caenorhabditis elegans* (10). The mechanism by which RNAi inhibits the conversion of mRNA into protein is briefly reviewed here. Small interfering RNA (siRNA) and micro RNA (miRNA) are central to RNA interference. Double-stranded RNA is recognized by an RNase type III enzyme, Dicer, and cleaved into small fragments of 21- 23 nucleotides called siRNAs. Each siRNA is unwound into a sense (passenger) strand and an antisense (guide) strand with respect to the target mRNA (**Figure 1.1**). siRNA binds to a protein complex called RNA-induced silencing complex (RISC) and the passenger strand is degraded, while the guide strand is directed mainly to the 3' untranslated region (UTR) of the complementary target mRNA (11). A cleavage enzyme within RISC (argonaute 2) degrades the target

mRNA, thus preventing translation. miRNAs also exist in cells and are pre-processed by a nuclear RNase III (Drosha) before export into the cytoplasm by nuclear transport receptor complexes. Due to limited complementarily to the target mRNA, miRNAs do not lead to the cleavage of mRNA with the RISC but, instead, result in translational suppression (12).

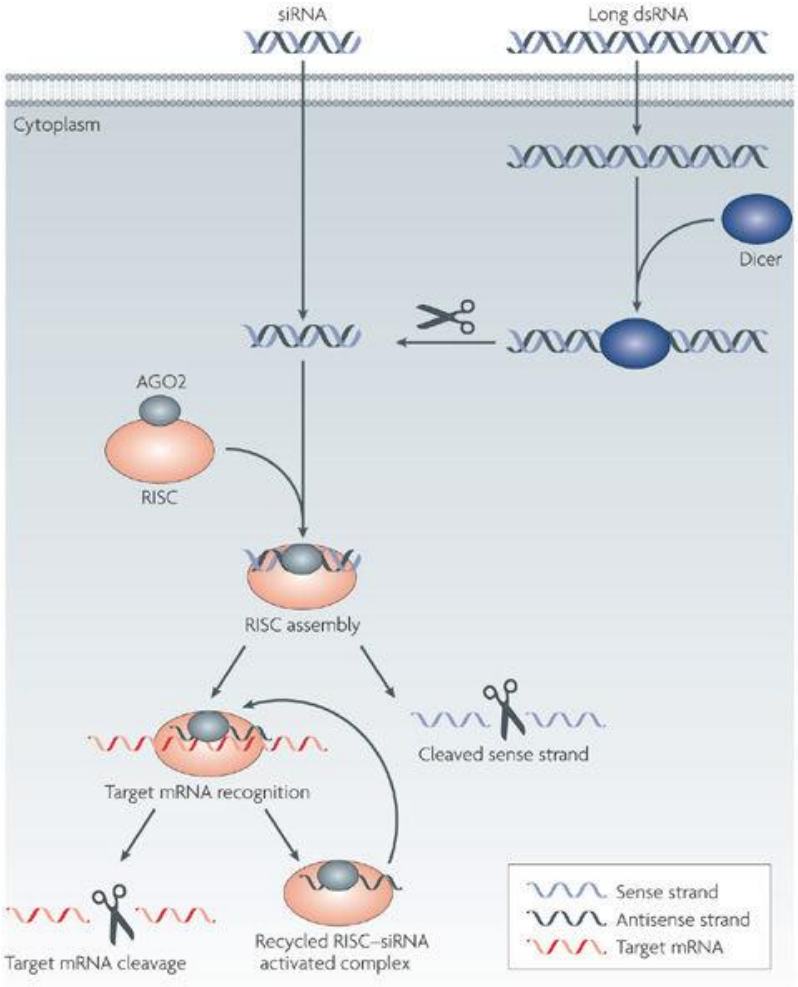

Figure 1.1 Mechanism of RNA interference (RNAi). After entering the cytoplasm, siRNA duplexes are incorporated into the RNA induced silencing complex (RISC), resulting in enzymatic cleavage of the sense strand of siRNA. The activated RISC complex cleaves target mRNAs with complementary domains due to its endonuclease activity resulting in gene silencing (13).

Then, the interest in using RNAi mechanism as one of the most promising new approaches for disease therapy has increased. The list of diseases that may be treated by RNAi is extensive, including cancers, Parkinson's disease (14), HIV infection (15), age-related macular degeneration (16), type 2 diabetes (17), obesity (18), hypercholesterolemia (19), and rheumatoid arthritis (20).

1.1.2 Off-target effects of siRNA

Off-target effects, defined as siRNAs effects on non-target genes causing change in their expression (21), can be an obstacle for usage of siRNA. Off-target effects depend on the concentration of siRNAs and similarities between the non-target genes and the 5' ends of siRNAs (22, 23). A second major limitation is an antiviral interferon response and apoptosis, however there are conflicting studies on dsRNAs that are less than 30 bases in length and able to silence gene expression in a specific manner without triggering the interferon response (24). RNAi may act on dendritic cells *in vivo* by activation of Toll-like receptors, leading to an unwanted immune response (25). Application of siRNA molecules as therapeutics is still challenging. Perhaps the most significant limitation is the safe, efficient and effective delivery of RNAi reagents.

1.1.3 SiRNA therapy in disease treatment

Since most cells in the body possess the intrinsic machinery required to process endogenous RNAi molecules and exogenous molecules designed to mimic endogenous RNAi (26), there exist a number of diseases resulting from abnormal gene expression that could be suitable candidates for siRNA therapy. In general, RNAi research has focused on areas where standard treatment options have been relatively ineffective or where improvement is desired and required.

Viral infection is a particularly useful area for gene silencing. Human immunodeficiency virus (HIV) is one of the most important examples. RNAi

machinery has been successful in silencing of viral (tat, rev, nef, and gag) and cellular (CD4, CCR5 and CXCR4) genes which are essential in viral infection, resulting in reduction the infection rate of HIV (27). Hepatitis C virus (HCV), is main cause of liver cirrhosis and cancer. RNAi machinery has great potential to inhibit viral replication in HCV infected individuals (28). Human papilloma virus type 16 (HPV-16) is a major causative factor of cervical cancer. Knocking down of E6 and E7 genes by RNAi molecules has resulted in inhibition of proliferation and senescence in HPV-positive cervical cancer cells (29). Hepatitis B virus (HBV) is an important cause of liver cancer. RNAi machinery may provide a promising therapy for this viral disorder because of its ability to inhibit HB virus replication *in vivo* (30). SiRNA molecules can also be used in influenza virus treatment, acting by inhibition of viral, but not cellular, mRNA accumulation (31).

Another possible group of applications relate to cancer therapy. Carcinogenesis can be generated either by overexpression of oncogenes (such as overexpression of P-glycoprotein) or by chromosomal translocation which is abnormal fusion of two separate chromosomal regions e.g. fusion of *M-BCR/ABL* resulting in leukemia. The RNAi approaches have been used successfully to inhibit oncogene expression (32, 33). Epidermoid carcinoma can also be treated with siRNA molecules by suppressing endogenous erbB1 expression (34). Furthermore, silencing of *c-raf and bcl-2* genes by siRNA molecules is an attractive method for treatment of leukemia (35). Vascular endothelial growth factor (VEGF) is believed to play a role in vascular angiogenesis and suppression of this angiogenic factor represents a new approach for cancer therapy (36).

While the main focus for genetic disorders is gene therapy, dominantly inherited genetic disorders occur as a result of single allele mutation. Therefore, silencing of the affected gene can promote cell regeneration by the normal allele.

Huntington's disease (HD) and spinobulbar muscular atrophy (Kennedy's disease) are neurological disorders caused by a trinucleotide (CAG) repeat expansion which is the codon for glutamine (Q), resulting in a polyglutamine tract. When these mutant proteins accumulate, it results in a toxic gain-of-function. Therefore, RNAi molecules directed against CAG repeats can provide a suitable method for treatment of these diseases (37, 38).

Inhibition by siRNA molecules can also be used in *Fas*-induced fulminant hepatitis, resulting in suppression of *Fas* expression in hepatocytes and subsequently prevention of liver fibrosis in mice (39).

SiRNA strategies have also become powerful research tools to explore the possibilities for gene silencing on progression in a wide variety of diseases. In one study, Karlas and colleagues utilized a genome-wide siRNA library composed of ~60,000 siRNAs targeting over 20,000 gene products to determine which host cell genes are critical for Influenza A virus replication (40). Their conclusion was that siRNA therapy has enormous potential to generate increased understanding and to be applied to treatment of many diseases. The actual implementation of siRNA strategies is easier said than done, however, since factors such as siRNA delivery remain the main obstacle.

Despite this promising research, a number of problems remain in the application of siRNA therapeutics. Most of these treatments are limited to local delivery of siRNAs, such as direct injection into the eye or skin. Targeting specific genes to different tissues and organs is accomplished with systemic delivery during treatment.

1.1.4 Challenges associated with siRNA delivery

Naked siRNA molecules (no delivery agent or molecule modification) do not enter cells efficiently for a number of reasons, especially when systemically administered, including: (1) limited cellular uptake across the plasma membrane due to repulsion of negative charges; (2) non-specific distribution and uptake into non-target tissues; (3) serum nuclease-mediated degradation; (4) reticuloendothelial system (RES) capture and renal elimination; and (5) inefficient capillary escape into tissues (extravasation) (41, 42). These drawbacks are intrinsically related to some of the unfavourable physicochemical properties of siRNA molecules, including large molecular weight, negatively charged surface, hydrophilicity, sensitivity to nuclease degradation and short plasma half-life of less than ten minutes (43). Consequently, to be implemented *in vivo*, siRNA molecules are usually administered in conjunction with some type of delivery agent. However, any systemically-delivered nanoparticle siRNA delivery agent must still overcome many hurdles: first it must evade filtration/renal excretion, phagocytosis by circulating and tissue-resident white blood cells, and degradation by plasma nucleases in the bloodstream. It must be capable of movement across the vascular endothelial layer; diffusion through the extracellular matrix (ECM). It must be able to be taken up by target cells; escape the endosome; and, finally have a productive association with RNAi-processing complexes in the cytosol (**Figure 1.2**) (13, 44). To solve the problems of protection from nucleases and uptake into cells the RNA needs to be encapsulated into a nanoparticle. Following systemic administration, siRNA loaded nanoparticles are preferentially taken up by the reticuloendothelial system (RES) composed primarily of macrophages and Kupffer cells present in RES organs such as the spleen and liver (45). This process is further enhanced by serum

proteins adsorbing to the surface of nanoparticles, thus promoting opsonisation (complement activation) and rapid clearance (46).

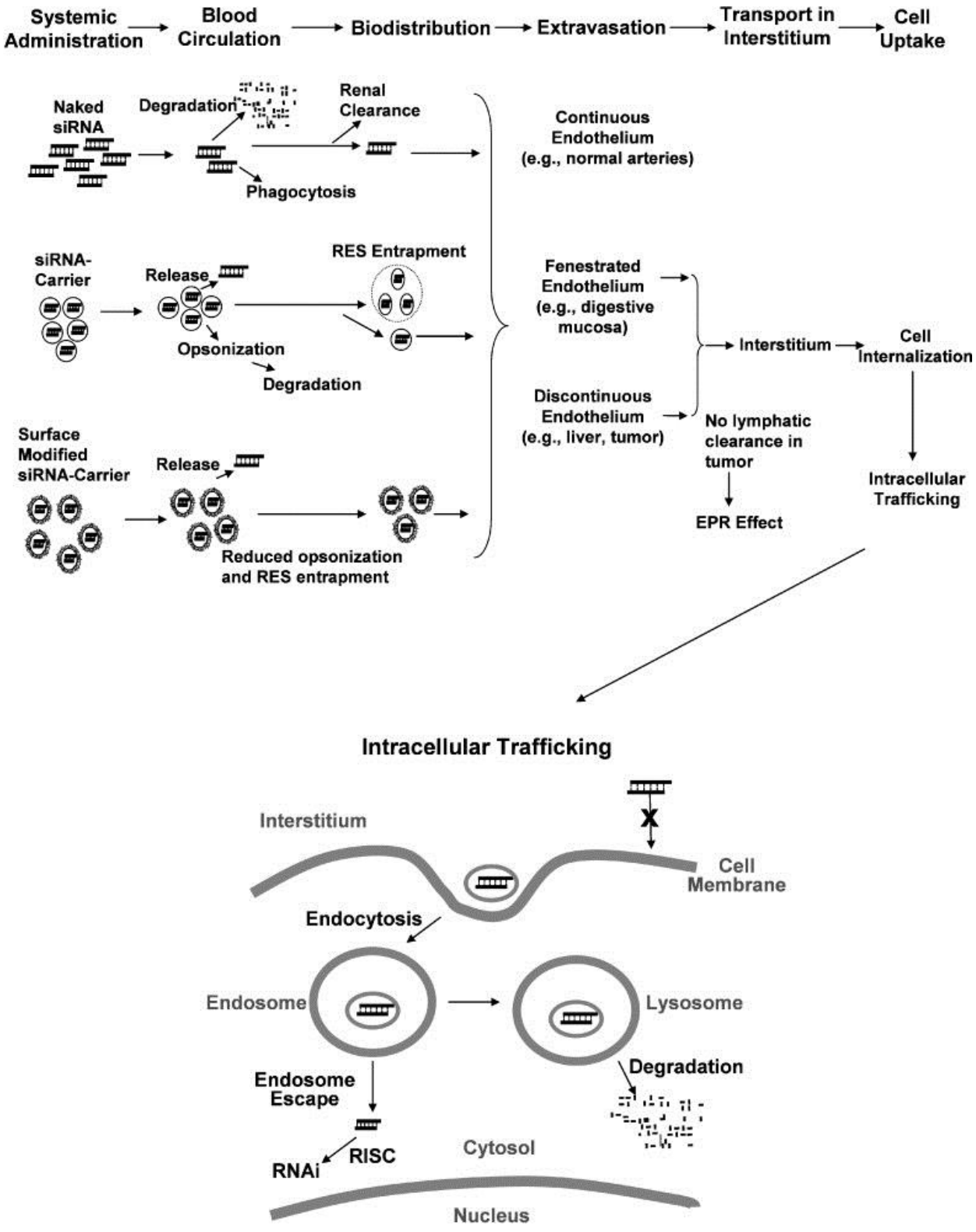

Figure 1.2 Barriers associated with various siRNA delivery methods. The three major areas depicted include circulation in the bloodstream, cellular uptake and intracellular trafficking (44).

After discussing the main barriers involved with the systemic delivery of siRNA delivery agents it is not surprising that an ideal delivery system should possess most or all of the following attributes: (1) safety: biocompatible, biodegradable and nonimmunogenic; (2) capacity to enhance tissue-specific distribution following intravenous injection; (3) deliver an effective amount of siRNA into target cells while protecting them from serum nuclease degradation and RES clearance; and (4) promote endosomal release, thus permitting the association of siRNA with RNAi machinery, which resides in the cytosol (42, 44). It is important to keep these general characteristics in mind when considering the advantages and limitations to the common siRNA delivery strategies described below.

In the search for effective siRNA delivery systems, a number of materials have been used, including virus vectors, liposomes, lipoplexes, cationic polymers, and peptides (44, 47). Among them, cationic polymers have been utilized for intracellular delivery of a variety of macromolecules, including proteins, peptide nucleic acids (PNA), and siRNAs (48, 49).

1.2 Delivery systems

1.2.1 Conjugate Delivery Systems

Conjugate delivery systems are developed by directly conjugating delivery materials to the siRNA cargo. To date, the delivery materials that have been used for conjugate delivery systems include cholesterol and other lipophilic molecules, polymers, peptides, antibodies, aptamers and small molecules. Two of the most-developed conjugate delivery systems are Dynamic PolyConjugates (DPCs) and GalNAc conjugates.

DPCs consist of several components: siRNA cargo, a membrane-disrupting polymer, PEG ligand and targeting ligand (50). The DPCs system silenced *apolipoprotein B*

(ApoB) and *peroxisome proliferator-activated receptor alpha (PPARα)* effectively in the liver with intravenous administration. In order to target other tissues besides liver, many types of targeting ligands have been studied, such as peptides, small molecules, lectins, antibodies, glycans, and nucleic acids (50). It is reported that two different conjugate delivery systems were co-injected to target the same gene in the liver (51).

GalNAc conjugates only include a chemically stabilized siRNA and a trivalent targeting ligand. In Alnylam Pharmaceuticals, three conjugates ALN-TTRsc (transthyretin), ALN-AT3 (antithrombin), ALN-PCS (Proprotein convertase subtilisin) are being examined for the treatment of transthyretin amyloidosis, haemophilia and hypercholesterolemia, respectively (52-54). This structure provides high affinity binding to its target ASGPR on hepatocytes. Study has shown that subcutaneous administration of this conjugate achieved better biodistribution of siRNA in the liver and higher gene silencing efficiency compared to intravenous administration. By changing the siRNA sequence, this conjugate can target different genes.

Another newly developed conjugate system, oligonucleotide nanoparticles (ONPs), is based on nucleic acids. ONPs include self-assembled complementary DNA fragments with chemically modified siRNAs. The size of these nanoparticles is about 29 nm in diameter. These ONPs were further modified through conjugation with a targeting ligand, such as folate. Folate-ONPs were evaluated *in vivo* and showed longer circulation time (55).

1.2.2 Lipid-based carriers

Liposomes, solid lipid nanoparticles, and micelles are all lipid-based siRNA delivery systems. Liposomes are globular vesicles, which comprise the phospholipid bilayer and an aqueous core. The amphipathic nature of liposomes allows the incorporation of

both hydrophilic and hydrophobic drugs. Liposomes are divided into three categories: neutral liposomes, anionic and cationic liposomes. Though neutral liposomes have achieved some success in delivering siRNA both *in vitro* and *in vivo,* cationic lipids remain the crucial components of lipid-based siRNA carriers (44).

Cationic lipids consist of three parts, a lipophilic tail group, a cationic head and a connecting linker. The structure of the cationic head group, the carbon chain length of the tail group and the nature of the linker affects the transfection efficiency and the toxicity of siRNA carriers. It is known that lipids with small hydrophilic groups and bulky alkyl chains favour endosomal escape and enhance the transfection efficiency (56). A variety of cationic lipids have been investigated, and Lipofectamine 2000 is a commercialized formulation used for *in vitro* transfection. However the toxicogenomics of cationic lipids including the initiation of immune response and changes in the expression of non-target genes limit the use of lipid *in vivo*. Meanwhile, several studies have shown that ionisable lipids, whose charge depends on the pH of the surrounding environment is more efficacious (57) and less toxic than cationic lipids that have a net positive charge. Consequently, the focus of recent study is on the development of new ionisable lipids (58).

Although liposomes have been used for some 50 years, the number of lipids that have been used for creating them has been limited. Recently, thousands of new lipids (59-61) have been generated and screened for siRNA delivery. This enables the creation of promising liposomes that require lower amount of siRNA to achieve specific gene knockdown.

1.2.3 Polymer encapsulation systems

Polylactide-co-glycolic acid (PLGA) is the most extensively studied copolymer as a carrier for controlled release of siRNA, with lower toxicity than cationic lipids and cationic polymers. PLGA nano-capsules are used to stabilize siRNA and provide sustained release (62). Recently, efforts have focused on modification of PLGA to get positively charged carriers to increase cellular uptake. For instance, chitosan coated PLGA nanoparticles improved the cellular internalization of siRNA in cultured cells (63, 64). Incorporation of PEI into PLGA nanoparticles improved siRNA loading and activity. PEI-PLGA nanoparticles showed 100% siRNA loading, protected siRNA and resulted in higher gene silencing activity in cultured cells than PEI alone (64, 65). Intratumoral injection of PEI-PLGA microspheres of anti-VEGF siRNA also showed improved effects on tumor growth suppression (66).

Cyclodextrin polymer-based delivery system was first used for plasmid DNA in 1999 (67) and re-optimized for siRNA delivery years later (54, 68-70). Less than a decade after their introduction, cyclodextrin polymer-based nanoparticles entered clinical trials for siRNA delivery and they were the first targeting delivery systems that entered clinical trials for cancer (71).

1.2.4 Cationic polymers

Cationic polymers have been used for delivery of plasmid DNA since 1990 and, more recently, for siRNA delivery. The positively charged polymers interact with the negatively charged phosphates of siRNA through electrostatic forces resulting in polymer-RNA complexes termed polyplexes. This process causes siRNA condensation and protects it from nuclease degradation. A number of polymers, either synthetic or natural, such as branched or linear polyethyleneimine (PEI), poly-L-lysine (PLL) and chitosan have been studied (72-74).

1.2.4.1 Cell penetrating peptide-based carriers

Cell penetrating peptide (CPP) mediated siRNA delivery systems can enter cells either through endocytic pathways or by directly crossing the cell membrane. CPP can be conjugated to siRNA through covalent cross-links, such as disulphide bonds. Disulphide bonds are cleaved in cells to release siRNA into the cytoplasm. For example, covalent conjugation of CPP penetratin or transportan to thiol-containing siRNA via a disulphide bond shows equivalent or better gene knockdown effects compared to cationic liposome siRNA carriers in several mammalian cell types (75).

CPP and siRNA can also form non-covalent complexes through electrostatic interactions. At the right molar and charge ratios, packaging of siRNA and CPP form the positively charged complexes aiding in cell membrane translocation. The advantages of this methodology include low cost of reagents, and easy preparation of CPP/siRNA complexes. MPG is a peptide derived from the hydrophobic fusion peptide domain of HIV-1 gp41 protein (Human immunodeficiency virus, glycoprotein 41) and hydrophilic nuclear localisation sequence from SV40 (Simian virus 40) T-antigen (76). SiRNA can form a non-covalent complex with MPG. The complexes enter cells through endosome-independent pathways followed by entry into the nucleus. The nuclear translocation requires an intact SV40 nuclear localisation sequence; alterations to this sequence prevented nuclear delivery and caused the rapid release of siRNA into the cytoplasm (77).

1.2.4.2 Polyamidoamine dendrimers (PAMAM)

Dendrimers are repetitively branched molecules (78). Dendrimers have been used as carriers of small molecule drugs and large biomolecules. Dendrimers with positively charged surface groups are used to deliver siRNA, and the precise core-shell nanostructures make it load siRNA by interior encapsulation, surface adsorption, or

chemical conjugation. The biocompatibility of dendrimers depends on their structure, molecular size and surface charge (79). Cytotoxicity and immunogenicity of dendrimers are related to their surface charge. Modifications are the main methods to improve their loading capacity and cellular uptake of siRNA.

Polyamidoamine dendrimers (PAMAM) are spherical, highly branched polymers, with a surface of primary amine groups that gives these polymers a high cationic charge density. The high density of their outer amine groups enable efficient condensation of nucleic acid, leaving the internal tertiary amines available for neutralisation during acidification within endo-lysosome, thus enabling more efficient endosomal escape (80, 81). PAMAM dendrimers are synthesised by the successive addition of methacrylate or ethylenediamine to ammonia or ethylenediamine core molecules (82, 83). Each round of additions is termed a generation (G), and leads to the molecular weight of the dendrimer being increased and the number of the primary amine surface groups being doubled. The number of generations, therefore, controls the diameter, molecular weight and surface charge of the dendrimers (82). Dendrimers are an attractive architecture for the development of gene delivery systems due to their well-defined polymer structure and their surface charge properties.

Different cell lines were efficiently transfected using starburst dendrimers such as liver hepatoblastoma (HepG2), rat embryonal fibroblast (RAT2), mouse embryonal (NIH), and monkey kidney fibroblast (COS-7) cells. The capability of dendrimers to transfect the cells were dependent on the size, shape and amount of dendrimer in the complex (84, 85). Complexation of DNA with high generation PAMAM dendrimers (G>5) forms monodisperse condensed particles (86). In addition, it offers higher transfection, due to increased flexibility of the dendrimers (87). Furthermore, generation 5 PAMAM modified with 3400 molecular weight PEG produced a 20-fold increase in transfection

efficiency compared with partially degraded dendrimer controls (88). Dendrimers appear to be non-cytotoxic in the concentrations relevant for gene transfer (89, 90). In a previous study by Malik, PAMAM dendrimers (G2, G3, G4, G8 and G10) were shown to cause haemolysis of rat red blood cells at concentrations of 1 mg.ml-1 (91, 92).

Haensler and Szoka first reported on the gene delivery applications of PAMAM dendrimers generations ranging from G2 to G10 *in vitro*, at a range of polymer to DNA ratios (93). It was found that the highest transfection efficacy was noticed for the 6th generation of dendrimer at polymer: DNA ratio of 6:1 and gave a superior level of gene expression compared to PLL and Lipofectin™.

1.2.4.3 Linear polyamidoamines (PAAs)

Polyamidoamines (PAAs) are regular linear cationic polymers, which are obtained by stepwise polyaddition of primary monoamines or bis(secondary amines) to bis-acrylamides (89, 94, 95). PAAs contain tertiary amines and amido groups regularly arranged along the macromolecular chain and therefore, the tertiary amino groups in the main chain can be protonated, giving the polymer an overall basic and poly-cationic character with amidic bonds, which are degradable in aqueous solution (89, 96).

PAAs are promising drug and gene carriers due to their combination of water solubility, biodegradability (89) and ability to change conformation with changing pH (97). The high buffering capacity is one of PAAs crucial properties because their net average charge alters considerably as pH changes from 7.4 to 5.5, which is accompanied by a change in the conformation from a coiled to an extended structure (98). Like PAMAM dendrimers, PAAs can provide buffering capacity in endosome and promote fusion and disruption of the endosomal compartment, releasing DNA into

the cytoplasm. PAAs can therefore be designed for intracellular drug delivery because they possess intrinsic endosomolytic properties (99).

Initial work in the development of PAA-based vectors for DNA delivery focused on the physicochemical characterisation and biological applications of complexes formed with different PAA structures. PAA based on methylene-bis-acrylamide and dimethylethylene diamine co-monomers (MBA-DMEDA) showed the most favourable DNA binding and complex properties (100). Interestingly, these structures were significantly less cytotoxic than PLL to hepatoma (HepG2) and lymphoblastoid leukaemia (CCRF) cell lines and produced complexes that were moderately efficient for *in vitro* transfection (90, 100).

1.2.4.3.1 Effects of charge density and flexibility of polyamidoamines on its properties

DNA binding capacity of PAAs depend on their structure, where PAA with two tertiary amino groups shows higher binding capacity than that with one tertiary amine groups. However, the DNA binding capacity is significantly decreased by the replacement of the methylene group in the diacrylamide unit by a piperazine ring. This is because of increasing rigidity of the polymer by the presence of two piperazine rings per repeating unit, resulting in difficulty for polymer to complex DNA closely. Moreover, the polyplexes with the smallest particle size and greatest colloidal stability have the higher charge density and flexibility in relation to other polymers. In contrast, the polyplexes with smallest DNA binding capability and stability against aggregation result in decreasing transfection efficacy. From all of these findings, it has been concluded that the polymer-DNA binding ability, colloidal stability and transfection efficacy of the polyplexes depend on the charge density and structural flexibility of the polymer (101).

1.2.4.3.2 Addition of carboxylic acid group to the bisacrylamide unit of polyamidoamines

When administered intravenously, polyplexes are normally present in the endosomes which acidify from early to late stages and ultimately, fuse with the lysosomes. In this intracellular environment, polyplexes are exposed to hydrolysis by the effect of endosomal acidity (pH 5-7) and lysosomal enzymes (pH 4.5). Escape of polyplexes from endosomes into cytosol is the main obstacle in gene delivery. Therefore, many vehicles have been developed to cause disruption of the endosomal membrane and overcome this barrier. These endosomolytic agents are either natural (viruses) or synthetic (melittin and INF-7), but these fusogenic peptides are exposed to conformational changes from a random coil to an α-helix at neutral pH and low pH, respectively. The addition of carboxylic acid moiety to the bisacrylamide segment can create amphoteric polyamidoamines. These polymers also undergo conformational changes at different pH upon protonation of the carboxylic acid and amino groups, resulting in greater hemolysis of RBCs at acidic endosomal pH than at neutral physiological pH. Therefore, addition of carboxylic acid moiety to PAAs can produce an amphoteric polymer that undergoes conformational changes at different pHs, resulting in promotion of the endosomolytic effect and an increase in transfection efficacy (101, 102).

1.2.4.3.3 Effects of polyethylene glycol incorporation into polyamidoamines

The highly positively charged complexes are favoured for their desirable electrostatic binding to the cell membrane, which leads to efficient internalisation and high level of gene expression *in vitro*. However, *in vivo* administration of highly positively charged systems was found to be the origin of many undesired non-specific interactions with blood components such as blood cells and serum protein, which result in a rapid

clearance of the complexes from the blood circulation by the reticuloendothelial system (RES) (103). This usually occurs by phagocytosis, which takes place after a process known as opsonisation. Opsonisation is the process by which certain blood components such as opsonin proteins adsorb onto the surface of the foreign particles or organism, thereby making it more recognisable to the phagocytic cells. The degree of opsonisation depends mainly on the surface characteristics of a particulate system, with serum protein adsorption occurring more with charged particles of a hydrophobic nature (104, 105). Therefore, one of the promising approaches to avoid clearance of the complexes from blood circulation and to increase their systemic circulation time is by incorporating hydrophilic moieties, for examples polyethylene glycol (PEG) and poly[N-(2-hydroxypropyl)methacrylamide] (pHPMA) into the complex structure in order to modify the surface character and to shield the surface charges (106-108). PEG is a non-ionic, hydrophilic polymer, well known for its biocompatibility, flexibility and non-immunogenicity. PEG has a number of features that can be used in gene delivery systems. The PEG layer strongly reduces interparticulate aggregation because of the formation of a sterically stabilised coating around the particles and thus improving the stability of the system. Furthermore, the steric barrier of the PEG layer inhibits the adsorption of proteins and other blood components, so that the opsonisation process does not occur, and the particles are not taken up by the RES. At the same time, it shields the particles from the immune system and prevents interaction of the particles with degradative enzymes, and in that way prolongs circulation times influencing the pharmacokinetics and biodistribution of the DNA delivery system (103, 106, 109). All of these features act to boost the chances of a particulate delivery system reaching its desired site of action.

Hydrophilic segments can be attached to cationic copolymers in two distinct architectures, either block copolymer (i.e. a linear structure of copolymer, in which the end of one segment is covalently attached to the head of another segment to form a diblock AB type or triblock ABA type copolymer) or graft copolymer, which is characterised with comb like structure with hydrophilic moiety attached to the cationic segment backbone (110). Two different PEGylation strategies have been developed. The first strategy is based on direct attachment of PEG to the cationic polymer prior to complexation (pre-PEGylation), whereas the second approach relies on coupling of PEG to the surface of the complexes after complex formation (post-PEGylation) (111). The majority of the researchers in the area of polycation-nucleic acid systems have concentrated on the formation of complexes with block copolymers consisting of cationic and hydrophilic polymer segments. The cationic segments of the copolymers interact with nucleic acid, forming a charge neutralised hydrophobic core, whilst the hydrophilic PEG segments are excluded from the core and thus form a surrounding hydrophilic corona. These undergo self-assembly to form micelle-like structures (112, 113).

Despite reported advantages of a polycation-hydrophilic segment for gene delivery, it seems that a careful manipulation of the construct composition will be required. For example, it has been reported that the transfection efficacy of PEG-grafted PEI was decreased when the proportion of PEG side chain increased (114). It is possible that the presence of PEG, which is known to sterically hinder interaction between particles, provides a steric barrier around these complexes thus preventing interaction with the cell membranes, and therefore the transfection efficacy is decreased. The morphology of complexes formed between PEG-polyamidoamine triblock copolymer and pDNA was investigated by atomic force microscopy (AFM) and transmission electron

microscopy (TEM) confirmed that the presence of PEG interferes with efficient DNA condensation (115). Therefore, careful selection of the appropriate cationic segment hydrophilic segment balance is key to the development of effective gene delivery systems.

Our group has previously used PEGylated PAA copolymer (2 kDa) and compared it with cationic homopolymer using a range of physicochemical properties and biological assays. Particle size results showed that the complexes formed from PEGylated copolymer were not aggregated at polymer/DNA ratios where severe aggregation occurred with homopolymer (115). Ethidium bromide displacement assay suggested that there were slight differences in the polymer-DNA binding abilities; this is possibly due to length of cationic polymer rather than being an effect of PEG. Incorporation of PEG on the surface of the complexes also results in reducing zeta potential of the complexes. Morphological studies showed that the complexes were not fully condensed owing to a high ratio of PEG to PAA segments, which prevented a tight condensation of the DNA and were susceptible to degradation by nucleases (115). To overcome these problems, mixtures of PEG-PAA and PAA were investigated. It was found that if the correct ratios of homopolymer to copolymer were used, well condensed; sterically stabilised polyplexes could be formed incorporating all the added polymer and DNA.

At lower RU/Nt ratios (1:1 and 1.33:1), small complexes were formed with no significant increase in size. At higher polymer/DNA ratios a reduced stability of the 3:1 blend was seen, with larger particle size measurements that increased with time. The observed particle size of slightly over 300 nm for the 1:1 ratio, suggested that condensation was not complete, but at an RU/nucleotide ratio of 1.33:1, small (< 200 nm) complexes were obtained. Therefore, it was believed that the amount of PEG

presented in the formulation was not sufficient to stabilise the particles; therefore, increasing amount of PEG was also investigated. At PAA/PAA-PEG ratio 1:1 large particle sizes were observed compared to ratio 2:1, this is attributed to absence of sufficient of cationic polymer to condense DNA. Complexes made with PEGylated polymer and the polymer blends both suffered from a reduced transfection activity. This is attributed to a low surface charge on the complexes, leading to a reduced interaction of the complex with the cell membrane and consequent reduction in uptake into the cell (116). Incorporation of targeting moieties were suggested to enhance uptake of the polymer blends, but these complexes still suffer from lower transfection efficiency (117).

1.2.4.3.4 Addition of disulphide bonds in polyamidoamines

The complexation of PEGylated cationic copolymers with nucleic acid produces complexes with a PEG corona that improves colloidal stability of the complexes owing to reduced interaction with blood components, resulting in prolonged circulation (106). However, PEGylated complexes showed significantly decreased transfection efficiency compared to positively charged complexes formed from cationic homopolymers, because of their lower surface charge. A strategy to improve stability and reduce cytotoxicity of the polymers while enhancing their transfection efficiencies is to incorporate reducible disulphide bonds into the polymer backbone to form bioreducible polycations facilitating intracellular redox-sensitive polymer breakdown (118, 119). These bioreducible complexes protect their contents from extracellular enzyme by forming stable complexes and uptake by the cell via the endocytosis pathway (120). The usage of disulphide bonds as cleavable linkers in drug or gene delivery systems has been reported in several publications (121-123). A disulphide bond (-S-S-) is a covalent linkage, which arises as a result of the oxidation of two

sulphydryl groups (SH) from two cysteine residues or other sulphydryl-containing materials. Disulphide bonds play also a key role in maintaining proper biological functions of living cells.Very wide range of metabolic processes involves thiol-disulphide exchange reactions, from protein stabilisation, enzymatic activity and cell signalling pathways to apoptosis (124, 125). Furthermore, many diseases have been recently associated with an imbalance of redox, including HIV, Parkinson and Alzheimer syndromes, cystic fibrosis and cancer (126-128).

There are two distinct characteristics that render disulphide bonds attractive for the design of gene delivery systems, which are the disulphide bond stability in plasma and its reversibility within cells (129). It is well-known that disulphide bonds are stable under extracellular physiological condition but are rapidly cleaved in a reductive intracellular compartment due to the presence of relatively high concentration of glutathione, the most abundant reducing agent in mammalian cells (128). The existence of these differences in reductive potential has been exploited for triggered intracellular delivery of a wide range of bioactive materials, such as pDNA (130), siRNA (131) and antisense oligonucleotides (132).

Disulphide bonds can be incorporated into gene delivery systems in two different strategies. The first strategy is the introduction of the disulphide linkages in the polymeric main chain or in the side chain (inter-chain disulphide linkages or disulphide-containing cationic polymers) (133). The second strategy is the formation of intra-chain disulphide linkages between two different components (intra-chain cross-linked) (134).

Linear bioreducible polyamidoamines containing oligoamines in their side chain showed strong DNA binding capability and the complexes formed were able to transfect COS-7 cells *in vitro*, with transfection efficiencies higher than 25 kDa

branched PEI (80). Notably, it has been demonstrated that the number of amine groups and length of the alkyl spacer between the amino groups displayed a distinct effect on their buffer capacity, transfection efficacy and cytotoxicity profile. The elongation of the alkyl spacer from ethylene to propylene between the amino units resulted in not only reduced transfection efficiency but also increased cytotoxicity (80).

Although cross-linking DNA complex via disulphide bonds enhances stability and extends systemic circulation of the complexes, the transfection efficiency decreases with increasing number of disulphide bonds. Oupicky *et al*, 2001 suggested that the reduction in the level of gene expression was due to the decreased endosomal escape of the cross-linked complex. It was proposed that too much stability through disulphide bonds leads to inefficient reduction and release of DNA from the complexes in the endosomal compartment (135).

1.2.4.3.5 Crosslinked polyamidoamines

Polyamidoamines (PAA) are a family of linear polymers synthesized by stepwise Michael-type polyaddition of primary mono-amines or secondary diamines with bisacrylamide. A polymer made with an amine monomer and a bisacrylamide is considered as a homopolymer. But, if the polymer is made of two different amine monomers and a bisacrylamide then it is regarded as a copolymer (136).

The main backbone of the PAA polymers used in this work is made of methylene bisacrylamide (MBA) and two monomers, dimethyl-ethylene-diamine (DMEDA) and cysteamine. Therefore, all polymers used in this thesis are copolymers, but for simplicity, non-PEGylated homo-block polymer containing a single-block linear PAA segment will be referred to as HP or homopolymer. PEGylated tri-block polymer (PEG-PAA-PEG) is a block copolymer of PAA and PEG, and will be referred as CP or copolymer.

PAA block of HP was synthesized with three monomers, DMEDA, cystamine and MBA (137).

PEGylated tri-block polymers (CP) is synthesized with DMEDA, mono-t-Boc cystamine and MBA. PEG chains are added on each end of the polymer (138). CP2K represents a co-block polymer containing 1.7 kDa PEG chains. CP2K contains thiol repeating units at each edge of the central PAA block (11 kDa). CP contains mono-Boc (t-butyloxycarbonylamino)ethyl-protected cysteamine groups (136) whereas HP contains thiopyridine protected cysteamine. These thiol-protecting groups prevent disulphide bridge formation during storage (137).

HP or CP-siRNA nanoparticles are complexes made by mixing one polymer, either PEGylated (CP) or non-PEGylated PAA (HP), with siRNA. HP-CP/siRNA complexes are prepared by mixing siRNA with a polymer blend solution, containing PEGylated (CP) and non-PEGylated (HP) polyamidoamine polymers in a required HP:CP ratio. The negatively charged siRNA self-assembles with the positively charged polymers (HP and CP), while the free thiols are expected to form disulphide bridges by crosslinking with adjacent thiols or by reacting with HP that contains dithiopyridine pendants. The reaction between a free thiol and a dithiopyridine results in the formation of a disulphide bond while releasing a thiopyridine group. This disulphide crosslinking stabilizes the polymer-siRNA nanoparticle.

1.2.4.3.6 Development of polyamidoamine-nucleic acid formulation

The basic understanding of the nature of interactions between polymer and siRNA is critical to successfully formulate polyplexes that will be functional under *in vitro* and *in vivo* conditions.

Initially, the nanoparticles were prepared by mixing a single polymer with nucleic acid, where electrostatic attraction reduces the distance between the polymer and nucleic

acid, bringing several polymer strands and nucleic acid together and the core of the polyplex becomes relatively hydrophobic and compact. Complexation and gene delivery was studied for homopolymers with different PAA backbones. The homopolymer NG30, p(DMEDA-MBA) showed efficient DNA condensing properties and transfection activity (100). Later development, multi-component systems involving PEGylated and non-PEGylated PAA for gene delivery was initially reported by Rackstraw *et al.* Homopolymer NG49 (DMEDA-MBA) and tri-block-copolymer NG47, PEG-(DMEDA-MBA)-PEG, were used for the delivery of plasmid DNA (116). In a later development, nanoparticles were prepared by mixing the plasmid DNA with a polymer blend consisting of PEGylated and non-PEGylated polymers, defined as three-component system which had several advantages like uniform size distribution, higher DNA condensation ability resulting in the formation of smaller, compact and stable nanoparticles and a quantitative incorporation of both polymer and nucleic acid components (116). Three component crosslinked nanoparticles formation has been also reported in Aljaeid's thesis and Danish's theses (139, 140). The crosslinkable PAA has been shown to self-assemble into stable nanostructures with plasmid DNA (139, 140), ODNs and siRNA (140).

Homopolymers (PAA) with three different molecular weights (44 kDa, >10 kDa and 5-10 kDa) and copolymers (PEG-PAA-PEG) with varying length of PEG chains (655, 1700 and 4600 Da) were investigated in Aljaeid's thesis (139). Aljaeid *et al.* showed that the thiol crosslinked complexes were much more tightly condensed than non-crosslinked complexes whereas, the *in vitro* transfection activity was inversely proportional to the length of PEG chain (655, 1700, 4600 Da). In contrast, *in vivo* assessment of the cross-linked complexes showed that complexes prepared with PEG655 provided strikingly higher luciferase activity in the liver, whereas PEG4600-

based complexes showed the best transfection in non-reticuloendothelial system organs expected to benefit from a longer circulation time. PEG1700-based complexes showed similar transfection in all organs. Therefore, the disulphide-based cross-link was validated as a suitable DNA delivery system for *in vivo* application (139).

A comparative study involving the packing of different nucleic acids (pDNA, ODNs and siRNA) with the crosslinked PAA polymer system was investigated in Danish's thesis (2009-2013). Copolymer (PEG-PAA-PEG) with 4600 kDa PEG was used along with three different homopolymers (44 kDa, >10 kDa and 5-10 kDa). The central PAA block of CP was 6700 kDa with randomly distributed cystamine residues. These nanoparticle formation data at high salt concentrations indicate that the condensation process of PAA with 4000–6000 bp DNA in relatively favourable compared to 21–23 bp siRNA. Crosslinked siRNA nanoparticles were prepared in 5 mM NaCl and the resulting complexes were found to be stable under physiological salt concentration after complexation (140). Danish *et al*. tested similar set of crosslinkable-polymers on A549 human lung cancer cell-line. The cells were exposed to free-polymer or polymer-siRNA complex in DMEM with no serum for 24 hours and the cytotoxicity assay was performed immediately after the treatment. Free polymer and polymer complexed with siRNA did not show any significant difference in toxicity profiles. The EC50 [Half Maximal Effective Concentration, EC50] was determined for HP as 255 μg/mL and a different PEGylated copolymer as 354 μg/mL [CP-05, PEG4600Da-PAA6700Da-PEG4600Da] (140).

Anthiya *et al.* tested a similar set of crosslinkable-polymers using miRNA or siRNA on a brain tumour cell line (117). Anthiya *et al.* showed that the thiols in crosslinked complexes increased nanoparticle stability in physiological medium, which in turn

would allow these nanoparticles to survive under harsh *in vivo* conditions which is lacking in the non-crosslinked systems.

Due to the disulphide mediated nanoparticle stabilization, the components self-assemble into nanoparticles with little excess free polymer or nucleic acid. The miRNA or siRNA loading into the nanoparticles is also high (~15 wt.% for RU/Nt ratio 5:1). However, the newly developed miRNA-PAAnanoparticles did not produce significant functional gene-knockdown after cell treatment.

1.3 Spleen Tyrosine Kinase (Syk)

The tyrosine kinase Syk was first described by Zioncheck et al. in 1986 (141). Subsequent work lead to Syk's isolation from the porcine spleen (141), hence its name. Syk is a 72 kDa non-receptor spleen tyrosine kinase recruited to the cell surface upon receptor activation to amplify downstream signalling events. Zap-70 is a closely related member of the Syk family mostly restricted to T cells and natural killer cells (142). Syk B is an alternative spliced variant that lacks a 23 amino acid segment of interdomain B (143).

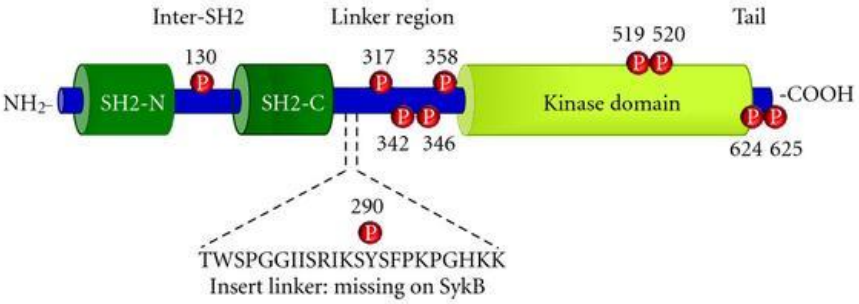

Figure 1.3 Molecular structure of Syk and isoform Syk B. Syk contains two tandem SRC homology domains (SH2), a kinase domain and two linker regions, interdomain A and interdomain B. Isoform Syk B, lacks 23 amino acid in interdomain B (144). P=phosphorylated.

Syk contains two tandem SRC homology domains (SH2), a kinase domain and two linker regions. Interdomain A connects the two SH2 domains, while interdomain B links c-terminal SH2 domain and kinase domain (**Figure 1.3**) (145).

Syk is highly expressed by haematopoietic cells including macrophages, mast cells, basophils, neutrophils, eosinophils, immature T cells and B cells, NK cells and dendritic cells (146, 147). Expression of Syk has also been detected in osteoclasts (148), fibroblasts (149) and epithelial cells (150).

The classical Syk-mediated signal transduction pathway involves association of the two tandemly arranged SH2 domains of Syk with the cytoplasmic consensus motif called immunoreceptor tyrosine-based activation motif (ITAM) (**Figure 1.4**) (151). The ITAM domain is present in the immunoreceptor tail (**Figure 1.4B**) or transmembrane adaptor chain (**Figure 1.4A**) and contains two adjacent consensus sequences that are tyrosine phosphorylated by Src family kinases upon receptor crosslinking (**Figure 1.4A-D**). Phosphorylated ITAMs serve then as binding sites for the two tandem SH2 domains of Syk resulting in protein recruitment and activation (152).

In certain cases, a single sequence is present in the cytoplasmatic tails of the receptor (hemITAM) (**Figure 1.4C**). In such instances, receptor dimerization provides the binding site for the two Syk SH2 domains (153). Examples include Syk-mediated signalling pathways of the platelet receptor CLEC-2 and the fungal recognition receptor Dectin-1 (153). Syk also associates with the ITAM-containing adaptor proteins DAP12, as well as with phosphorylated tyrosine residues in ITAM-like motif-containing ezrin –radixin –moesin ERM family proteins (151, 154).

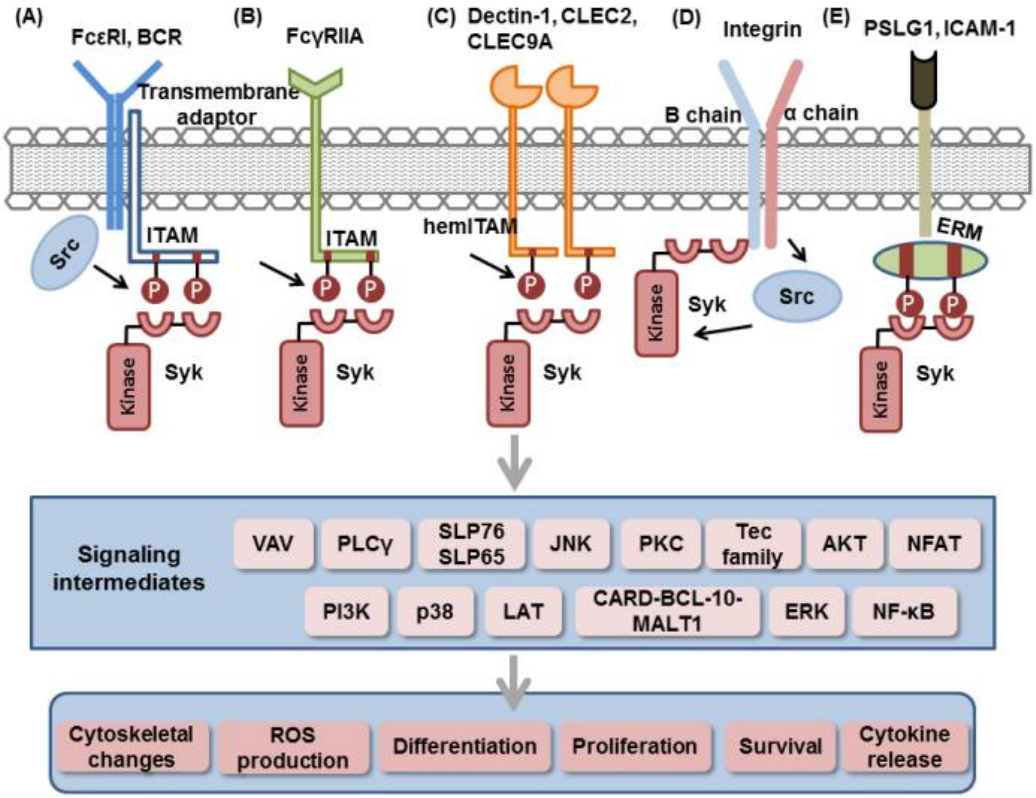

Figure 1.4 Mechanisms of Syk mediated-signaling. Syk is recruited to the plasma membrane upon receptor crosslinking through binding of the two SH2 domains to the phosphorylated tyrosine residue of ITAM (by SRC family kinases) in the receptor complex. ITAMs are present in the receptor associated transmembrane adaptor **(A)**, in the cytoplasmic tail of the receptor **(B)**, or in two separate receptor peptide chain **(C)**. Syk also interacts with the integrin β-chain through the non-phosphorylated tyrosine-binding surface of the amino-terminal SH2 domain **(D)** and with phosphorylated tyrosine residues in ITAM-like motif- containing ezrin-radixinmoesin ERM family proteins **(E)**. Downstream signaling pathways involve other signalling molecules and leads to a variety of cellular responses (147).

In the absence of phosphorylated ITAM binding, Syk adopts an autoinhibited conformation in which the regulatory region, containing the two SH2 domains and interdomain A, interacts with the catalytic domain in the C-terminal region (155). In addition to ITAM binding, tyrosine phosphorylation in interdomain A or B also results in Syk activation (156). Syk phosphorylation is essential for kinase activation and downstream signalling (152).

Activation of Syk leads to in the regulation of several intracellular signalling pathways. Downstream Syk targets include the VAV, LAT and SLP76 as well as phospholipase Cγ (PLCγ), phosphoinositide 3-kinase (PI3Ks) and the mitogen activated protein (MAP) kinase (**Figure 1.4**). These molecules turn on further downstream signalling processes leading to different biological outcomes including cytoskeletal rearrangement, reactive oxygen species (ROS) production, respiratory burst and phagocytosis (142, 143, 145, 148-155).

1.3.1 Inhibition of Syk

The wide biological role of Syk has motivated researchers to find several approaches to block protein expression and kinase activity. Genetic deletion, pharmacological inhibition and knockout mice have been used to interfere with Syk function. The first attempt to generate Syk deficient mice showed a perinatal lethal phenotype in mice null for the Syk gene (157, 158).

Short interfering RNAs (siRNA) have been used to supress Syk expression. Blockade of Syk with siRNA inhibits mast cell signalling, antibody-mediated platelet ingestion in human macrophages (159), B-cell lymphoma cell proliferation (160), and downstream Syk signalling in chronic lymphocytic leukemia cells (161).

Antisense oligo nucleotides (ASO) were also used in silencing Syk mRNA. Matsuda et al. synthesized the first ASO directed to Syk (162). Syk ASO nebulized as liposome complexes was assayed by Stenton et al. in a rat model of airway inflammation (163). The authors demonstrated significant reduction of the allergic inflammatory response in mice pretreated with Syk-ASO.

In 2001, Novartis patented a 2,6-disubstituted purine compound, NVP-QAB-205, that exhibited inhibitory activity against Syk. NVP-QAB-205, with an IC50 of 10 nM, has been shown to effectively inhibit mast cell degranulation and airway hyper-reactivity

in response to adenosine in ovalbumin sensitised Norwegian Brown rats and blocked the acute bronchoconstrictor response to ovalbumin in these animals. Bioavailability of the NVP-QAB-205 after intra-tracheal administration is 70 %, thus making the compound suitable for administration via intra-tracheal nebulization (164, 165).

In summary, the large variety of Syk-mediated signalling pathways has motivated the development of several small molecule inhibitors with therapeutic potential for the treatment of various diseases. In addition, knockdown of Syk expression offers another alternative to target Syk for therapeutic applications.

1.3.2 Syk inhibition in allergic disease and asthma

Syk mediates important signalling events in asthma such as the allergic response, driven by mast cells (166) and basophils (167), following allergen challenge via high affinity Immunoglobulin E receptor (FcεRI) leading to degranulation, de novo synthesis and the release of mediators of allergic inflammation. Therefore, Syk inhibition interferes with signal transduction and may be effective for the treatment of asthma. In fact, Matsubara et al. (168) used this approach in an acute murine model of ovalbumin (OVA)-induced airway inflammation. In this study, OVA-sensitized animals were treated twice daily with Syk inhibitor R406 beginning 1 day before the first OVA challenge and continuing for 10 days until the day before the experimental outcomes were obtained. R406 inhibited the development of airway hyper-responsiveness (AHR), eosinophilia and goblet cell metaplasia. A similar study by the same group used a sub-acute murine model of OVA-induced asthma, and also showed that pre-treatment with Syk inhibitor R406 prevents the development of OVA-induced Airway hyper-responsiveness and airway inflammation (169). A third study by Yamamoto *et al.* (170) demonstrated that administration of Syk inhibitor BAY61-3606 for 21 days blocked the development of antigen-induced inflammation,

bronchoconstriction and bronchial oedema in this rat model of asthma. In addition, aerosolised anti-sense oligonucleotides (ASO) to Syk administered 3 days before the antigenic challenge to OVA-sensitized Brown Norway rats significantly inhibited inflammation, lung eosinophilia and antigen-induced contraction of isolated tracheas (163).

In humans, the first clinical trial with Syk inhibitor R112 alleviated the symptoms of patients with allergic rhinitis (168) and showed therapeutic potential for the treatment of asthma as well.

In summary, Syk inhibition is a promising therapeutic strategy for allergic diseases including asthma. Several animal studies support this statement from a prophylactic approach (171).

1.3.3 Development of Syk assay for siRNA

Although there no good human mast cell or basophil cell lines available, well characterised rat basophilic cell lines exist (172), called rat basophilic leukaemia (RBL) which were isolated from a Norwegian brown rat (*Rattus norvegicus*, Rn). One clone, RBL-2H3 (173), is commonly used by researchers. These cells have abundant expression of the tetrameric FcεRI high affinity IgE receptor (174).

Degranulation results in the release of the preformed granular content and these can be measured. For example, basophil granules contain histamine and beta-hexosaminidase which can be measured using established assays (175).

Our group has generated an RBL cell line which is stably transfected with a neuropeptide Y-red fluorescent protein fusion construct (NPY-mRFP). These cell lines store the NPY-mRFP fluorescent protein in the granules and release it into the medium upon degranulation (176).

This system can very conveniently be used for quantification of degranulation as it does not need any substrates or buffers (needed for beta-hexosaminidase activity measurement) or expensive ELISA kits (needed for histamine quantification). Instead, the release of fluorescent protein from the granules can be measured directly in the supernatant without any additional treatment, cutting down on cost, duration and sources of experimental errors encountered with the other assays.

In this research, newly designed thiol crosslinkable polyamidoamines were characterized and their potential as a siRNA delivery system was evaluated using Syk gene as a model target gene. The degranulation inhibition, gene silencing efficiency, and cytotoxicity of the crosslinked PAA in complex with siRNA were investigated.

1.4 Aims and objectives

The aim of this study was to develop an effective and safe PAA based siRNA delivery system for treatment of allergic diseases based on knockdown of the Syk gene.

Objectives

I. Development and characterisation of polyplexes based on linear polyamidoamines with thiol cross-links.

II. Investigate the use of the NPY-mRFP system as a degranulation reporter system and screening of efficient PAA-siRNA nanoparticles for *in vitro* performance using degranulation inhibition and cytotoxicity assay.

III. Validate gene silencing results of thiol crosslinked PAA-siRNA complexes with Western blot and RT-PCR methods.

Chapter 2

2 Materials and Methods

This chapter describes the generic experimental methods and protocols used throughout the project. Most of the common chemicals and reagents were obtained from Sigma and Invitrogen unless specified.

2.1 Small interfering RNA

The four types of Syk-targeted siRNA sequences were based from Sanderson's article and the individual siRNA duplexes were purchased from Sigma Aldrich, UK (**Figure 2.1**) (177). Syk-targeted and scrambled siRNAs were supplied as lyophilized powder which were then diluted with nuclease free water and stored at -45 ^{O}C as 1 mg/ml stock solution for further use. SiRNAs used in this project are 21 base pair-double stranded unmodified nucleotides with species specificity of complete homology against mRNA of either rat, human or mouse Syk (**Table 2.1**).

SiRNA	Sequence (5′-3′)	Location in rat mRNA	MW (g/mol)
G	CCUCAUCAGGGAAUAUGUG (Sense strand) CACAUAUUCCCUGAUGAGG(Antisense strand)	CDS bp: 697-715	13304
H	GCCUGCUGCACGAAGGGAA (Sense strand) UUCCCUUCGUGCAGCAGGC (Antisense strand)	CDS bp: 936-954	13349
I	GUCAUGCAGCAGCUGGACA (Sense strand) UGUCCAGCUGCUGCAUGAC(Antisense strand)	CDS bp: 1570-1588	13334
J	GUGCUGAUGAAAACUACUA (Sense strand) UAGUAGUUUUCAUCAGCAC(Antisense strand)	CDS bp: 1862-1880	13274

Table 2.1 Specifications of siRNA used in the project.

```
   1 GCAAGTGGAG GCTCCCTCTC CTTCCCTCCG TCTCTGTGGC CACCCCCATT TTTAAGCCTG
  61 CCAGTTTGGT CCTTTCCACG CTCCATGCTG CCTGGTGCCC GGGAGCCCAG GCCATCTGCG
 121 ACTCCAGGAC AGGAAGTCAG AAGAGGGGAG CTCAGACATG ACAGGCAAGC CACATGGCTG
 181 GTACAATGAG TACCATGGAA CCTGAAGGAG CGCATGTGTT TGATAGTGTT GGCTCTTCAA
 241 GAGGCATCAT CTATGGAAGT GCCAAGGGTG TGTACAAGAG CTATTCTCCA CATACCTCCC
 301 AGAGCTCTGA AGGGGTGCAG ACATGGCGGG CAATGCTGTG GACAATGCCA ACCACCTGAC
 361 CTACTTTTTT GGCAACATCA CCCGGGAAGA GGCCGAAGAC TACCTGGTCC AGGGAGGCAT
 421 GACCGATGGG CTCTACCTGC TACGCCAGAG CCGCAATTAC CTGGGTGGTT TTGCTTTGTC
 481 GGTGGCACAC AACAGGAAGG CACACCACTA CACTATCGAG AGAGAACTTA ACGGCACCTA
 541 CGCCATCTCC GGGGGCAGGG CCCATGCCAG CCCGGCAGAC CTCTGCCATT ACCACTCCCA
 601 GGAACCCGAA GGCCTGGTCT GCCTCCTCAA GAAGCCCTTC AACCGGCCCC CGGGGGTACA
 661 GCCCAAGACT GGACCCTTTG AGGACCTGAA GGAGAACCTC ATCAGGGAAT ATGTGAAACA  <-- SiRNA G
 721 GACCTGGAAC CTTCAGGGCC AGGCTCTGGA GCAAGCCATC ATAAGTCAGA AGCCCCAACT
 781 GGAGAAGTTG ATCGCCACGA CGGCTCATGA GAAGATGCCC TGGTTCCATG GCAACATCTC
 841 CAGAGACGAG TCAGAGCAGA CGGTCCTCAT AGGGTCAAAG ACCAACGGAA AATTCCTGAT
 901 CAGGGCCAGA GACAACAACG GCTCCTTTGC ACTGTGCCTG CTGCACGAAG GGAAGGTATT  <-- SiRNA H
 961 ACACTATCGC ATCGACAGGG ACAAGACCGG GAAGCTTTCC ATCCCCGAGG GGAAGAAGTT
1021 TGACACCCTC TGGCAGCTAG TGGAACATTA CTCTTACAAG CCAGATGGGC TATTAAGAGT
1081 CCTCACGGTA CCATGTCAAA AGATTGGCGT GCAGATGGGC CACCCAGGAA GTTCAAATGC
1141 CCATCCTGTG ACTTGGTCAC CAGGTGGAAT AATCTCAAGA ATCAAATCCT ACTCCTTCCC
1201 AAAGCCTGGC CACAAAAAGC CTCCCCCACC CCAAGGGAGC CGTCCGGAGA GCACCGTGTC
1261 CTTCAATCCC TATGAGCCAA CGGGAGGGGC CTGGGGCCCA GACAGAGGCC TTCAGAGAGA
1321 AGCCCTGCCC ATGGACACCG AGGTATATGA GAGTCCTTAC GCTGACCCTG AAGAGATCCG
1381 GCCCAAAGAG GTCTACCTGG ACAGGAAACT GCTGACCCTG GAGGACAATG AACTGGGCTC
1441 TGGCAACTTC GGGACTGTGA AAAAGGGATA CTACCAAATG AAAAAAGTTG TAAAAACAGT
1501 GGCTGTGAAA ATCCTGAAGA ATGAGGCCAA CGACCCGGCT CTGAAGGACG AGCTGCTGGC
1561 GGAGGCCAAC GTCATGCAGC AGCTGGACAA CCCCTACATT GTGCGCATGA TCGGAATCTG  <-- SiRNA I
1621 TGAGGCGGAG TCGTGGATGC TGGTGATGGA GATGGCGGCA TGGGGGCCCC TCAACAAGTA
1681 CCTGCAGCAG AACAGGCACA TCAAGGATAA GAACATCATC GAGCTGGTTC ACCAGGTTTC
1741 CATGGGAATG AAGTATTTGG AGGAGAGCAA TTTTGTGCAC AGAGATCTGG CCGCGAGGAA
1801 CGTGCTTCTG GTCACCCAGC ACTACGCCAA GATCAGTGAC TTCGGTCTTT CCAAAGCCCT
1861 CCGTGCTGAT GAAAACTACT ACAAGGCCCA GACCCACGGG AAGTGGCCGG TGAAGTGGTA  <-- SiRNA J
1921 CGCCCCCGAA TGCATCAACT ACTTTAAGTT CTCCAGTAAG AGTGATGTCT GGAGCTTCGG
1981 AGTCCTGATG TGGGAAGCGT TCTCCTACGG GCAGAAGCCA TACAGAGGGA TGAAAGGGAG
2041 CGAAGTGACT GCCATGCTGG AGAAAGGAGA GCGGATGGGG TGCCCTCCAG GATGCCCGAG
2101 AGAGATGTAC GACTTGATGT TCCTATGCTG GACTTACGAT GTGGAGAACA GGCCAGGATT
2161 CGCGGCTGTG GAACTGCGGC TTCGCAATTA CTACTACGAC GTGGTTAACT AAGAGCTTGG
2221 GTGCCTGTCC GCGGCCACCT CGAATTCTCA AGCGATCGCA GGAAATTTAT TCAGATGAAC
2281 TGGCTCTCAG AGTTTCATCT CCCTCTGCCC AGAGGAGAGC TAACCAAGCA AAGCTAGGAA
2341 CTCACTCTCG CAACAGTTCT GGTCCCAAAA GACAGACAAG CAGCAAGCCC GCGGGACCTG
2401 AGGACTTGTC TGTCTGGCTT TTGTTTCCAT CTGTGTGGTT TTCGTCTTGG GTCACGTTCC
2461 GGGAACCATT TCCAAATTCG CTTGACGTCA TTCCGTTGCT CTGGGGCCAG GATTTCAGTG
2521 TCGCCCCCTG CAGGTCAGAA AGAGAAGTGC TTCGCCATTT CAGCAAAGGA CTGAGAGAAA
2581 CCTCACCAAT GCCGTTCGGA AGGCGGAAGA CGGTTAAGGA AAATGACAGA CTCAGGCACT
2641 GCTTTTGCTC TCAGCACTGA GACTGAAACA CCACGTGAAT GGGATGCTGA GACATGGCTG
2701 GCTTGCTTGC ACGCCCCTGG AGTCCGCCTC CTTGTAGAAT GACTTGAAGT CCGCTGTTGT
2761 GTGCTTACAG GAGGAGGCGT GAATAGCATT CTGCATGAAG GCTGCCAGGC AGGGTGGGCT
2821 CCCATGATCC TCTGCGACTG AGCCAAGTGT ATCAGGCATG GGTCAGAGTC CCTTTCTCTG
2881 CAGAAGGAAT GAATGCATCC AGGACTCCTT GTTGCGGCCA CAATACCTGA CCAGCAACCT
2941 CAGGGAGGAA ACGCTTGTTT GGGCTCACAG GCCATCATGG TGGCAAAGAC TTTACAACAG
3001 GCAGGAAAGA CTTGAGGGCA TGAACAAGAA GCTGTAAGGT CACGTGGTAT CCACACAGAG
3061 GAAGCGAAGA ATGAACAGGA AGTAGGACCA GGCTATAAGG CCCCAAAGCC CACCCACCCC
3121 ACCCCACCCC CCATCCCCCA CCCCCCGTGA CCCACTTTCC TTCAGCAAGA CCCCACTTCC
3181 CAAAGGTTCC ACAGGTCTCT CAGACAGTGA ATGCCAACAG CTGGGGACCA AAGTGTTCAA
3241 ATATACGAGC CTCTGTGGGG AGCCTTTCAC ATTCAAACTG CAAGAGGTTC CATCCATTTT
3301 CTGATGCTAT GACTGAACAC CTAGATAGGG TGGTGACAAA GAGAAGCAAT GTATCTCTTA
3361 GCTGTACATC CCTCTCCAAG GGTCGGAACT GCCCCCAGTG AGATGCAGTG CCAGGCAGCA
3421 GCCTTCCTGA ATGTCACAGG GTGATATCCC GATCAGAGGG GGGAAGCCTT CTCAGGTGTG
3481 TCCTTCTCTT ATGAGCCCCT GATACCGTCC CAGAGCCTCC TCAGGCCCCA CTTCTTCTTA
```

```
3541 ACCATCCCCC AAGGTCCCAT CTCCAAACAC CATGCTGTGA ACCTAGGCAC TAAGTCTTCA
3601 ACACATGAGC CCTGAGGGGA CACATTCATA CTAGAGCAGA CGGCAACACA GTGACCAGGA
3661 CCACCTCAGG ATGAGCTCGC GGATGGAATT TTAATTCAGA ATAAAACCAG AGAGGTGACC
3721 TTCCCCACAA GTAAGCCTTG CTAAGTGTGA CTTTGAGCTC TATCCTCCTG ACTTGCATAA
3781 GGTTCGGCTA ACTACCGACC ACACACCAAG TGTCACCTGT CCATAGCACA GTTGCTGAGG
3841 ACATAAAAGT TACAAAGGCA TAGCCTTCCG TCTAGGTCTA GGGGAATGTA CAAAGGAAGC
3901 ATCTCATCCT CACCCCTGAG ACACTGACAA ACACAGCCAG GGACGGCATG GGAGGCCCCA
3961 CTGGCGGCGG GTTCGATGAA CAGAGCCGGT GAAATGGGTT CCCCTCTTTA GACCAGTAGT
4021 TCTCAACCGA GACCCTCCAG TACAGTTCCT AGTGCTGTGA TGACCCCCAA TCATCAAGTT
4081 ACTTTGTGGC TACTTCATAA CTGTAATTTT GCTACTGTTA TGAATCATAG TGTGAATATC
4141 TGTTGATATG CAGGATATGC AATGTGCATC CCCCAAGGAG GGCACACCCA CAGGTTGGGA
4201 ACCACTGCCT TTGATATGGA GGCGCTACAC TTAGAAGCTA TGGTGTGTCT TGGAACTGTG
4261 CTAGTAGGTC AGTCGCCCTG TTGGGGGCAG ATCCCTGTGT GTTGCTGGCT GAGTGGGCCT
4321 GCAGAACACC TCCTTGGTGA GGAAATCCCG TGGGTCACTG CCTGATTGAG TCAAGGGAGG
4381 AAGAGACACT GTGTTGGTTA TGGAGGACAG GACCGTCTAG TCTGAGGAAG AAGCTCTCTG
4441 CTGAGCTCCT GGCCTACCTT CCCCTGTCCT CAGGGTAGGG CTATTAAAAG GCCACCTTGA
4501 AGGTCTGGGG GTGGTTGTGC GAGAACCCTA TGGAGGCCTC TGTCTTTTTC AGTCTTGTTT
4561 GCTTTCTGGC CTCTCTAGTA GTGCCTCTCC TTTCCAGGGG GTTGGACTGA CCATTCGTTA
4621 TCGGATGTGA CCAAGCAGAA CGGAGGGAGA CACGGCTTTG TCTCCCTTCA GAAGGTCGAA
4681 ACTGGCTCCT GGACGCAGAA GTCATGTGTG GCTATTGTCC AGGGCTCTCA TCTGTTGAAA
4741 ACTGTGTCTT GCTGTCAAGA TTAATTCTCT CCCCTGGGGC CACAGAGAGG AGGGCGGATG
4801 GAGAGAGGAT CCTCCTGGAG GGTTTAGATT CTGAATGCAC CATAAATTTG CAAGGTCGGA
4861 AACAAGGTCC TTCTCAGGCG TCTATACTTG GCCTAGGTCT GCTCACAAGC TGCCTCTGGT
4921 GCTCCGAATC CCTTCTGCCT GGCGCTGGGC TCACTGTGTG CCTTCACCTA TGACCCTTTA
4981 ATCAGCAGAG CACACGGAGC ACCTAATCTG CCTCGCCACA TCCTACTGAC CTCGCCACAC
5041 CACATACCTC ATGCAGAACC GAATGTCTCT CCATGAAACG CCCAAGCCAG CCATTCATAA
5101 AAACCTGTCT CTGTGTGCAC TGGAACGTGT CCTCCCTGTA CCCAAACCCA CTTTGTGTGC
5161 CAGACAGTGA CTCCACAGGG ACGCCAGGCC TGTGATCGCA TTGCTCGTTG CAGAGGGAAG
5221 CCCCGGGTTG TCCGTCTCAG GGATTACTCC CACCCAGAGC AGCACACAGT GTTCCCCTGT
5281 TATTTCAGAA ATTATTTTTA ATAAAGATCT ACTATTA
```

Figure 2.1 Spleen associated tyrosine kinase (Syk), mRNA sequence. The sequence of the Syk siRNAs G, H, I and J is shown along with the specific location on rat Syk mRNA (RefSeq_dna: NM_012758). Brown highlighted sequence refer to coding sequence while non-highlighted sequence refer to untranslated regions.

2.1.1 Thiol-modified siRNAs

The Syk-targeted and scrambled siRNA carrying thiohexyl protected group were purchased from ATDBio (CO, UK) as shown in **Figure 2.2**. The thiol aliphatic group was placed at the 5'-terminus on antisense strand of siRNA to allow reaction of the thiol PAAs while maintaining the binding affinity of Syk-targeted siRNA with RISC complex. Thiolated siRNA supplied in reduced form from company.

Syk-targeted siRNA sequence (5′-3′)	Location in rat mRNA	MW (g/mol)
GCCUGCUGCACGAAGGGAA(Sense strand) UUCCCUUCGUGCAGCAGGC (Antisense strand)	CDS bp: 936-954	13539

Table 2.2 Specifications of thiol-modified siRNA used in the project.

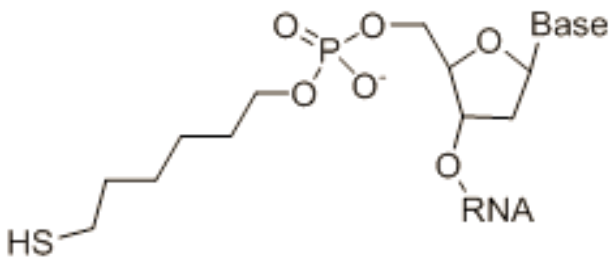

Figure 2.2 Structure of 5'-thiohexyl linker in in thiol-modified siRNA.

2.2 Cell culture

Rat basophilic leukemia (RBL)-2H3 cell line were obtained from the European Collection of Cell Cultures (ECACC), UK. Our group has generated an RBL cell line which is stably transfected with a neuropeptide Y-red fluorescent protein fusion construct (NPY-mRFP), a 36 amino acid peptide (178). This cell line store the NPY-

mRFP fluorescent protein in the granules and release it into the medium upon degranulation (179).

NPY-mRFP RBL-2H3 cells (passage 7) grew as adherent monolayers in cell culture-treated 25 cm^2 or 75 cm^2 flasks, with 0.2 μm vent caps (Corning, USA), in a cell culture incubator set to 37°C, 5% CO_2 with a humidified atmosphere. The flasks contained 5 mL or 15 mL RBL medium: minimum essential medium supplemented with 10% v/v heat-inactivated foetal bovine serum, 100 U/mL penicillin, 100 μg/mL streptomycin and 2 mM L-glutamine. Medium in the flasks were refreshed every two to three days. Cells were passaged 1/5 or 1/10 when 80-100% confluent. For each flask, the cells were detached by discarding the medium, washing the cells once with 10 mL Ca^{2+}/Mg^{2+}-free Dulbecco's phosphate-buffered saline (DPBS) (Sigma-Aldrich), adding 2 mL trypsin-EDTA to the cells, and placing the flask in a cell culture incubator. After the cells were sufficiently trypsinised, 8 mL RBL medium was added. The volume of cells appropriate to the split proportion i.e. 1/5 or 1/10 were discarded (or used for experiments), which was replaced with the same volume of fresh RBL medium for continual growth of the cells. Then, 10 μl of 1 μg/mL G418 sulphate antibiotic (Fisher, UK) was added to maintain NPY-mRFP gene expression in transfected cell lines. For simplicity, NPY-mRFP RBL-2H3 cell line will be referred as RBL- NPY in this work.

2.3 Polyamidoamines polymers

The polyamidoamine polymers used in this study were provided by Prof Paolo Ferruti, and Prof Elisabetta Ranucci University of Milan, Italy. These PAAs are hydrophilic and composed of repeating units of amido and amino co-monomers. Both homopolymer and copolymer are based on MBA-DMEDA (prepared from methylene bis acrylamide and dimethylethylenediamine co-monomers). A non-PEGylated mono-

block PAA with molecular weight greater than 10 kDa was used in this study and will be referred as homopolymer or HP>10 KDa (**Figure 2.3**). The homopolymer was used as a cross-linker and also contained random pendent sulfhydryl units on the central PAA backbone activated with sulfapyridine groups. A PEGylated tri-block PAA was referred as a copolymer (CP) and indicated as CP2k based on the length of the PEG chain on the polymer. CP2k has cystamine repeating units distributed at the either ends of PAA block as $PEG_{1.7kDa}$–$Cystamine_{2.4kDa}$-PAA_{11kDa}–$Cystamine_{2.4kDa}$–$PEG_{1.7kDa}$ (**Figure 2.4**). The cystamine monomers had BOC protected pendent sulfhydryl group to prevent disulphide bridge formation during storage. The PEGylated copolymer was prepared for use by removal of the protecting BOC group using Dithiothreitol (DTT) as a reducing agent. When the activated co-polymer (CP-Reduced) were mixed with the cross-linking homopolymer (HP) in a certain ratio in the presence of siRNA, they could form stable encapsulated cross-linked siRNA polyplexes with PEG at its surface.

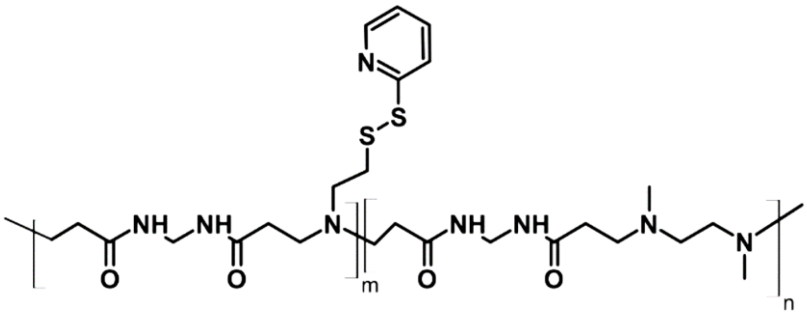

Figure 2.3 Chemical structure of homopolymer (HP>10 kDa). HP contains thiol (MBA and Cysteamine-containing group) and non-thiol (MBA-DMEDA) repeating units. Thiol repeating units are randomly distributed in the PAA structure.

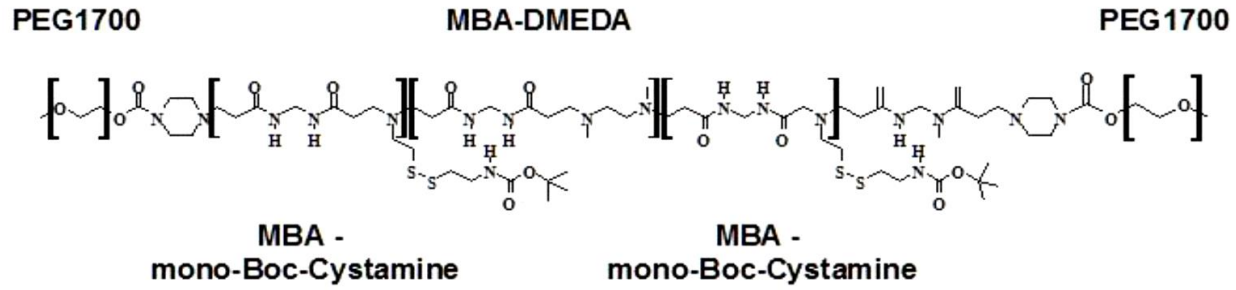

Figure 2.4 Chemical structure of copolymer (CP2k). PAA segment of CP2k contains thiol (MBA-Cystamine-Boc pendant) and non-thiol (MBA-DMEDA) repeating units. The thiol repeating units are present at the edges of the PAA block.

Table 2.3 Polymer data sheet.

Polymer	**Other names**				**Mw (Da)**
Homopolymer	Mono-block PAA	HP	HP>10 kDa	Non-PEGylated	>10
Copolymer	Tri-block PAA	CP	CP2k	PEGylated	19.2

2.3.1 Copolymer reduction

The thiol group (-SH) pendant on the backbone of PEGylated copolymer was reduced to remove the protecting BOC group to prepare the polymer for use. Reduction of copolymer was processed by deoxygenation of 1 L of HPLC water by passing nitrogen through it for 30 minutes under magnetic stirring. Then, 100 mg of copolymer was dissolved in deoxygenated water (10 ml) in a sealed vial covered with parafilm and stirred with magnetic stirrer for 10 minutes until the polymer was completely dissolved. Nitrogen was also passed through a sodium hydroxide solution (1M) in a separate vial for 6 minutes and NaOH solution was poured drop wise into the polymer solution to return the pH to 7.4. Polymer solution was kept for 30 minutes on the magnetic stirrer and then DTT (4.6 mg) was added in to the polymer solution and kept stirring for at least one hour in dark. After an hour, the pH of the reaction mixture was set to pH 3.5 to 4.0 by adding appropriate amounts of HCl [2 M]. Then, the above

solution was transferred to an Amicon Ultrafiltration Stirred Cell 250 ml filled with deoxygenated water and pressurized to 4 bar using a compressed nitrogen source. Deoxygenated water was passed through three times and reduced polymer was cooled with liquid nitrogen and freeze dried for 48 hours using VirTis® Sentry 2.0 SP Scientific Freeze dryer.

The physicochemical characteristics of siRNA-PAA nanoparticles were studied using agarose gel electrophoresis and dynamic light scattering..

The biological characteristics were evaluated using degranulation inhibition assay, resazurin cell viability assay, gene silencing efficiency and western blot in NPY-mRFP RBL-2H3 cells.

2.4 Agarose gel electrophoresis

Polyplexes were prepared by the addition of equal volumes of polymer to siRNA solution and incubated for 30 minutes at room temperature to form stable complexes. Two component complexes were made by mixing one polymer, either PEGylated or Non-PEGylated PAA, with siRNA whereas three component polyplexes contain a mixture of two polymers, PEGylated and Non-PEGylated PAA, with siRNA. The agarose gel [1.2 wt.%] was prepared in 40 mM Tris-acetate, 1 mM EDTA (TAE, pH 7.4) running buffer. The agarose was dissolved by heating the mixture in a microwave oven. The mixture was cooled down to 55˚ C and ethidium bromide was added to a final concentration of 0.5 μg/mL. Polyplexes containing 1μg of siRNA prepared at different Polymer Repeating Unit/ RNA Nucleotide (RU/Nt) ratios, 0.5:1 to 6:1 in each well. Then complexes were mixed with loading buffer (2.5 ul) and loaded into wells. Then the gel was allowed to run at 80V for 50 minutes in TAE buffer. Free, semi or completely bound siRNA was viewed by UV-transilluminator gel imaging system (The Bioimaging Company UK) by using Syngene software. For the visualization of

free polymer, the gel was stained with Coomassie blue staining solution [0.1% Coomassie Brilliant Blue R250, 50 % methanol, 10% acetic acid in water] followed by background elimination with de-staining solution [5 % methanol, 7.5 % acetic acid in water] for 24 hours. Coomassie stained gels were imaged against a white background using the trans-white mode with the same imaging software.

2.5 Particle size measurement of siRNA polyplexes using DLS technique

Dynamic Light Scattering (DLS) or Photon Correlation Spectroscopy (PCS) is a non-invasive, well-established technique to determine the particle size and size distribution for complexes in fluid. This technique is the easiest to implement, the quickest to perform, and the least destructive to the sample. DLS requires very small amount of colloidal solution (in microliters) for measurement. It refers to the interpretation and measurement of light scattering data on a microsecond time scale. This technique is one of the most popular methods used to determine the size of colloidal particles. It is applicable in range from about 0.001 to several microns, which is difficult to achieve with other techniques. DLS also has the ability to detect the trace amount of aggregates in the sample solution. Thus, DLS is considered a powerful light-scattering technique for studying the properties of suspensions and solutions of colloids, biological solutions, macromolecules, polymers and siRNA and DNA complexes.

Polyplexes containing 1.5 μg of siRNA were formed with different homopolymer to copolymer (HP:CP) ratios. Aliquots of the polymers with the required ratios were added into the siRNA solutions to obtain the desired polymer (RU) to nucleotide (Nt) ratios. The solutions were mixed by gentle agitation to avoid bubbles and complex formation was allowed to occur for 30 minutes. Then, 30 μL of the sample was transferred to Hellma quartz cuvettes. Size of the polyplexes was determined by using Viskotek DLS 802. The count rate was set between 300-500 kcps by adjusting the

LASER power between 5–20%. The acquisition time was set as 30s for each measurement and the size was obtained as an average of minimum 10 measurements.

2.6 Degranulation Assay

NPY-mRFP RBL-2H3 cells were harvested from flasks (see **2.3 Cell culture**). Samples of cells were taken for counting using a Neubauer modified haemocytometer, and the 50 mL tube was centrifuged at 300g for five minutes to pellet the cells. After discarding the medium, the cell pellet was re-suspended into 10 mL antibiotic-free complete MEM to obtain to obtain a cell concentration of $15x10^4$ cells/mL. RBL cells were seeded in a 12-well plate (1 mL/well) and incubated at 37°C with 5% CO_2 overnight for attachment. On the next day, the cells were sensitised with 0.5 μg/mL SPE-7 clone-derived mouse anti-DNP IgE. The plate was then placed in a cell culture incubator overnight. The next day, the cells in the plate were viewed under a light or fluorescence microscope to check for viability. Stimuli were prepared in phenol red-free RBL medium. For each well, the medium was removed and 1 mL prepared stimuli was added: medium only (negative control), 1 μg/mL calcium ionophore (A23187) or 1 μg/mL BSA-DNP. Lysis buffer (1% v/v Triton X-100 in DPBS) was used as a positive control (100% release). The plate was then placed in the cell culture incubator for one hour. Supernatants (200 μL) were transferred to wells of black, flat-bottomed, untreated 96-well polystyrene plates (Corning, USA). Fluorescence in well plates was measured with a plate reader (TECAN Spark® 10M multimode microplate reader, Switzerland) using 530 nm excitation and 590 nm emission.

2.6.1 Degranulation Inhibition Assay

Samples of cells were taken for haemocytometer counting, and the 50 mL tube was centrifuged at 300 g for 5 minutes to pellet the cells. After discarding the medium, the cell pellet was re-suspended into 10 mL antibiotic-free complete MEM to obtain a cell

concentration of $15x10^4$ cells/mL. RBL cells were seeded in a 12-well plate (1 mL/well) and incubated at 37°C with 5% CO_2 overnight for attachment. On the next day (24 hours), polyplexes were prepared by the addition of polymer solution to siRNA solution and incubated for 30 minutes at room temperature to allow time to form stable complexes. Prior to siRNA addition, the medium was removed and the wells were washed with 1 mL of PBS without Ca^{2+} and Mg^{2+}, and then replaced with siRNA containing medium. The cells were treated with these polyplexes in serum free medium for 4 hours and then replaced by MEM complete medium. On the next day, the cells were sensitised with 0.5 μg/mL monoclonal anti-dinitrophenyl antibody (anti-DNP IgE, Sigma Aldrich, UK) produced in mouse which is bound to FcεRI and stimulate cellular responses. Then, the plate was placed in a cell culture incubator overnight. On the next day, the cells were viewed under a light or fluorescence microscope to check for viability. Stimuli of 2,4-dinitrophenylated- albumin from bovine serum (DNP-BSA) (1 μg/ml) were prepared in phenol red-free RBL medium without serum and antibiotics and then added to the wells. The plate was placed in the cell culture incubator for one hour. DNP-BSA induces the cross-linking of receptor-bound IgE molecules resulting in the degranulation of the cells and the release of fluorescent materials. Supernatants (200 μL) were transferred to wells of black, flat-bottomed, untreated 96-well polystyrene plates (Corning, USA). Fluorescence in well plates was measured with a plate reader (TECAN Spark® 10M multimode microplate reader, Switzerland) using 530 nm excitation and 590 nm emission. Degranulation inhibition was measured 24, 48 and 72 hours after the polymer exposure before performing resazurin cell viability assay.

2.7 Resazurin cell viability assay

Resazurin assay was performed on the same cells following the degranulation inhibition assay. Resazurin sodium salt (5 mg) was dissolved in 50 mL HBSS (1x Hank's balanced salt solution with calcium and magnesium ions) to prepare a stock dilution of 100 µg/mL. Following degranulation inhibition assay, the BSA-containing medium was replaced with resazurin-containing medium [diluted (1/10) resazurin to phenol red-free MEM (Gibco™, Life technologies)], supplemented with serum (10%). The cells were incubated for 45-60 minutes in a cell culture incubator set to 37°C, 5% CO_2 with a humidified atmosphere. Supernatants (200 µL) were transferred to wells of black, flat-bottomed, untreated 96-well polystyrene plates (Corning, USA). The fluorescence was read with a TECAN plate reader [Excitation: 540 nm; Emission: 590 nm]. Fluorescence from blank wells (resazurin medium without cells) was subtracted from rest of the samples. The fluorescence from untreated cells was considered as 1 (100 % viability).

2.8 Reverse transcription polymerase chain reaction (RT-PCR)

2.8.1 RNA isolation

Total ribonucleic acid (RNA) was isolated from cells using GenElute™ mammalian total RNA miniprep kit (Sigma-Aldrich) following manufacturer's protocol. Briefly, cells in a 12-well plate were lysed with 250 µl of lysis solution containing 2-mercaptoethanol, then scraped and the lysate removed into 2 mL filtration column and separated by centrifugation (14,000 × g for 2 min). An equal volume of 70% (v/v) ethanol was then added to filtrate (250 µl) and spun for 1 minute. The RNA pellet was washed with 500 µL of wash solution and 1 mL of wash solution 2 and centrifuged at 14,000 × g for 2 minutes to remove ethanol. The pellet was then transferred to a new

collection tube and 50 µL of elution solution added and centrifuged for 2 minutes to get the pure total RNA. The Purified RNA was then storage at -80 °C.

2.8.2 cDNA synthesis

Complementary deoxyribonucleic acid (cDNA) was synthesised by reverse transcription (RT) of RNA. For each sample of RNA to be converted to cDNA, the following reagents were added (GeneAmp® RNA PCR core kit, Applied Biosystems Life Technologies): 1.8 µL RNA, 4 µL 25 mM $MgCl_2$, 2 µL 10X PCR bufferII, 2 µL 10 mM dATP, 2 µL 10 mM dCTP, 2 µL 10 mM dGTP, 2 µL 10 mM dTTP, 1 µL 50 µM Oligo $d(T)_{16}$, 1 µL 20 U/ µL RNase inhibitor, 1 µL 50 U/µL MuLV RT and 1.2 µL ultrapure™ DEPC-treated water to reach a final volume of 20 µL per well. The reaction mix was heated to 42˚C for 15 minutes, 99ºC for 5 minutes and 5ºC for 5 minutes in MJ research PTC-200 DNA engine thermal cycler thermocycler. The cDNA was either used immediately for qPCR or kept at -20˚C until required.

2.8.3 Quantitative real-time PCR (qRT-PCR)

For each sample of RNA to be analysed, 6 wells were prepared (3 for Syk gene and 3 for GGT1 as a reference gene) in strip tubes 0.1ml (Qiagen, Germany). To each well, the following were added: 1 µL cDNA template, 5 µL KAPA SYBR® FAST qPCR kit master mix (2X) Bio-Rad iCycler™ (Kapa Biosystems), 0.5 µL PrimePCR™ SYBR® green assay: Syk, rat (Bio-Rad) or PrimePCR™ SYBR® green assay: Ggt1, rat (Bio-Rad) and 3.5 µL ultrapure™ DEPC-treated water (Invitrogen) to reach a final volume of 10 µL per well. The reaction mix was then ran on a Rotor-GeneQ Real-Time PCR system (Qiagen) for amplification. with an initial step of 95˚C for 3 minutes followed by programme running for 40 cycles (95˚C for 3 seconds, then 60˚C for ≥ 20 seconds). Syk silencing efficiency was calculated using the Pfaffl method (180). Each

value was corrected for background by subtracting the negative control. Corrected values were then expressed as a percentage of Syk silencing.

2.9 Western blot

2.9.1 Preparation of cell lysate

All steps have been performed on ice. Following degranulation inhibition and resazurin assay, the medium was removed carefully, the wells were washed twice with ice cold PBS (1 mL) and replaced with cold RIPA (Radioimmunoprecipitation assay) lysis buffer (400 μL) (AMRESCO). Protease inhibitor cocktail (1X final concentration) (Sigma-Aldrich) was added to RIPA buffer immediately before applying to cells because RIPA Buffer does not contain any protease inhibitor. The composition of lysis buffer is as follows, 149 mM sodium chloride, 50 mM Tris pH 7.5, 0.1% sodium dodecyl sulfate, 1% NP-40, 0.5% deoxycholic acid, sodium chloride (NaCl, 150 mM). After 15 min, the cells were scraped from the wells and collected in cold 1.5 ml microcentrifuge tubes on ice. They were vortexed for few seconds to facilitate complete lysis and centrifuged for 15 minutes at 14,000xg at 4^{o}C to separate the total protein (supernatant) from the cellular debris (pellet). The lysate was carefully transferred to a new cold tube and used for protein estimation.

2.9.2 Total Protein Estimation - BCA Assay

The BCA protein assay is based on bicinchoninic acid (BCA) for the colorimetric detection and quantitation of total protein. This method combines the reduction of Cu^{+2} to Cu^{+1} by protein in an alkaline medium (the biuret reaction) with the colorimetric detection of the cuprous cation (Cu^{+1}) using a reagent containing BCA. The purple-coloured reaction product is formed by the chelation of two molecules of BCA with one cuprous ion. This water-soluble complex exhibits a strong absorbance at 562nm

that is nearly linear with increasing protein concentrations. The macromolecular structure of protein, the number of peptide bonds and the presence of four particular amino acids (cysteine, cystine, tryptophan and tyrosine) are reported to be responsible for colour formation with BCA. Protein concentrations generally are determined and reported with reference to standards of a common protein such as bovine serum albumin (BSA). The assay was performed in a 96-well transparent plate following the manufacturer's protocol using Pierce's BCA™ Protein Assay Kit (Thermo-scientific, cat.no. 23227). Working solution of BCA reagent was prepared by mixing Reagent A [sodium carbonate, sodium bicarbonate, bicinchoninic acid and sodium tartrate in 0.1M sodium hydroxide], Reagent B [4 wt.%, cupric sulfate] and albumin standard ampule, containing bovine serum albumin (BSA) at 2 mg/mL in 0.9% saline and 0.05% sodium azide. A series of BSA standard solutions, ranging from 25 to 2000 μg/mL, were prepared in ultrapure™ DEPC-treated water. An equal volume of sample (25 μL) and BCA reagent (200 μL) were added in each well. Each sample was prepared in triplicate. The plate was incubated at 37°C for 30 minutes. The absorbance at 562 nm was measured with a Tecan Spark® 10M multimode plate reader.

2.9.3 SDS-PAGE gel electrophoresis

Western Blotting was started with electrophoresis to separate proteins mixture according to molecular weight. The separated mixture was transferred to a rigid support. Then the blotting membrane was blocked, washed, probed with a primary antibody, washed again, and probed with an enzymatically labelled secondary antibody, which is then developed with a suitable substrate.

The protein samples were denatured with 2x reducing buffer (0.1M Tris-HCl pH 6.8, 5% SDS, 0.01% Bromophenol Blue, 10% β-mercaptoethanol, 20% glycerol) at 100ºC for 5 minutes and then centrifuged at 16,000xg in a microcentrifuge for 1 minute.

Equal amounts of protein (13 µl) were loaded into wells of a 4-20% mini-PROTEAN® TGX™ precast polyacrylamide gel (Bio-Rad, UK) along with 7 µl of precision plus protein™ Kaleidoscope™ prestained protein standards ladder (Bio-Rad, UK). Gel was run in SDS-PAGE sample buffer [62.5 mM Tris-HCI (pH 6.8), 25% glycerol, 2% SDS, 0.01% bromophenol blue] at a voltage between 80-200V for 35 to 45 minutes until the blue dye reaches the black reference line. After electrophoresis, the separated proteins were transferred onto a trans-blot® Turbo™ mini nitrocellulose transfer membrane using trans-blot® Turbo™ transfer system (Bio-Rad) in as little as 3 minutes. The transferred protein was then complexed with an antibody and detection probe (e.g. enzyme, fluorophore, isotope) using iBind™ flex Western system.

2.9.4 Protein detection using iBind™ flex Western system

The Invitrogen™ iBind™ flex western device is an automated device that offers flexible blot processing to perform blocking, washing, and antibody binding steps.

After electrophoresis and transfer of proteins to membranes, the blots were probed (for detection of Syk protein) with an anti-Syk antibody (mouse monoclonal IgG1, κ antibody, clone SYK-01, BioLegend) (1:500 dilution, using 4 µL antibody for the iBind flex device method and 10 µL antibody for the manual method) and anti-mouse IgG (whole molecule)–peroxidase antibody produced in goat (Sigma-Aldrich) (1:1,000 dilution, using 2 µL antibody for the iBind flex device method and 5 µL antibody for the manual method) was used as a secondary antibody. After 3 hours, antibody binding was detected using Pierce™ ECL western blotting substrate detection kit. The membrane was then imaged using an LAS-4000™ system (Fujifilm) with chemiluminescence mode using the auto exposure time setting.

The same blot was stripped with MILLIPORE re-blot plus Western blot strong antibody stripping solution for 15 minutes. After stripping, the NC membrane was re-

probed (for detection of GAPDH protein as a negative control) with a GAPDH loading control monoclonal antibody (1:1,000 dilution, using 2 µL antibody for the iBind flex device method and 5 µL antibody for the manual method) and anti-mouse IgG (whole molecule)–peroxidase antibody produced in goat (1:1,000 dilution, using 2 µL antibody for the iBind flex device method and 5 µL antibody for the manual method) was used as a secondary antibody. Images of the membranes were obtained using a Fuji LAS-4000™ imager (Fujifilm, Japan) under the high binning mode with chemiluminescence-luminol reagent (3 µL of 30% H2O2(BDH, UK), Tris/HCl 0.1 mM, pH, 8; 2.5 mM luminol (Sigma, UK) and 400 µM coumaric acid (Sigma, UK).

Chapter 3

3 Development of siRNA-PAA Nanoparticles

3.1 Introduction

Cationic polymers have been widely applied to improve siRNA gene delivery. But, the formation and stability of the nanoparticles that depends on charge-charge interaction still low, mainly because of the low negative charges and rigid rod-like structure of siRNA, which are the main obstacle underlying widespread use of this application (181). Our study described a new approach to improve binding and stability of PAA nanoparticles with siRNA using thiol-modified delivery system. Other studies showed that cationic polymers cannot tightly bind and condense siRNA depending on electrostatic interactions, resulting in a loose complex formation which is vulnerable to nuclease degradation in the blood before reaching the target tissues (182, 183). Many reports tried to develop a stable polymerized siRNA nanoparticle either by producing excess cationic charge on the polymer or excess anionic charge on siRNA. Raising the positive charges of cationic polymers can produce tight binding between polymer and siRNA, but with increasing unwanted charge-mediated cytotoxicity (184). In contrast, the bonding ability and stability improved with higher molecular weight and increasing anionic charges on siRNA (185-187). Kwon and co-workers designed a stable self-crosslinking nanoparticle by the thiol modification at the 5'-terminus of both siRNA strands, hence forming reducible disulphide linkage with cationic polymer (185). Alternatively, another approach entails the use of a third anionic compound like hyaluronic acid and poly-γ-glutamic acid as a compatibility enhancer and also enhance the binding ability with cationic polymer to co-encapsulate

the siRNA is one of the most prevalent approaches to form stable cationic polymer/ siRNA nanoparticles. But, the inclusion of the third anionic agent increases the complexity of polyplex formation, which in turn renders the optimization of the polyplex difficult (188-190). On comparison with these reported publications, we designed and developed a new approach to improve binding and stability of PAA nanoparticle using thiol-modified siRNA based delivery system. In order to develop a stable and tight encapsulated PAA-siRNA nanoparticle, a thiohexyl group was linked at the 5'-terminus on antisense strand of siRNA to improve the binding affinity of Syk-targeted siRNA with PAAs.

The formation of compact well-condensed nanoparticle consist from the formation of loose polyplexes formed by electrostatic interactions between cationic polymers and anionic siRNA. Then, these charge interactions decrease the distances between thiol groups, leading to increased intra- and intermolecular crosslinking reaction and formation of stable and tight encapsulated complexes (191). In addition to the extracellular stability of the polymer-siRNA nanoparticle, these self-polymerized thiol crosslinked polyplexes can be degraded in the presence of reducing reagent that enhanced the cytosolic release of siRNA. The intracellular unpacking of siRNA from the polyplex is depend on glutathione reduction of the disulphide linkage. In the intracellular environment, the disulphide linkage is susceptible to cleavage by enzymatic reduction and the polyplex becomes unstable and the release of siRNA from the complex into cell cytosol is expected (192). This strategy offers an effective method for controlled delivery of siRNA, in comparison with other siRNA delivery vectors that depend on electrostatic interactions with unpredictable intracellular siRNA delivery profiles and unknown mechanism.

3.1.1 Effects of pH and salt concentration on siRNA binding

Polyamidoamines have a considerable attention in the formulation of siRNA. Because of its cationic surface charge, PAA can readily form nanoparticle with negatively charged siRNA upon simple mixing. Moreover, the biocompatibility and biodegradability of PAA make it a good siRNA delivery vehicle.

The interactions between polymer and siRNA are critical to successfully formulate polyplexes that would be functional under *in vitro* and *in vivo* conditions. Hence, the aim of this chapter was to determine optimal conditions for siRNA nanoparticle formation using two types of polymers: homopolymer (HP) and copolymer (CP2k). It includes an initial step of optimization focusing on the effect of ionic concentration and pH on siRNA binding to the polymer. Followed by preparation of both two-component (HP-siRNA) and three-component (HP-CP-siRNA) polyplexes at different polymer repeating unit to RNA nucleotide ratios (RU/Nt) and HP: CP ratios.

All these different polyplexes were characterized by agarose gel retardation assay and size measurements (DLS). Based on the results obtained from these physicochemical characterisations, suitable formulations that satisfy defined selection criteria were selected for *in vitro* testing. The selection criteria for the selection of polyplexes are: complete incorporation of siRNA into nanoparticles with no or minimal free polymer in the polyplexes to avoid excess free-polymer mediated cytotoxicity, in addition to the particle size of the polyplexes. Biological characterisation included degranulation inhibition assay and resazurin cell viability studies of PAA-siRNA nanoparticles on a rat basophilic leukemia reporter cell line, NPY-mRFP RBL-2H3. The *in vitro* performance of siRNA-polyplexes were evaluated based on Syk-gene knockdown efficiency and protein blotting using qRT-PCR and western blot, respectively.

3.2 Results

3.2.1 Effect of salt concentration on polymer-siRNA binding

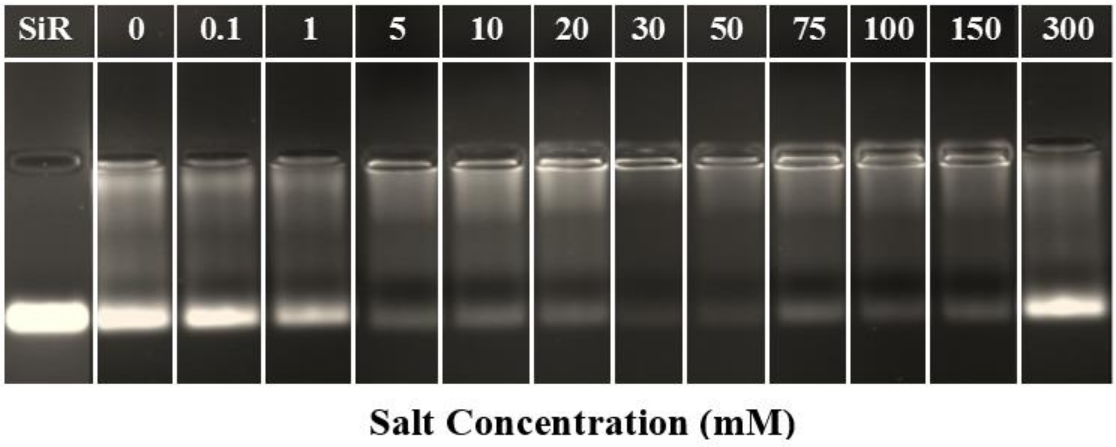

Figure 3.1 Effect of NaCl concentration on HP-siRNA interaction using agarose gel electrophoresis. All complexes were prepared using 1 µg of non-thiolated siRNA at RU/Nt ratio 2:1 and pH 7.4.

In order to study the effect of ionic strength, we evaluated the siRNA-PAA binding ability at fixed RU/Nt (2:1) ratio and increasing salt concentration from 0-300 mM, at pH 7.4. Briefly, the polymer solution was prepared at NaCl concentration from 0-300 mM and pH was set to pH 7.4. Then, an appropriate amount of salt solution wAS added to the siRNA solution and mixed with polymer. After a 30-minute incubation, the complexes containing 1 µg of non-thiolated siRNA were subjected to gel retardation assay.

Polymer-siRNA interaction prepared with ultrapure™ DEPC-treated water and at low salt concentrations (0–1 mM NaCl) produced three different bands which include unbound or excess siRNA (lower band), low molecular weight soluble complexes (intermediate band) and large molecular weight neutral complexes (fluorescence remaining in the wells). As polymer binds to siRNA it becomes partially neutralised, the electrophoretic mobility of the complexes is reduced (1 to 20 mM NaCl), until the

complexes become completely neutral and/or aggregated and remain within the loading wells (5 and 150 mM NaCl), as indicated by the reduced fluorescence in those lanes due to exclusion of ethidium bromide from siRNA (**Figure 3.1**).

A small amount of salt can improve the binding affinity between oppositely charged polymers, PAA and siRNA by reducing the electrostatic interactions, which in turn favours easier polymer chain rearrangement and adapting flexible polymer conformations for optimal binding (193-195). Maximum binding was observed between 30 – 50 mM salt concentrations. Hence, 30 mM NaCl was decided as a minimum salt concentration to be used for further complexation studies to obtain maximum and effective siRNA loading into the complexes.

3.2.2 Effect of pH on PAA-siRNA interaction

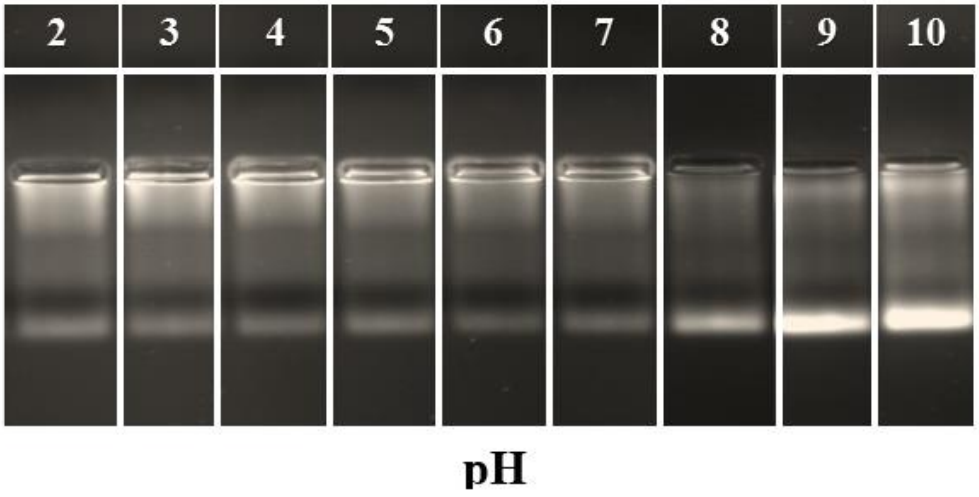

Figure 3.2 Effect of pH on HP-siRNA binding using agarose gel electrophoresis. All complexes were prepared using 1 µg of non-thiolated siRNA at RU/Nt ratio 2:1.

To find the optimal siRNA-PAA binding pH, the polymer was dissolved in 150 mM NaCl and set to required pH between 2.0 and 10.0. The complexes were formed by mixing the polymers with non-thiolated siRNA at a fixed RU/Nt ratio (2:1) and analysed by gel retardation assay. The maximum binding occurred between pH 6 – 7, **Figure 3.2**. In the crosslinked system, the free thiols for copolymer and thiolated siRNA are expected to form disulphide bridges by crosslinking with adjacent thiols or by reacting with homopolymer that contains dithiopyridine pendants. This disulphide crosslinking stabilizes the polymer-siRNA nano-complex. Both these reactions can occur between pH 4 - 8, while the optimal pH for thiol-thiol oxidation is between pH 6.5 - 8.0 and pH 4.0 - 5.0 for the thiol-dithiopyridine binding. However, the thiol-dithiopyridine binding can occur at physiologic pH, although it takes longer time than in acidic environments (196). Hence, pH 6.5 was selected for further studies as it favoured maximal siRNA binding and expected to support crosslinking system.

3.2.3 Homopolymer-siRNA and copolymer-siRNA complexes

In this section, PAA-siRNA polyplexes were analyzed by agarose gel electrophoresis in order to select suitable polyplexes for further use. Gel retardation assay provided information about the binding ability and complexation behaviour of siRNA with the polymer, in addition for detecting the presence of free polymer by using Coomassie blue staining. Subsequently, the size of the polyplexes were determined from DLS measurement.

For each experiment, polyplexes were prepared by mixing HP>10 kDa or CP2k and siRNA at different polymer to nucleotide (RU/Nt) ratios (**Figure 3.3**). For homopolymer gel image lane 1 contains naked siRNA only as a control, lanes 2 - 9 contain polyplexes with different polymer to nucleotide (RU/Nt) ratios of 0.25:1, 0.5:1, 1:1, 1.5:1, 2:1, 2.5:1, 4:1, and 5:1, respectively and lane 10 contains homopolymer or copolymer as a control prepared in 30 mM NaCl and pH 6.5. Polymer appears on the cathodic side (upper portion) of gel stained by Coomassie blue dye, while migration of siRNA can be seen on the lower portion of gel by EtBr staining visualized by UV transilluminator for the same gel. Both upper and lower images show the same gel. Appearance of fluorescence in the wells is indicative of complexation, but this fluorescence may be reduced or absent if binding of the polyplexes is tight. Therefore, disappearance of EtBr stained migrating siRNA from the gel provides evidence of complete incorporation of siRNA. Polymer staining within the well can also confirm the presence of complex formation.

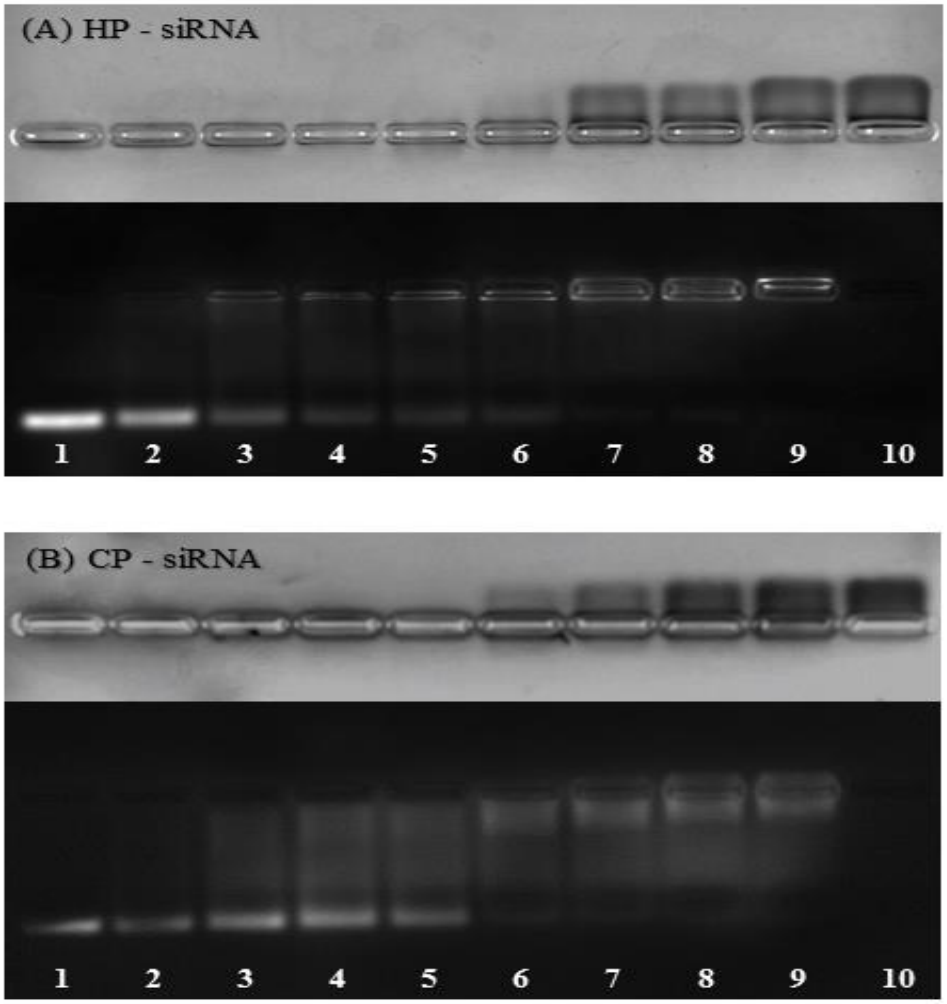

Figure 3.3 Agarose gel electrophoresis of HP-siRNA and CP2k-siRNA complexes. **(A)** HP-siRNA complexes; **(B)** CP2k-siRNA complexes. For homopolymer gel image lane 1 contains naked siRNA only as a control, lanes 2 - 9 contain polyplexes with different polymer to nucleotide (RU/Nt) ratios of 0.25:1, 0.5:1, 1:1, 1.5:1, 2:1, 2.5:1, 4:1, and 5:1, respectively and lane 10 contains homopolymer or copolymer as a control prepared in 30 mM NaCl and pH 6.5. In each image, the top panel represents Coomassie blue staining for the polymer and the bottom panel represents the fluorescence image of ethidium bromide stained gel detecting the siRNA.

PAA homopolymer (HP>10 kDa) and copolymer (CP2k) showed a gradual decrease in mobility of free siRNA on gel with increasing polymer addition with complete disappearance at RU/Nt ratio of 2.5:1 (lane 7) and 2:1 (lane 6) for HP and CP, respectively. Fluorescence began appearing in the wells at a ratio of 0.5:1 for HP onward together with anionic soluble complexes formed particularly near the loading

wells. By further increasing the amount of polymer, siRNA bands disappeared on anodic side of gel and appeared instead on the cathodic side at RU/Nt ratio of 5:1 (lane 9) for HP, forming positively charged soluble complexes with excess amount of polymer seen on the upper portion of gel. The siRNA fluorescence pattern created by CP was not similar to HP. CP2k-siRNA complexes produced a distinctive fluorescence immediately above and below the wells while this was not observed with HP. This is because the PEG helps to maintain the solubility of the complexes through the formation of non-stoichiometric polyelectrolyte complexes which can migrate intermediate distances on the gel. Moreover, the complete complexation for CP indicated that the PEG chains on CP2k did not interfere with siRNA accessing the PAA chain.

3.2.4 Complexation of HP with SH-siRNA

Homopolymer was complexed with SH-siRNA at different RU/Nt ratios, 0.5:1 to 6:1. The gel retardation assay showed complete complexation at an RU/Nt ratio of 2.5:1 (**Figure 3.4**), where as in the case of non-thiolated siRNA at RU/Nt 2.5:1, the complexation was complete but with excess or unbound free polymer (**Figure 3.3**). Charge-based interaction of homopolymer with non-thiolated siRNA showed unbound or free polymer at the optimal ratio, but in the case of the HP/SH-siRNA, free polymer started to appear at RU/Nt ratio 4:1, indicating that siRNA could be completely and effectively condensed by the homopolymer resulting in compact crosslinked nanoparticles and increase the ability of complexes to protect siRNA from nuclease degradation. Moreover, the unbound free polymer amount is reduced when using thiol-modified siRNA, hence reducing toxicity issues arising from free polymer.

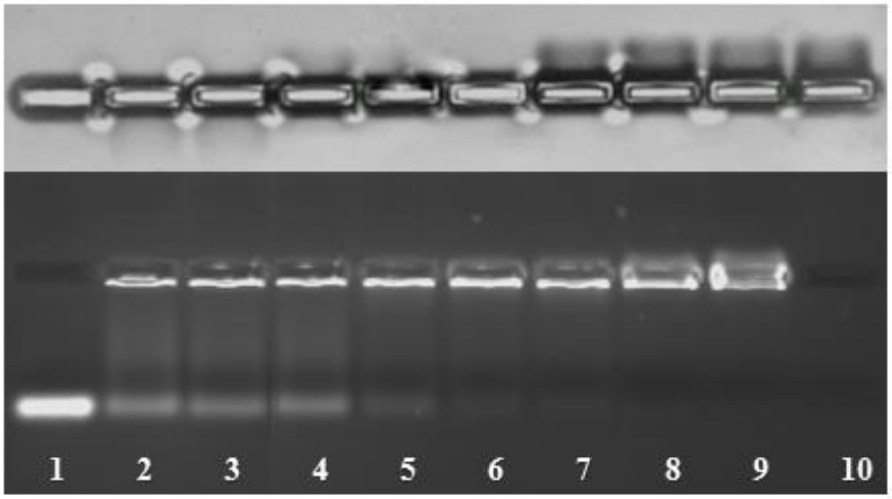

Figure 3.4 Agarose gel electrophoresis showing thiolated siRNA condensation by crosslinked homopolymer. For each image lane 1 contains naked siRNA only as a control, lane 2-9 contain polyplexes with different RU/Nt ratios of 0.5:1, 1:1, 1.5:1, 2:1, 2.5:1, 4:1, 5:1, and 6:1, respectively. Lane 10 contains only homopolymer as a control. Upper images show the migration of polymer components by staining with Brilliant blue dye, while lower images show the migration of siRNA component by EtBr staining and U.V visualization. Both upper and lower images show the same gel.

Taken together, the gel images showed clear differences in the siRNA complexation behaviour between SH-siRNA and siRNA using HP. Complete complexation (~100%) occurred around RU/Nt ratio 4:1 for HP using SH-siRNA with minimal excess free polymer than that for non-thiolated siRNA. More than 90% of the thiol-modified siRNA was bound to the HP at RU/Nt as low as 2:1 ratio.

3.2.5 Particle size of HP-siRNA and HP/SH-siRNA complexes

The particle size is of great importance in facilitating uptake and cellular interaction. Therefore, homopolymer was complexed with thiolated and non-thiolated siRNA at different RU/Nt ratios 0.5:1 to 5:1, and their size were determined from DLS measurement.

Particle sizes of HP/siRNA polyplexes prepared at low RU/Nt ratios of 0.5:1 and 1:1, were slightly larger than those formed at higher RU/Nt ratios 1.5:1 to 2.5:1. In addition, particle sizes of the HP/SH-siRNA complexes were smaller than that for non-thiolated siRNA at all RU/Nt ratios (**Figure 3.5**). The electrostatic interaction formed between oppositely charged polymers (e.g. cationic polymer and nucleic acid) will reduce particle size as the RU/Nt ratio increases. In addition, particle size will be further reduced in case of SH-siRNA because of the interaction between thiol groups (SH) of reduced siRNA and thiopyridine of homopolymer (HP) to form disulphide bonds. The electrostatic interactions between siRNA and HP decrease the distances between thiol groups, leading to increase intra- and intermolecular crosslinking reaction (191).This may explain the reduction in particle size of the HP/SH-siRNA nanoparticles in comparison with non-thiolated siRNA, possibly due to the presence of thiolated cross-linked reactions in addition to charge-based interactions.

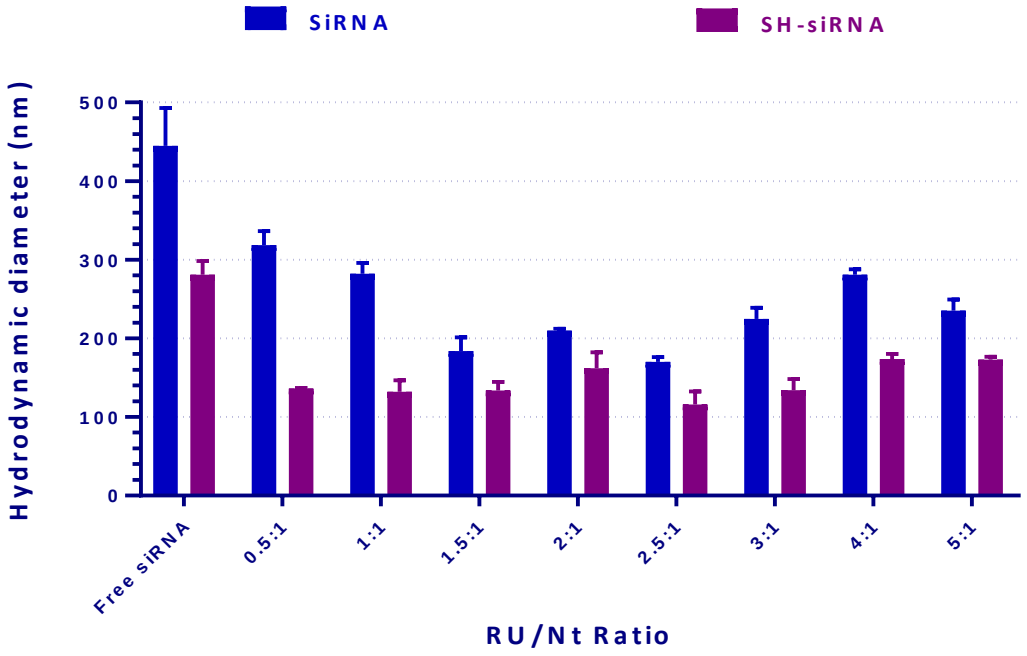

Figure 3.5 Hydrodynamic dimeter (nm) of HP/siRNA nanoparticles using dynamic light scattering (Viskotek DLS). HP/siRNA polyplexes were prepared at different polymer to nucleotide (RU/Nt) ratios including 0.5:1, 1:1, 1.5:1, 2:1, 2.5:1,

3:1, 4:1 and 5:1 respectively. All comparisons between thiolated and non thiolated siRNA were statistically significant; these results have been omitted for clarity.

3.2.6 HP-CP polyplexes using non-thiolated siRNA

These complexes are formed by mixing a homopolymer (HP) and a PEGylated copolymer (reduced CP) with a nucleic acid molecule. This kind of system permits varying the amount of PEG and thiol ratios by simply varying the HP:CP ratio.

The polymer blends were prepared by mixing homopolymer [HP] and reduced copolymer (CP2k) in different HP:CP ratios. Once the polymer blends were prepared, they were added to siRNA in appropriate concentrations to obtain different polymer PAA repeating unit to RNA nucleotide ratio (RU/Nt).

Maximum complexation was seen for HP: CP ratio of 1:1 followed by 2:1 and 3:1 (**Figure 3.6**). At all polymer blend ratios, complete complexation was observed above RU/Nt ratio of 2.5:1, the free polymer started to appear at RU/Nt ratio of 2:1. It would be desirable to have a large number of PEG chains on the surface of the nanoparticles to increase their colloidal stability while more PEG might reduce the cellular uptake because of charge neutralization. Hence, to achieve nanoparticles with a lower surface PEG density, HP: CP ratio 1:1 could be used (**Figure 3.6**). All of these complexes were selected for particle size analysis.

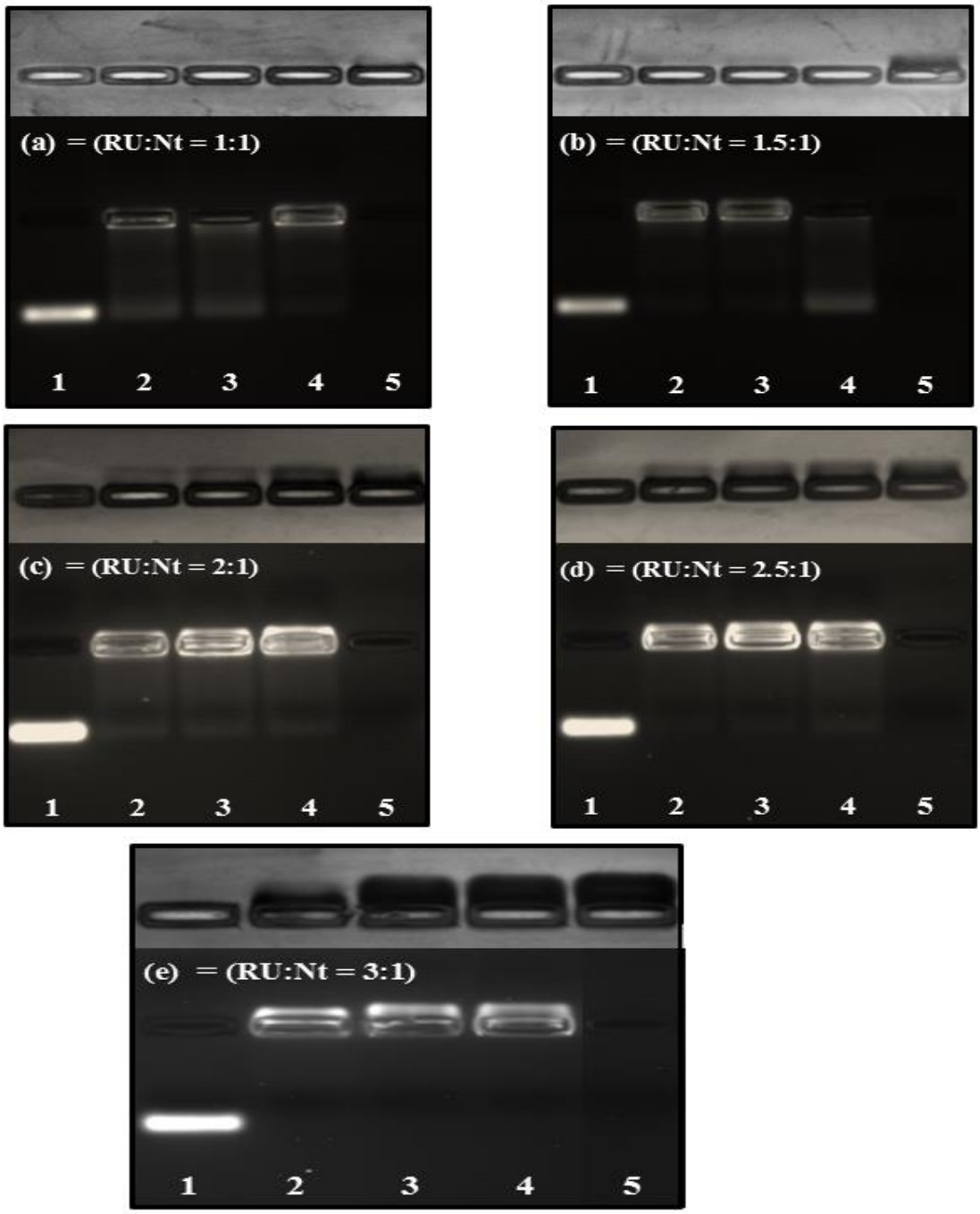

Figure 3.6 Agarose gel electrophoresis of HP:CP2k/siRNA complexes. Cross-linked siRNA polyplexes were prepared at polymer to nucleotide (RU:Nt) ratios of (a) 1:1, (b) 1.5:1, (c) 2:1 and (d) 2.5:1 and (e) 3:1 respectively. In each gel image lane 1 contains naked non-thiolated siRNA only and lane 5 contains free polymer mixture only as controls, while lane 2-4 contain polyplexes prepared with different homopolymer to copolymer (HP: CP) ratios of 1:1, 2:1 and 3:1, respectively. **Top image**: Show the migration of polymer components by Coomassie blue staining; **bottom image:** Show the migration of siRNA component by EtBr staining Agarose gel stained with ethidium bromide to represent thiolated siRNA complexation ability. Both upper and lower images show the same gel.

3.2.7 HP-CP complexes using thiol-modified siRNA

Herein, we mixed a thiol-modified siRNA with a blend of homopolymer and copolymer to produce a well-condensed compact nanoparticle with no or minimal free polymer in order to reduce cytotoxicity.

The polymer blends were prepared by mixing the homopolymer (HP) and reduced-copolymer (CP2k) in three different HP: CP ratios, 1:1, 2:1 and 3:1. Once the polymer blends were prepared, they were added to reduced-thiolated siRNA in appropriate concentrations to obtain different polymer PAA RU to RNA nucleotide ratio, 2:1 to 6:1.

The complexation studies conducted between blend of polymers (HP and CP) and thiolated siRNA revealed stronger binding activity (**Figure 3.6**) than that of non-thiolated one (**Figure 3.7**). By using the thiol-modified siRNA, as the homopolymer amount and RU/Nt ratio increased in the polyplex, the complexation with siRNA increased probably due to increase the formation of stable inter- and intramolecular disulphide bonds. The complete complexation was observed at an RU/Nt ratio of 4:1 and HP:CP ratio of 2:1 with no or minimal excess unbound polymer, where as in the case of non-thiolated siRNA the complexation was not complete and with free polymer (**Figure 3.6**).

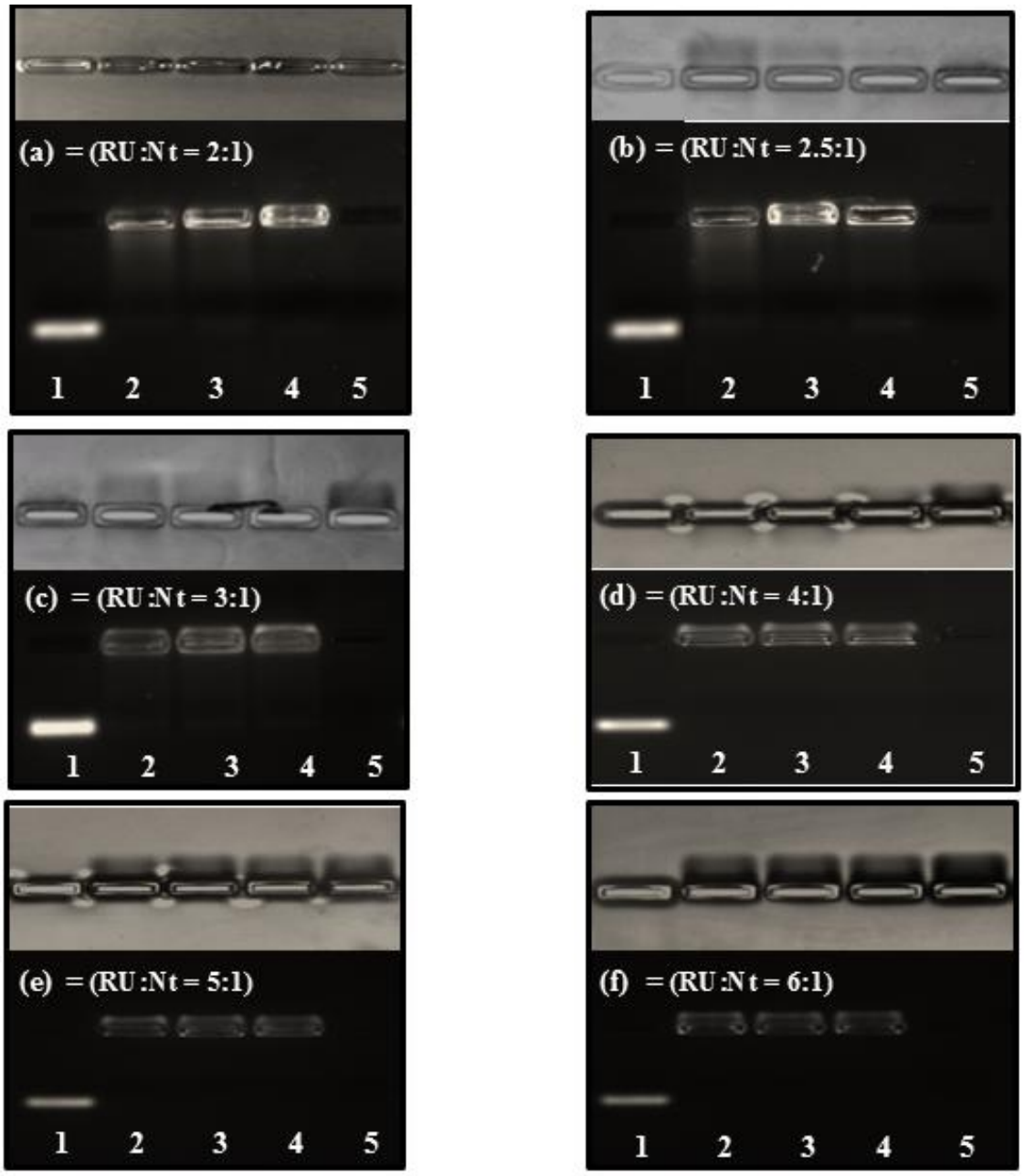

Figure 3.7 Agarose gel electrophoresis of HP:CP2k complexes using thiol-modified siRNA. Cross-linked siRNA polyplexes were prepared at different polymer to nucleotide (RU:Nt) ratios of (a) 2:1, (b) 2.5:1, (c) 3:1, (d) 4:1, (e) 5:1 and (f) 6:1, respectively. In each gel image lane 1 contains naked thiol-modified siRNA only and lane 5 contains free polymer mixture only as controls, while lane 2-4 contain polyplexes prepared with different homopolymer to copolymer (HP: CP) ratios of 1:1, 2:1 and 3:1, respectively. **Top image**: Show the migration of polymer components by coomassie blue staining; **bottom image:** Show the migration of siRNA component by EtBr staining Agarose gel stained with ethidium bromide to represent thiolated siRNA complexation ability. Both upper and lower images show the same gel.

3.2.8 Particle size of HP-CP complexes using thiolated and non-thiolated siRNA

The thiolated and non-thiolated siRNA nanoparticles were characterized for size by Viscotek DLS instrument. At all ratios, the thiol-modified siRNA nanoparticles showed mean particle size smaller than that of non-thiolated siRNA nanoparticles, indicating relatively well condensed compact polyplexes (**Figure 3.8**).

At low RU/Nt ratio of 2.5:1, slightly larger polyplexes appeared to be formed at the highest HP:CP ratio (i.e. lowest PEG amounts) than that formed at higher (RU/Nt) ratios and lowest HP:CP ratios. However, the optimal RU/Nt and HP:CP ratios of thiolated and non-thiolated siRNA complexes were found to be smaller in size than those prepared at higher HP:CP ratios.

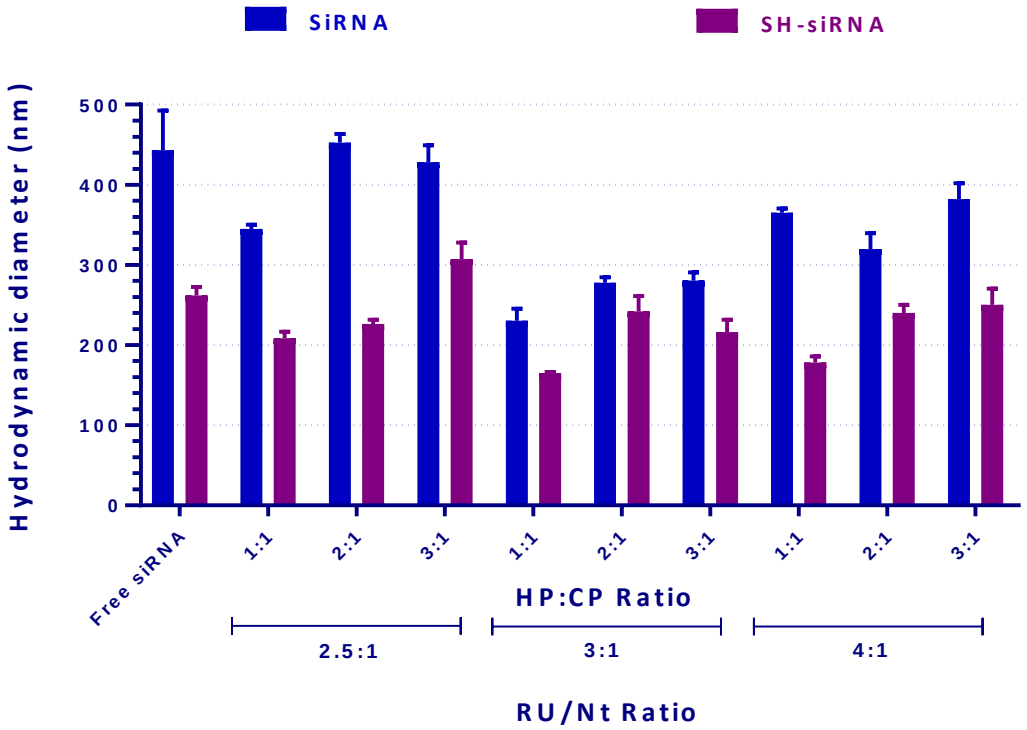

Figure 3.8 Hydrodynamic dimeter (nm) of HP:CP/siRNA nanoparticles using dynamic light scattering (Viskotek DLS). HP:CP/siRNA polyplexes were prepared at different polymer to nucleotide (RU/Nt) ratios including 2.5:1, 3:1 and 4:1 respectively and HP:CP ratios of 1:1, 2:1 and 3:1. All comparisons between thiolated and non thiolated siRNA were statistically significant; these results have been omitted for clarity.

3.3 Discussion

3.3.1 Effect of Salt and pH on PAA-siRNA interaction

The delivery of siRNA and achieving gene silencing depend on formation of polyelectrolyte complexes (PEC), which are formed by electrostatic interaction between oppositely charged polymers [e.g. cationic polymer and nucleic acid] (197, 198). The stability of this complex is strongly affected by concentration of polyelectrolytes, ratio of polyelectrolytes (stoichiometry), salt concentration (ionic strength), concentration of surface stabilizing molecules and pH (198). Mixing of high concentration polyelectrolytes which have high charge densities tends to form large aggregates. At a proper concentration, they can form nano-size complexes, but these complexes can start to aggregate in the absence of a surface stabilizing agent. However, The aggregation can be reduced when the surface is stabilized by excess charge [e.g. excess polymer] or steric hindrance [e.g. PEG] (136). Here, we investigated the effect of salt and pH on the PAA-siRNA binding activity. Our results showed that, based on gel electrophoresis and DLS, the optimal PAA-siRNA interaction when the complexes were formed in the presence of salt (30-50 mM) and pH 6-7. The presence of salt can significantly affect the complex formation, where the low salt concentration causes a drastic decrease in the aggregation, providing an additional probability, beside the difference of the polyelectrolyte concentration, to control size of the PEC (194, 199). However, it is very difficult to predict the influence of salt on complex formation, due to the complexity of the internal structure of PEC, where it depends on the specific properties of polyelectrolyte compounds. Between pH 6 and 7 the binding ability was optimal. But, outside this pH range, the PAA capability to complex with siRNA decreased. The pH of the aqueous dilution solution affects the conformational freedom of the polymer binding. At acidic pH, protonation increases

the positive charges on the polymer which repel each other and hence, the polymer assumes a more rigid conformation. While the repulsion of the charges is reduced by increasing the pH to basic condition or by addition of salt, and the polymers attain a more flexible conformation. However, the cationic groups become less positively charged at higher pH, so bind to siRNA less effectively. Under the right conditions of pH and salt, the oppositely charged polyelectrolytes can form tight complexes (136, 194, 195, 200). Usually, the presence of low concentration of sodium chloride is favoured for most PECs, because it causes a drastic reduction in the formation of aggregation by reducing the charge densities, whereas higher ionic concentration results in increased aggregation level. Higher ionic concentrations result in increased aggregation and loose complexes formated due to high shielding effect of the salt (194, 195). By using homopolymer and non-thiolated siRNA at a fixed RU/Nt ratio (2:1), the maximum complexation was obtained at pH 6.5 and 30 mM NaCl. This indicated that this low ionic concentration enabled the polymer to adapt flexible conformations to complex maximum amount of siRNA (193).

3.3.2 SiRNA binding ability with PAAs

The polyelectrolyte complexes of non-thiolated siRNA/PAAs were formed by the charge-based interaction between the phosphate and amine groups of siRNA nucleotide and PAAs, respectively. Because of low charge density and short chain length of siRNA, it is difficult to form well condensed and stable nanoparticles depending on electrostatic interaction between cationic polymer and anionic siRNA (201, 202). Therefore, these interacting particles must be stabilized further to resist aggregation, which is ensured by the tight binding of the primary molecules (194). In our study, a thiolation reaction was used to form a compact well-condensed PEC, resulting from interactions between thiol groups (SH) from the reduced copolymer

(CP) or reduced siRNA and thiopyridine from the homopolymer (HP) to form disulphide bonds.

HP-CP or HP was complexed with thiolated and non-thiolated siRNA at varying RU/Nt ratios. The complete incorporation of siRNA and SH-siRNA was observed at a RU/Nt ratio of 2.5:1 using HP in agarose gel electrophoresis. Depending on the electrostatic interaction, non-thiolated siRNA showed unbound or free excess polymer at low RU/Nt ratio (2.5:1), in contrast to the thiol-modified siRNA, where no or minimal free polymer was observed in the optimal selected ratio (2.5:1) and hence, would be expected to reduce the excess free-polymer mediated cytotoxicity. Moreover, the free polymer only started to appear at RU/Nt ratio 4:1 by using SH-siRNA, indicating that siRNA could be more completely and effectively condensed by the homopolymer at lower ratios using thiolated siRNA resulting in compact crosslinked nanoparticle and increase the ability of complexes to protect siRNA from nuclease degradation (187, 191, 203). The electrostatic interactions between siRNA and PAA decrease the distances between thiol groups, leading to increased intermolecular crosslinking reaction (191). Therefore, we can conclude that the binding ability of the thiolated-siRNA and HP became easier than non-thiolated one, possibly due to the presence of thiolated cross-linked reactions in addition to charge-based interactions.

The HP-CP polyplexes also revealed improvement in complexation ability and particle size with thiol-modified siRNA, but at higher RU/Nt (4:1) and HP: CP (2:1) ratios, indicating that SH-siRNA could be effectively and tightly condensed by the HP-CP blend after disulphide bridges formation between the free thiols of reduced CP and free thiols of reduced SH-siRNA or with dithiopyridine pendants of HP. The reaction between a free thiol and a dithiopyridine results in the formation of a disulphide bond while releasing a thiopyridine group. This disulphide crosslinking increases the intra-

and inter-molecular disulphide bond formation and stabilizes the polymer-siRNA nano-complex (74, 185). Moreover, using thiol-modified siRNA an increased number of homopolymer chains are required to produce charge neutralisation (195). These findings explain the increasing in RU/Nt and HP: CP ratios by using thiol-modified siRNA. Non-thiolated siRNA was unable to form well condensed complex without free unbound polymer even at low starting RU/Nt ratios, which further enhanced the relevance of SH-siRNA in producing compact well condensed nanoparticles.

As such, complexation and binding efficiency of siRNA with no or minimum excess free polymer was notably improved, and the size of the polyplexes was also markedly enhanced. After a successful incorporation of siRNA in polyplex, PAA could be an ideal candidate for safe intracellular siRNA delivery. Hence, the next aim of this study was to analyse whether the improvement in polyelectrolyte complex formation as assessed by physicochemical characterisation affects the biological siRNA performance.

3.4 Conclusion

The optimal siRNA-PAA complexation conditions were determined by agarose gel electrophoresis [Optimal salt: 30 mM NaCl, pH: 6.5]. These conditions were used in the preparation of polyplexes with thiolated and non-thiolated siRNA and different polymers [HP, CP2k and HP:CP] to find the optimal ratios for further use in biological investigations. HP showed efficient siRNA binding at RU/Nt ratio of 2.5:1. Moreover, HP:CP revealed complete siRNA incorporation at RU/Nt 2.5:1 and HP:CP 1:1 ratio for non-thiolated siRNA and RU/Nt 4:1 and HP:CP 2:1 ratio for thiolated siRNA evaluated by agarose gel electrophoresis. DLS measurements showed smaller siRNA nanoparticles diameter using thiol-modified siRNA, around 100-150 nm for HP and 200−250 nm for cross-linked HP:CP.

Therefore, we can conclude that the chemical binding of PAA and thiol-modified siRNA became easier than that of non-thiolated one, in association with particle size that control gene silencing activity.

Based on these facts, a cross-linked system based on bio-reducible PAA and thiolated siRNA may be a promising approach to improve intracellular silencing activity and will be discussed in ***Chapter 4.***

Chapter 4

4 Effects of siRNA polyplexes on RBL-2H3 degranulation & resazurin cell viability assay

4.1 Introduction

4.1.1 Bioreducible polyamidoamines as siRNA delivery vehicles

As reported in ***chapter 3***, HP-siRNA and HP-CP-siRNA polyplexes were prepared at different polymer repeating unit to RNA nucleotide ratios (RU/Nt) and HP to CP ratios (HP: CP). All these different polyplexes were characterized by gel-retardation assay and particle size measurements (DLS). Based on the results obtained from these physicochemical characterisations, suitable formulations that satisfy defined selection criteria were selected for *in vitro* testing. The three major selection criteria for the selection of polyplexes are, (a) Efficient siRNA incorporation; (b) No or minimal free polymer in the siRNA-polyplexes to avoid excess free-polymer mediated cytotoxicity; and (c) Size of the polyplexes. The complexes were selected based on their ability to effectively complex siRNA with no or minimal free polymer to avoid excess free-polymer mediated cytotoxicity. Additionally, the size of the complexes measured by DLS did not vary across formulations except at very low RU/Nt ratios. These properties make PAA a promising candidate for siRNA delivery which requires the above two conditions to be selected for further biological investigation. Biological characterisation included efficiency study using degranulation inhibition and toxicity study using resazurin cell viability assay in NPY-mRFP RBL-2H3 cell line.

Hence, the aim of this chapter was to biologically evaluate the optimal formulations required for siRNA nanoparticle formation using two sets of homopolymer (HP) and copolymer (CP2k) polyplexes, with thiolated and non-thiolated siRNA.

4.1.2 Thiol-mediated siRNA delivery

Several barriers still exist affecting the polymerization and transfection efficiency of the PAA-based siRNA delivery system, including the poor extracellular stability of the delivery system. In the last decade, several chemical strategies have been developed for improving the extracellular stability and intracellular delivery of siRNA (204). A promising strategy for the delivery of siRNA from the nanoparticle is the incorporation of cleavable bonds into the functionalisation to enable controlled molecular release from the nanoparticle, thus creating delivery vehicles with improved functionality in chemical and biological settings (205). Moreover, PAA required further development to increase nanoparticle stability and achieve high transfection efficiency. For these reasons, we developed and tested a nanoparticle of PAA-siRNA targeting Syk using thiolated and non-thiolated siRNA complexed with homopolymer and/or copolymer. In this study, we investigated whether the use of the thiol-modified siRNA promotes the extracellular stability of the siRNA nanoparticles while still enabling the cytosolic release of siRNA to achieve high transfection efficiency. Here, the extracellular stability of the siRNA nanoparticles should be increased due to the presence of thiols (dithiopyridine pendants) in the polymeric backbone (homopolymer) which enable the formation of intermolecular crosslinked disulphide bonds with the free thiols, present in copolymer and thiol-modified siRNA. Moreover, the free thiols are expected to form disulphide bridges by crosslinking with adjacent thiols which increased nanoparticle stability in physiological medium and this

property does not occur in the non-crosslinked systems. These thiolation reactions stabilize the polymer-siRNA nanoparticle extracellularly. In addition, the self-polymerized thiol crosslinked nanoparticles can be degraded in the presence of reducing reagent enabling the cytosolic release of siRNA. L-Cysteine and Glutathione (GSH) are the major molecules in the cell that are capable of reducing disulphide bonds. The plasma and extracellular compartments contain relatively low concentrations of reducing agents, while the intracellular compartments contain very high concentrations of glutathione (206). This highly reducing intra-cellular environment is expected to facilitate selective delivery of cargo from the disulphide crosslinked nanoparticles. Taken together, the ionic or electrostatic interaction between the negatively charged siRNA and the positively charged polymers, in addition to the chemical binding through the formation of disulphide bonds make these nanoparticles good candidates for the safe and efficient delivery of siRNA.

4.1.3 NPY-mRFP fluorescence release assay

Among various proteins of the complex signalling cascade involved in the pathway of degranulation and allergic inflammation, spleen tyrosine kinase (Syk) enzyme is the first kinase involved in the complex, branched signalling pathway resulting in the release of pro-inflammatory mediators and induction of allergic symptoms. A stably-transfected RBL-2H3 cell line expressing high levels of an NPY-mRFP fusion protein was generated in our group; this offers a simpler and faster degranulation assay than the commonly-used β-hexosaminidase assay. Neuropeptide Y (NPY) is a 36 amino acid peptide, discovered in 1982 by Tatemoto et al. (207). It is targeted to the granules, even after fusion with a fluorescent protein. Therefore, the cell lines store the NPY-mRFP fluorescent protein in the granules and release it into the medium upon sensitisation with IgE and exposure to the corresponding allergen. Secreted NPY-

mRFP can be measured by quantifying fluorescence in the supernatant. This assay is faster than the β-hexosaminidase assay, as there would be no requirement for a substrate developing step, and would be a direct reporter of degranulation.

4.1.4 Resazurin reduction assay

Resazurin assay is a reduction method used for monitoring cell proliferation and toxicity. Resazurin is a water soluble oxidized non-fluorescent blue dye that can be reduced by living cells to a red fluorescent compound resorufin by the mitochondrial enzymes. The fluorescent product is then quantified by fluorescence measurement (Excitation: 540 nm; Emission: 590 nm) (208).

4.2 Results

4.2.1 Degranulation assay (NPY-mRFP fluorescence release assay)

After overnight sensitisation mouse anti-DNP IgE, the RBL 2H3 cells were stimulated with BSA-DNP. Whereas, the other wells were left unstimulated (controls), lysed, or stimulated with calcium ionophore A23187 or BSA-DNP. After 1 hour stimulation with either BSA-DNP, calcium ionophore A23187 or lysis buffer, fluorescence was measured in supernatants (**Figure 4.1**). As can be seen in lysis, calcium ionophore A23187 and BSA-DNP stimulation of IgE-sensitised cells triggered higher NPY-mRFP release than unstimulated cells. Untreated, unsensitised cells exposed to BSA-DNP and unstimulated cells sensitised with SPE-7-derived mouse anti-DNP IgE did not release NPY-mRFP.

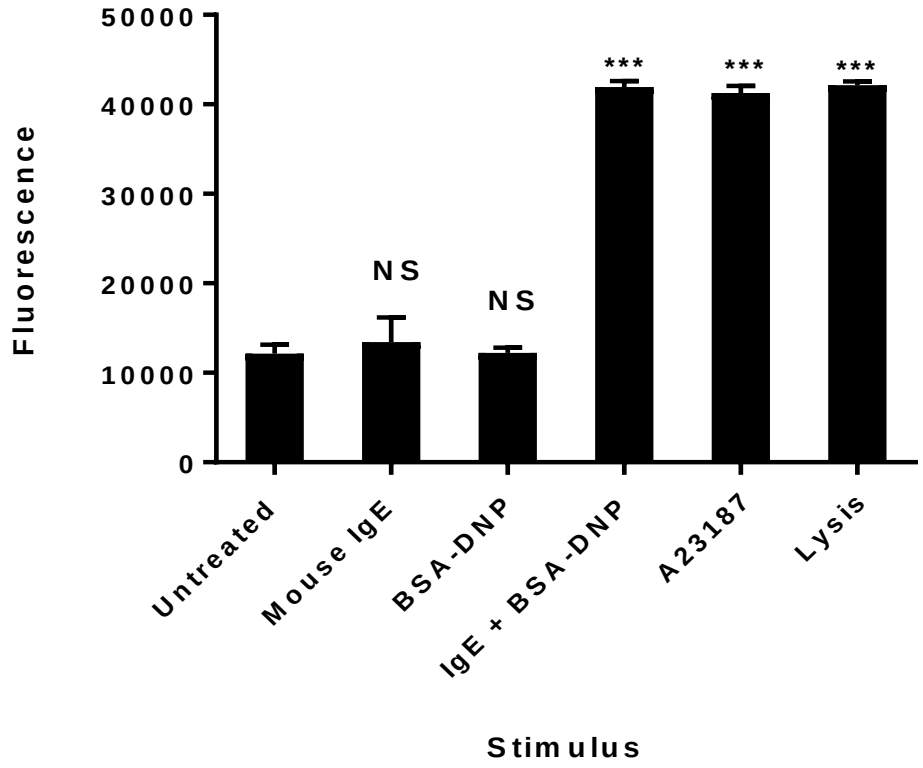

Figure 4.1 Cell stimulation triggers NPY-mRFP release. Measurement of fluorescence in medium used to stimulate cells, after transferring from the clear 12-well plate containing cells, to wells of a black 96-well plate.BSA-DNP, anti-DNP and calcium ionophore are used in 1 μg/mL concentration. All treated cells compared to unstimulated cells (control). Error bars show standard deviation. Statistical significance obtained from Dunnett's multiple comparisons test (One-way ANOVA), NS: not significant; P≤0.001 (***). N=3.

The NPY-mRFP RBL-2H3 cell line was incubated with increasing concentrations of mouse anti-DNP IgE before stimulation with 1 µg/mL BSA-DNP in order to determine the optimal concentration of IgE for cells to secrete NPY-mRFP. The NPY-mRFP RBL-2H3 cells bound to mouse anti-DNP IgE in a dose-dependent manner (**Figure 4.2**), with the highest binding at a concentration of 0.5 µg/mL. After that, the IgE binding decreased again in a dose-response curve at suboptimal IgE concentrations (100 ng/mL–10 pg/mL).

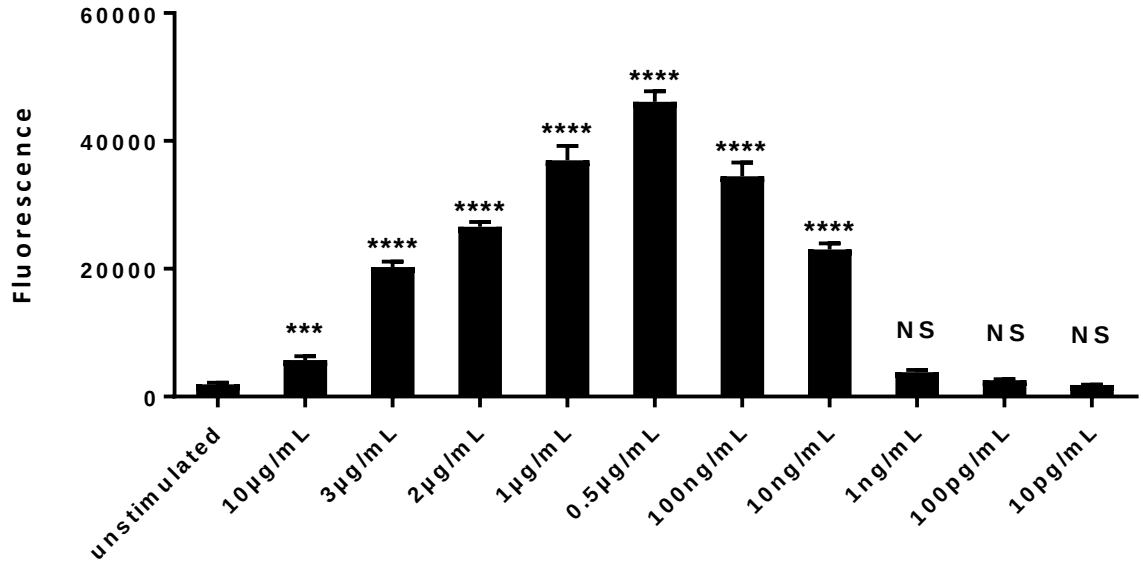

Figure 4.2 Degranulation assay using different concentrations of mouse anti-DNP IgE and stimulated with 1 µg/mL BSA-DNP. Error bars show standard deviation. Above the bars are results of Dunnett's multiple comparisons test (One-way ANOVA) against unstimulated cells, NS: not significant; P≤0.001 (***); p < 0.0001 (****). n=3.

NPY-mRFP RBL-2H3 cells were sensitised with 1 µg/mL of mouse anti-DNP IgE before stimulation with increasing concentrations of BSA-DNP in order to determine the optimal concentration for FcεRI crosslinking to secrete NPY-mRFP. Statistics showed that IgE-sensitised RBL cells bound to BSA-DNP in a dose-dependent manner (**Figure 4.3**), with the highest binding at a concentration of 1 µg/mL. After that, increased BSA-DNP concentrations caused a decrease in NPY-mRFP release at suboptimal BSA-DNP concentrations (0.5 µg/mL-1 ng/mL).

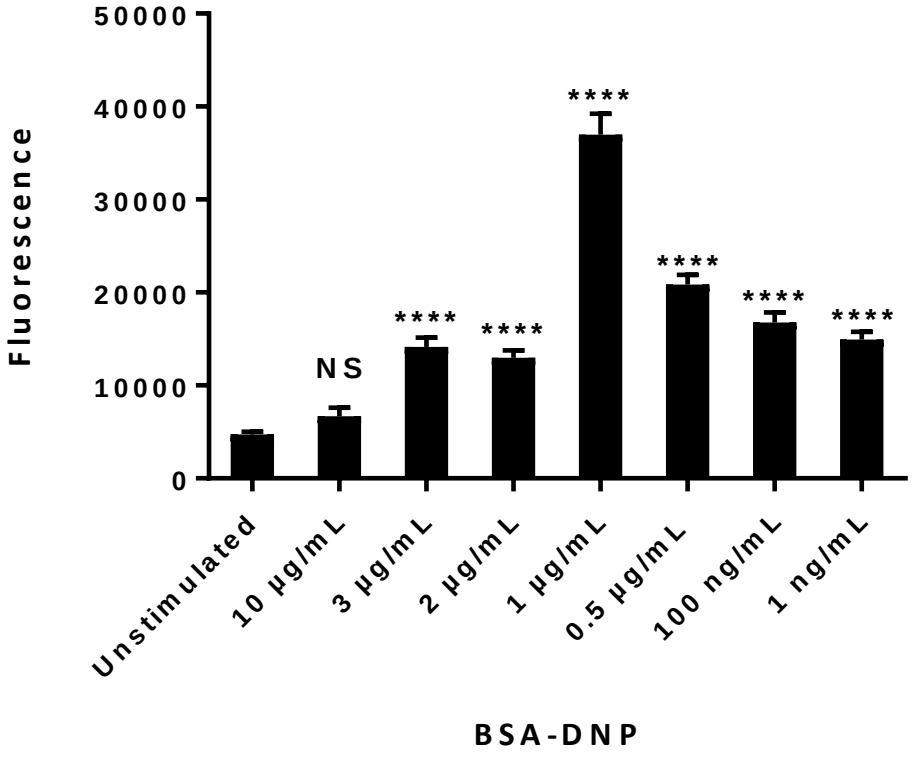

Figure 4.3 Degranulation assay using NPY-mRFP RBL-2H3 cells sensitised with 1 µg/mL mouse anti-DNP IgE and stimulated with different concentrations of BSA-DNP. Error bars show standard deviation. Above the bars are results of Dunnett's multiple comparisons test (One-way ANOVA) against unstimulated cells, NS: not significant; $p < 0.0001$ (****). n=3.

4.2.2 Determination of active siRNAs against Syk

Four different siRNA sequences (G-H) were transfected into rat RBL-2H3 cell line to identify the active siRNA against Syk gene. Degranulation inhibition and cell viability were determined using a non-PEGylated homopolymer (RU/Nt 2.5:1) and 150 nm siRNA concentration after 48 hours polyplex incubation. The four types of siRNA sequences led to a significant decrease in RBL-2H3 degranulation compared to scrambled negative control. Sequence H was the most potent siRNA in degranulation inhibition and cell viability. Meanwhile sequence I, was the least potent (**Figure 4.4**).

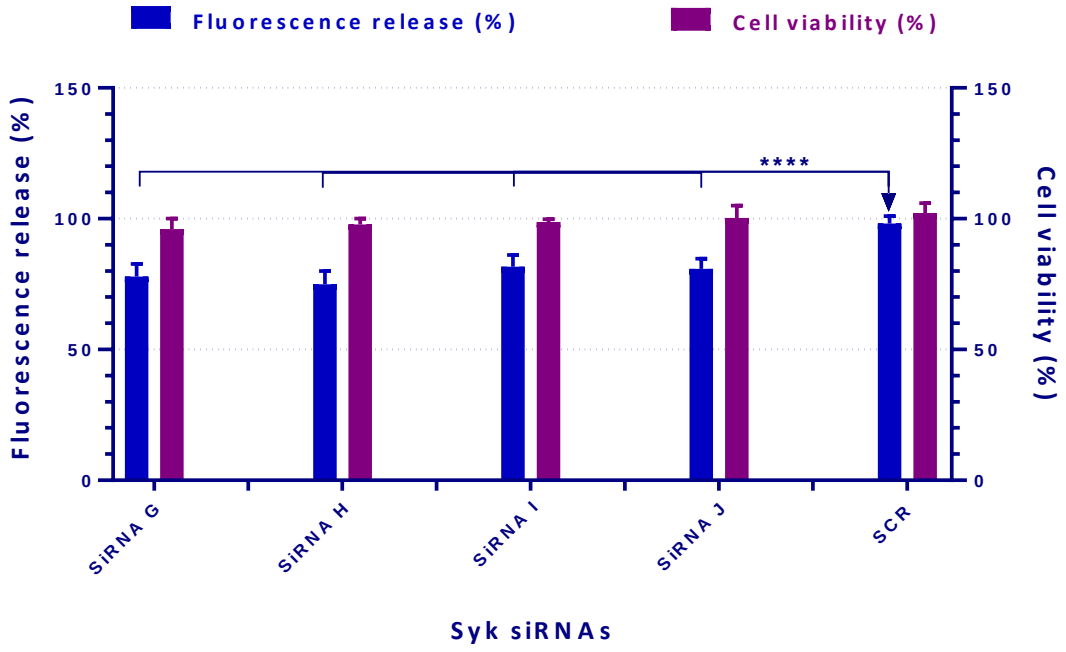

Figure 4.4 Degranulation inhibition and resazurin cell viability assay using NPY-mRFP RBL-2H3 cells sensitised with 1 µg/mL mouse anti-DNP IgE and stimulated with 1 µg/mL of BSA-DNP. Non-thiolated siRNA concentration is 150 nM corresponds to ~ 2 µg of siRNA per well (1 mL). homopolymer (2.5:1 RU/Nt ratio) was used in this this experiment. Error bars show standard deviation. Above the bars are results of Tukey's multiple comparisons test (Two-way ANOVA), $p < 0.0001$ (****), but cell viability statistics have been omitted for clarity because they were not statistically significant. n=3. Syk-targeted and scrambled siRNA treated cells for degranulation inhibition comparisons were also significant in 250 and 300 nM siRNA concentration; these results have been omitted for clarity.

4.2.3 Optimization of siRNA concentration

Homopolymer-siRNA polyplexes were prepared at RU/Nt ratio of 2.5:1 and different concentrations of non-thiolated siRNA H to evaluate the efficiency of increasing concentration of siRNA. **Figure 4.5** showed an increase in downregulation for fluorescence release by increasing the concentration of siRNA from 50 nM to 300nM. The HP-siRNA nanoparticles (300 nM) were able to significantly reduce the release of NPY-mRFP protein, whereas none of the scrambled siRNA treatments produced any inhibition, hence confirming the fact that non-targeted siRNA delivery does not cause functional effect on cells. However, there was a reduction in cell viability treated with high concentration of SiRNA H. Therefore, 300 nM siRNA used for further experiments.

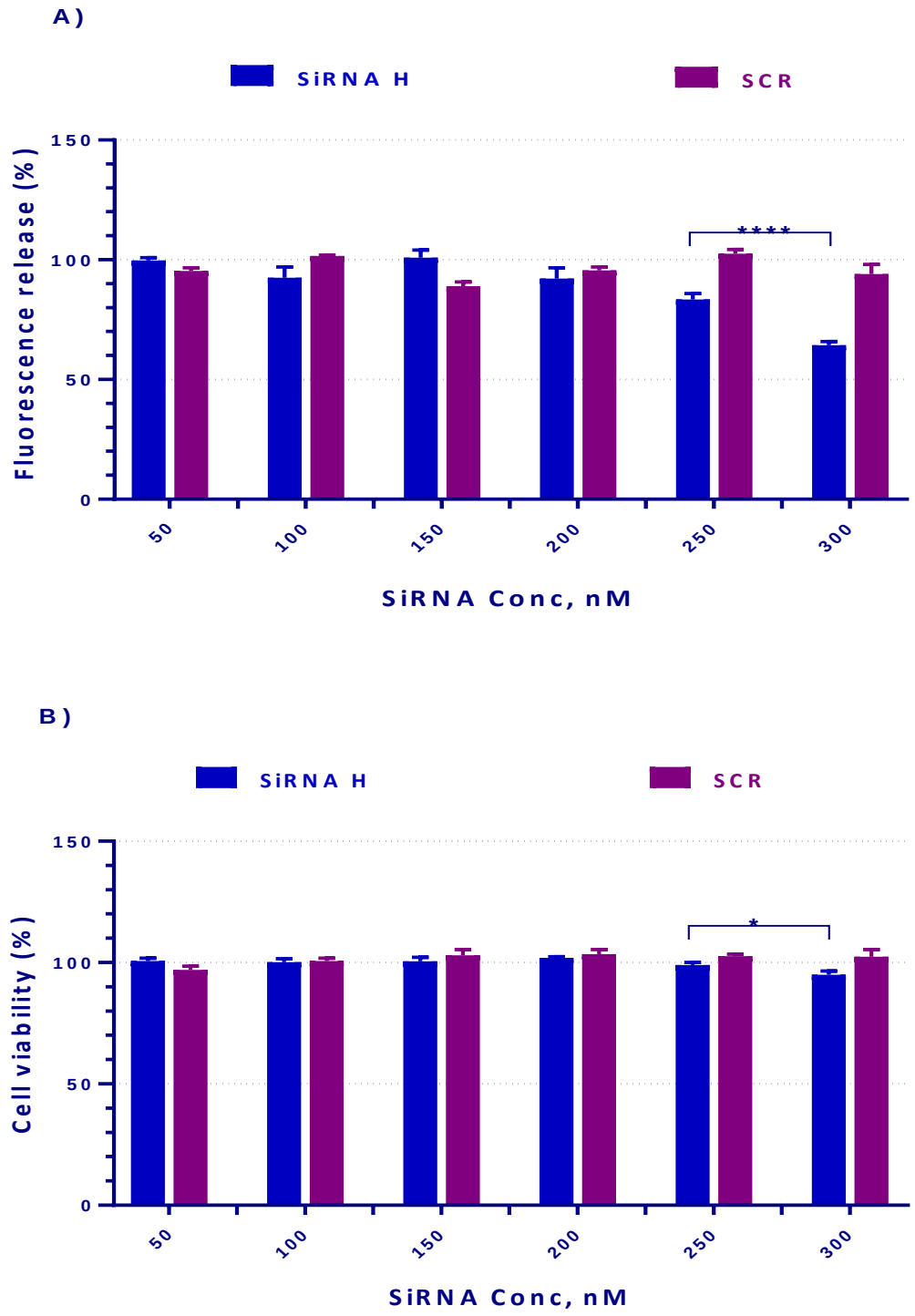

Figure 4.5 (A) Degranulation inhibition and (B) Resazurin cell viability assay of HP-siRNA polyplexes using NPY-mRFP RBL-2H3 cells sensitised with 1 µg/mL mouse anti-DNP IgE and stimulated with 1 µg/mL of BSA-DNP. Polyplexes were prepared using HP>10 kDa at RU/Nt ratio of 2.5:1 and non-thiolated siRNA H or scrambled control at 50, 100, 150, 200, 250 and 300 nM concentrations. Error bars show standard deviation. Above the bars are results of Tukey's multiple comparisons test (Two-way ANOVA), $p = 0.0218$ (*), $p < 0.0001$ (****). n=3.

4.2.4 Effect of siRNA on NPY-mRFP RBL-2H3 cells degranulation and viability using two components system

Based on the results obtained from the physicochemical characterisations, suitable formulations that satisfy defined selection criteria were selected for *in vitro* testing. The three major selection criteria for the selection of polyplexes are, (a) Efficient siRNA incorporation; (b) No or minimal free polymer in the siRNA-polyplexes to avoid excess free-polymer mediated cytotoxicity; and (c) Size of the polyplexes. Biological characterisation included degranulation inhibition and toxicity studies of free polymer on NPY-mRFP RBL-2H3 cell line.

The objective of these experiments was to initially examine the effect of thiolated and non-thiolated siRNA using a non-PEGylated homopolymer (RU/Nt 2.5:1) on RBL-2H3 degranulation, in which RBL-2H3 cells were sensitised with mouse IgE and stimulated with BSA-DNP. Degranulation of RBL-2H3 was determined by measuring the release of the granule protein NPY-mRFP with different exposure times. As shown in

Figure 4.6, BSA-DNP stimulated RBL-2H3 cells treated with non-thiolated siRNA H caused a significant down regulation in degranulation after 48 hours of polyplex exposure compared to stimulated RBL-2H3 cells treated with non-thiolated siRNA H at 24 and 72 hours post-transfection with nanoparticles. None of the scrambled non-thiolated siRNA-treatments produced any knock-down, hence confirming the fact that non-targeted siRNA delivery does not affect the Syk mRNA expression levels and thus, does not cause any functional effect on cells. These results suggest that the optimal degranulation can be significantly down regulated when RBL-2H3 cells are treated with Syk-targeted siRNA.

The same experiments were then conducted to study the effect of thiol-modified siRNA on degranulation inhibition and resazurin cell viability assay, **Figure 4.7.** The results showed that the thiolated siRNA nanoparticles significantly down regulate degranulation at 24, 48 and 72 hours compared with the non-thiolated polyplexes that

reduce degranulation at only 48 hours incubation. However, although stronger binding ability and smaller particle size have been observed with thiolated siRNA, a similar degranulation inhibition (~40 %) effect was seen in comparison with the non-thiolated siRNA.

Moreover, there was a general trend for significant increase in cell proliferation with thiolated and non-thiolated siRNA after 24 hours nanoparticles exposure. However, the use of thiolated siRNA does not have more effect on cell proliferation compared with the non-thiolated siRNA as expected.

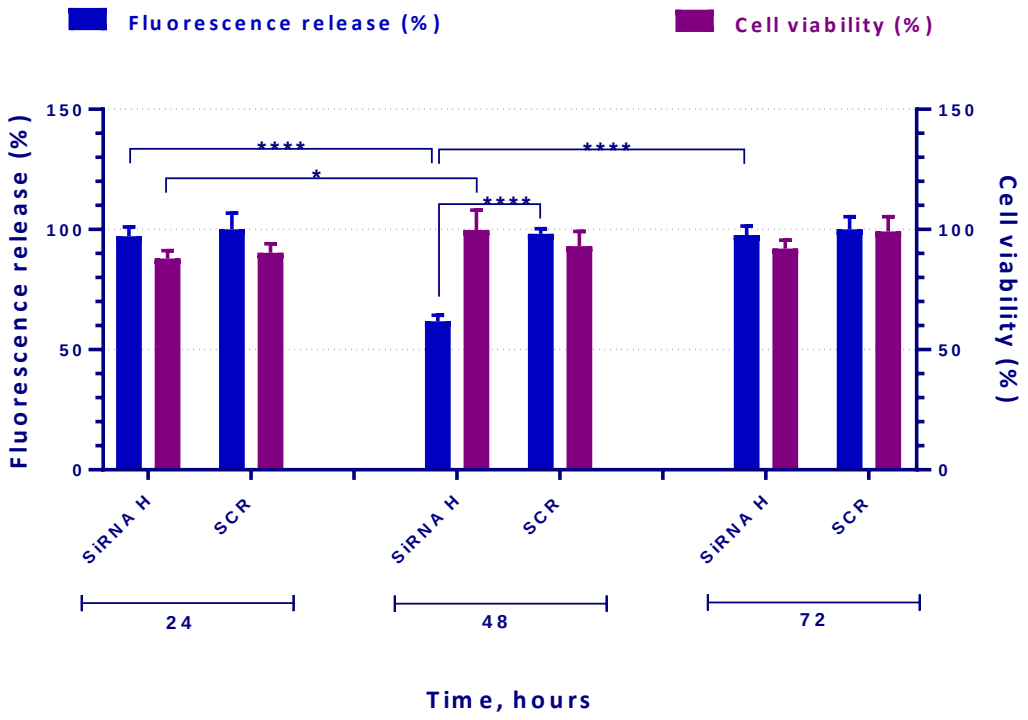

Figure 4.6 Degranulation inhibition and resazurin cell viability assay of non-thiolated siRNA polyplexes. NPY-mRFP RBL-2H3 cells were sensitised with 0.5 µg/mL mouse anti-DNP IgE and stimulated with 1 µg/mL of BSA-DNP. The complexes were prepared with non-thiolated siRNA (300 nM) corresponding to ~ 4 µg of siRNA per well (1 mL) and homopolymer at a constant RU/Nt ratio 2.5:1. The data are representative of 3 separate experiments, in which each condition was analysed in quadruplicate per experiment. Error bars show standard deviation. Above the bars are results of Tukey's multiple comparisons test (Two-way ANOVA), $p = 0.02$ (*); $p < 0.0001$ (****).

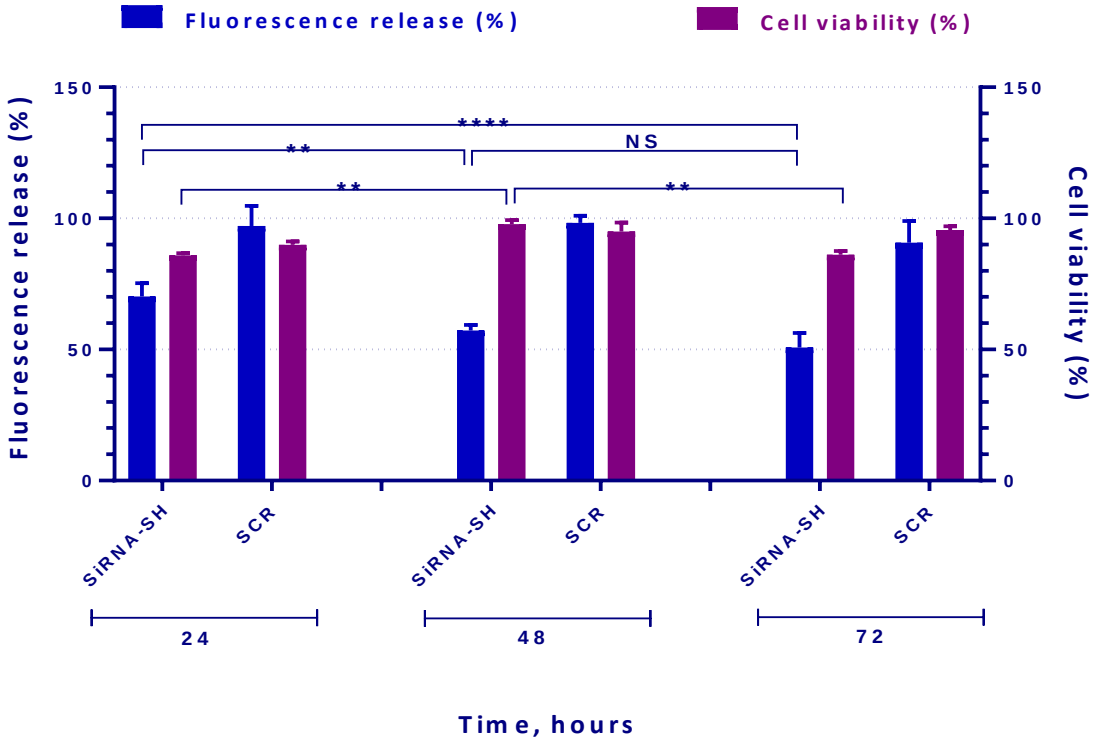

Figure 4.7 Degranulation inhibition and resazurin cell viability assay of thiol-modified siRNA polyplexes. NPY-mRFP RBL-2H3 cells were sensitised with 0.5 µg/mL mouse anti-DNP IgE and stimulated with 1 µg/mL of BSA-DNP. The complexes were prepared with thiol-modified siRNA (300 nM) corresponding to ~ 4 µg of siRNA per well (1 mL) and homopolymer at a constant RU/Nt ratio 2.5:1. The data are representative of 3 separate experiments, in which each condition was analysed in quadruplicate per experiment. Error bars show standard deviation. Above the bars are results of Tukey's multiple comparisons test (Two-way ANOVA), NS: not significant; $p < 0.01$ (**); $p < 0.0001$ (****). All syk-targeted and scrambled siRNA treated cells for degranulation inhibition comparisons were significant; these results have been omitted for clarity.

4.2.5 Effect of siRNA on NPY-mRFP RBL-2H3 cells degranulation and viability using three components system

Cross-linked polymeric systems were then investigated on the same cell line. The rationale for cross linking of the polymer constituents into nanoparticles is to improve the physicochemical and biological properties by increasing nucleic acid loading and *in vivo* stability of nanoparticles, reduce toxicity by increasing biodegradability and to control the release of cargo in response to specific stimuli. Hence, the optimized nanoparticle [RU/Nt (2.5:1) HP: CP (1:1)] was biologically tested for its ability to down regulate degranulation by measuring fluorescence in supernatants.

The results showed that the non-thiolated siRNA nanoparticles (300 nM) were able to downregulate the release of NPY-mRFP fluorescent protein (~15%) after 48 hours nanoparticle exposure.

None of the scrambled siRNA-PAA nanoparticles treatments produced any knock-down, hence confirming the fact that scrambled siRNA delivery does not cause any functional effect on cells due to lack the probability of cross-hybridization which cause non-specific silencing response (209). Moreover, treatment with active and negative control siRNA did not showed noticeable toxicity. None of the active siRNA complexes tested showed significant difference in reducing cell viability between 24 and 72 hours after siRNA transfection (**Figure 4.8**).

The optimal RU/Nt (4:1) HP: CP (2:1) ratio was tested with thiol-modified siRNA using the same assays. Treatment with thiolated complexes not only significantly reduced degranulation (~35%) but also induced cell proliferation after 48 hours polyplex exposure as expected (**Figure 4.9**). Whereas treatment with scrambled thiol-modified siRNA did not reduce NPY-mRFP release, and showed noticeable over proliferation (~100% viability).

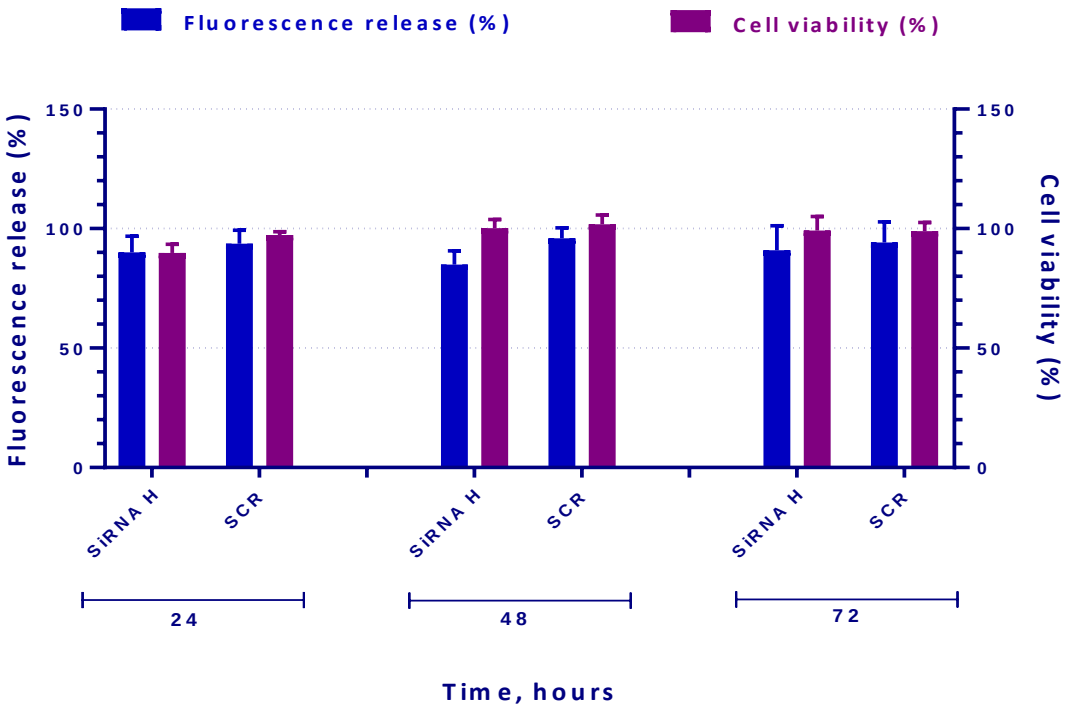

Figure 4.8 Degranulation inhibition and resazurin cell viability assay of non-thiolated siRNA polyplexes. NPY-mRFP RBL-2H3 cells were sensitised with 0.5 µg/mL mouse anti-DNP IgE and stimulated with 1 µg/mL of BSA-DNP. The complexes were prepared with non-thiolated siRNA (300 nM) corresponds to ~ 4 µg of siRNA per well (1 mL) and cross linked polymeric system (HP-CP)at a fixed RU/Nt (2.5:1) HP: CP (1:1). Error bars show standard deviation. Above the bars are results of Tukey's multiple comparisons test (Two-way ANOVA). The data are representative of 3 separate experiments, in which each condition was analysed in quadruplicate per experiment. All compared siRNAs were not statistically significant; these results have been omitted from the graph for clarity.

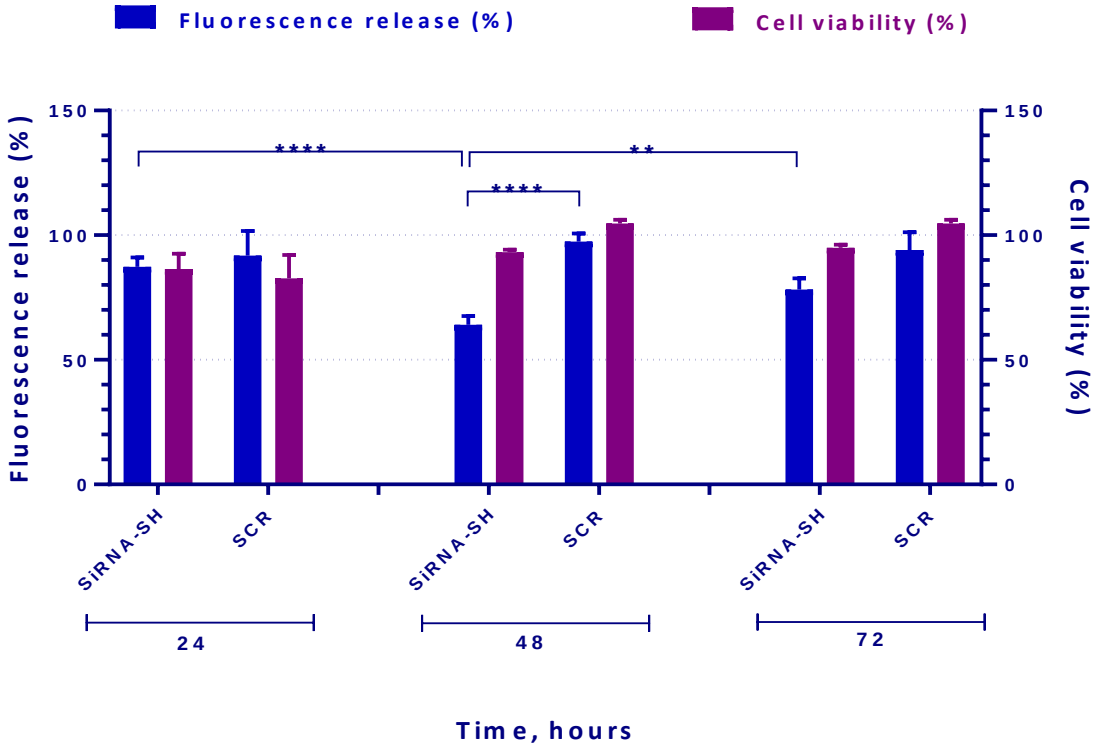

Figure 4.9 Degranulation inhibition and resazurin cell viability assay of thiol-modified siRNA polyplexes. NPY-mRFP RBL-2H3 cells were sensitised with 0.5 µg/mL mouse anti-DNP IgE and stimulated with 1 µg/mL of BSA-DNP. The complexes were prepared with non-thiolated siRNA (300 nM) corresponding to ~ 4 µg of siRNA per well (1 mL) and cross linked polymeric system (HP-CP)at a fixed RU/Nt (2.5:1) HP: CP (1:1). Error bars show standard deviation. Above the bars are results of Tukey's multiple comparisons test (Two-way ANOVA), $p < 0.01$ (**); $p < 0.0001$ (****). The data are representative of 3 separate experiments, in which each condition was analysed in quadruplicate per experiment.

4.2.6 Degranulation inhibition and cell viability of siRNA polyplexes using bio-reducible PAA nanoparticles and commercial transfection reagent

The optimal results for degranulation inhibition of homopolymer and crosslinked polyplexes loaded with thiol-modified siRNA were compared with the degranulation inhibition of Lipofectamine 2000 tested on RBL-2H3 cells (**Figure 4.10**). All the complexes were treated at 300 nM siRNA concentration and showed significant inhibition efficiency (~30-40%) of which Lipofectamine 2000 reagent had similar effect to homopolymer (~40% degranulation inhibition). Among the polyplexes tested, Lipofectamine 2000 polyplex showed higher cytotoxicity than homopolymer and crosslinked polyplexes. However, none of the complexes tested show statistically significant difference in degranulation inhibition between Lipofectamine 2000 and PAA-polyplexes treatments, while the toxicity observed was minimal with homopolymer and crosslinked polymers.

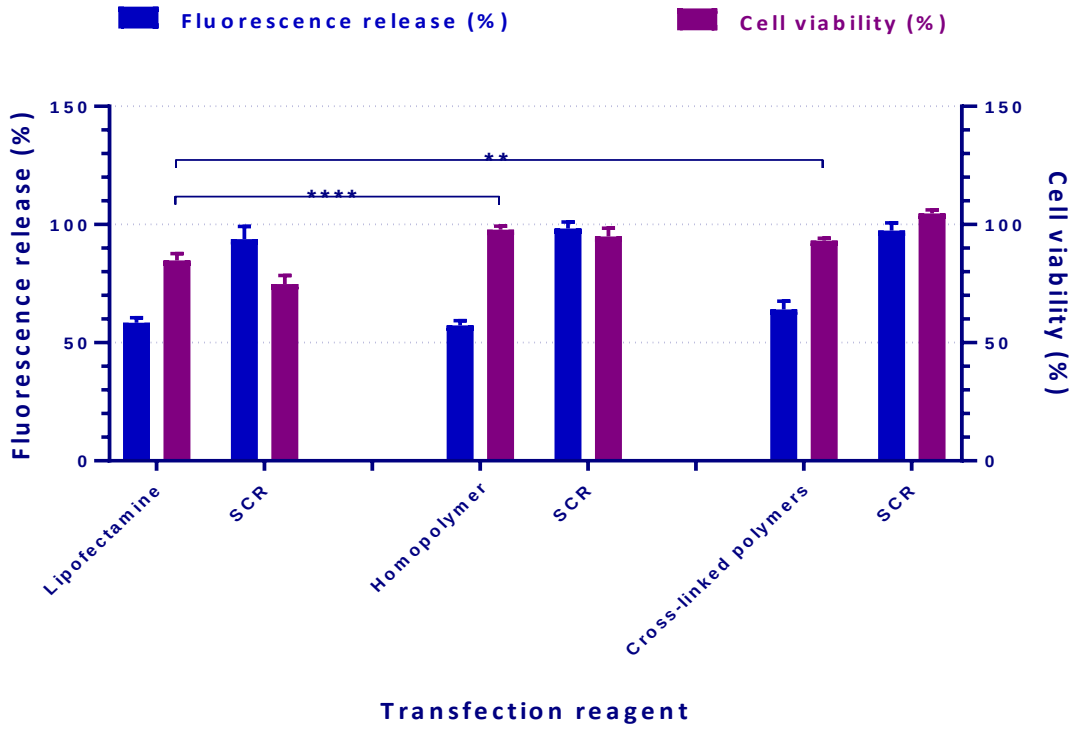

Figure 4.10 Degranulation inhibition and resazurin cell viability assay using homopolymer, cross-linked polymers and Lipofectamine 2000. After 48 hours of polyplex exposure, the NPY-mRFP fluorescence proteins were measured in supernatant. NPY-mRFP RBL-2H3 cells were sensitised with 0.5 µg/mL mouse anti-DNP IgE and stimulated with 1 µg/mL of BSA-DNP. The complexes were prepared with thiol-modified siRNA (300 nM) corresponding to ~4 µg of siRNA per well (1 mL). Error bars show standard deviation. The data are representative of 3 separate experiments, in which each condition was analysed in quadruplicate per experiment. Above the bars are results of Tukey's multiple comparisons test (Two-way ANOVA), $p < 0.01$ (**); $p < 0.0001$ (****).

4.3 Discussion

4.3.1 NPY-mRFP Fluorescence Release Assay

RBL-2H3 cell line was used as a model to study degranulation and potential intervention in allergy (210, 211). In basophils, the activation of Syk enzyme and the subsequent release of pro-inflammatory mediators is a crucial process resulting in degranulation and the release of allergic mediators (212). Degranulation results in the release of pro-inflammatory mediators (histamine, cytokines, proteases and leukotrienes) and NPY- mRFP fluorescent protein (in our study) from basophils after a stimulus that can be IgE/antigen (IgE-dependent) or calcium ionophore A23187 (IgE-independent) (213). These preformed granular contents can be measured using established assays like histamine and beta-hexosaminidase (175). Our group has generated an RBL cell line which is stably transfected with a Neuropeptide Y-red fluorescent protein fusion construct (NPY-mRFP) (176). These cell lines store the NPY- mRFP fluorescent protein in the granules and release it into the medium upon degranulation.

To activate degranulation, RBL-2H3 cells were stimulated with two different activating stimuli for degranulation (IgE/antigen and calcium ionophore) (214). Calcium ionophore (A23187) causes an increase in intracellular calcium and simulates steps that directly precede degranulation (215).

The results of degranulation assay were as expected, wells containing untreated cells, cells sensitised with mouse anti-DNP IgE and cells stimulated with BSA-DNP contained lower levels of fluorescence than wells containing cells treated with IgE and BSA-DNP, cells treated with calcium ionophore (A23187) and lysed cells. A study by Kitaura et al. found that SPE-7-derived IgE is “highly cytokinergic”: capable of aggregating FcεRI and triggering preformed mediator release without allergen

stimulation (31), but we found that SPE-7-derived mouse anti-DNP IgE did not efficiently increase NPY-mRFP release by the cells.

4.3.2 Selection of the active siRNA sequences

Basophils play an important role in the initiation of allergic inflammation. To understand the function played by Syk in IgE-mediated basophil stimulation, siRNA molecules that target silencing rat Syk gene were transfected in a rat basophilic leukemia cell line, NPY-mRFP RBL-2H3. In this work, four different siRNA molecules targeting the Syk gene were selected and investigated for their ability to inhibit Syk in RBL-2H3 cell line. The results showed that all the active Syk-targeted siRNAs G-J had increased degranulation inhibition efficiencies in comparison with scrambled siRNA. Interestingly, 2 out of the 4 siRNA molecules had similar effects on inhibition. SiRNA G and H were the most potent sequences in down regulating NPY- mRFP fluorescent protein release.

There are two key parameters important for siRNA activity, thermodynamic stability and accessibility of the mRNA target site. The thermodynamic stability profile of the duplex could determine the strand selected by RISC so that the strand with the lower 5′ end thermodynamic stability is more likely to compete and be selected by RISC. Two independent reports proposed that a major factor in siRNA activity was the thermodynamic stability profile of the duplex (216, 217). They suggested that the functionally active siRNAs presented with a low internal stability at the 5′ end of the antisense (guide) strand in comparison with the non-functionally active siRNA duplexes. Furthermore, the tight secondary structure of the targeted region of mRNA might prevent the accessibility of binding site in siRNA, subsequently inhibiting silencing efficiency (218). Moreover, the presence of freely accessible terminal nucleotides on the antisense strand of siRNA duplexes were found to be relevant in

the efficiency of siRNA silencing (219).The determination of these sequences and their desirable *in vitro* profile, increases the possibility for using these sequences in further biological investigation.

4.3.3 Degranulation inhibition and cell viability

Previous reports demonstrate that Syk plays a key role in the activation of immune system, where the stimulation of Syk enzyme is the first detectable signalling response in degranulation and release of pro-inflammatory mediators (220). This has led to the development of therapeutic agent targeting Syk gene as another form of anti-allergic therapy (221, 222). In this study, we investigated the degranulation inhibition ability of different sequences of Syk-targeted siRNAs in NPY-mRFP RBL-2H3 cell line. Then, the most potent siRNA sequence in degranulation inhibition with low toxicity was used for further experiments. The main aim of this chapter was to investigate the potential of thiol crosslinked PAA-siRNA nanoparticles, using thiolated and non-thiolated siRNA molecules, in inhibition of degranulation and their effect on cell viability in the same sample. In this chapter, it was decided to combine both activity and toxicity elements together to afford more logical presentation and discussion of results. This is particularly pertinent because the reduction in NPY-mRFP fluorescence release after siRNA nanoparticle treatment indicates either successful RNAi delivery and associated degranulation inhibition or cytotoxicity of the PAA-siRNA nanoparticles or a combination of both these effects.

For the siRNA delivery system to be functional, it should be able to reduce the release of fluorescence in supernatant. Hence, the optimized nanoparticle (HP: CP2k and HP) using either thiolated or non-thiolated siRNA, was tested for its ability to inhibit the degranulation on NPY-mRFP RBL-2H3 cells in order to study the functional gene-silencing activity.

Based on the results obtained from physicochemical characterisation, non-thiolated siRNA H was prepared with homopolymer at the optimal RU/Nt ratio (2.5: 1) in order to avoid toxicity issues that could arise from free polymer present in the mixture. As there was no significant toxicity observed in this experiment for HP-siRNA complexes with increasing concentrations of siRNA, this amount was increased further to 300 nM, **Figure 4.5**. This indicated that PAA-siRNA formulation was able to act functionally at higher concentrations. Hence, the inhibition of Syk was specific and strongly depended on the concentration of the selected sequence Syk target siRNA.

In this section, we have a close comparison between cross-linked polymer and non-PEGylated homopolymer of the same cationic polymer using non-thiolated siRNA, in terms of degranulation inhibition and cell viability. Comparison of degranulation inhibition by homopolymer nanoparticles with the cross-linked polymer, showed that higher degranulation inhibition (~40%) was achieved at 48 hours incubation with 2.5:1 ratio of HP-siRNA polyplex, whereas none of the scrambled siRNA treatments produced any significant inhibition. However, the better silencing performance for homopolymer is likely to be due to its positive surface charge, which act as a surface stabilizer for nanoparticles to avoid aggregation and also will tend to bind to negatively charged cell surface and enhance endocytosis of polyplexes. Hence, confirming the significance of producing discrete well-condensed nanoparticles to present the best transfection efficiency. Additionally, the introduction of PEG into polymeric structure resulted in shielding of the charges and prevent of aggregation due to its charge neutralization. However, PEG can adversely affect the cellular uptake due to its steric effect that prevent the association of the nanoparticles with cell membranes (116, 223). Unmodified polymers may cause potential membrane damage and have already been reported to cause apoptosis in different human cell lines (224). Changes in degree of

branching and chemical structure or the introduction of hydrophilic moieties (e.g. PEG) into a polymer can reduce the cytotoxicity to an acceptable level (225, 226). Introduction of PEG into polymeric structure resulted in shielding of the charges on the polymer backbone due to the steric effect of PEG chains. PEG reduces the association of the complexes with cell membranes and hence a reduced cytotoxicity in comparison to their non-PEGylated counterparts (227). However, unexpected nonsignificant differences in cytotoxicity were observed between HP and cross-linked polyplexes, where none of the PAA complexes tested showed significant difference in cell viability. This may be related to the basic structures of the three monomers in polymer units, DMEDA, cystamine and MBA. Additionally, it has been shown that cellular toxicity strongly depends on the molecular weight and increased number of cationic charges on the interacting polycations with the anionic cell membrane (90, 228, 229).

4.3.4 Thiol-mediated delivery

Because of the rigid rod shape, low charge density and small size of siRNA in comparison to plasmid DNA, stability of polyplexes formed by electrostatic interaction with cationic polymers is considered to be a major hurdle for *in vivo* applications (140, 181). Additionally, the linear structure of cationic polypeptides may further weaken the binding with nucleic acid. This work describes a new approach to improve the extracellular stability of polyplexes and intracellular delivery of siRNA. Mok et al. reported that stable and condensed siRNA polyplexes with linear polyethyleneimine (LPEI) could be successfully prepared using a disulphide linkage at the 5′ end of both siRNA strands. Polymerised-siRNA nanoparticles showed excellent cellular uptake and efficiently inhibit TNF-α gene expression (187, 191). Another study also include using of disulphide linkage in binding siRNA to the

delivery agent can effectively knockdown endogenous gene in mouse hepatocytes (50).

In comparison with these reported studies, we developed and tested a formulation of polyplexes prepared from thiolated SiRNA complexed with homopolymer in order to increase its extracellular stability and intracellular delivery of siRNA. Thiols from the siRNA would form disulphide bridges with other active thiols (thio-pyridine moieties) from the homopolymer which are in close proximity. This new crosslinking might result in compaction of the nano-structure, which in turn might promote further crosslinking, compaction and stabilization.

NPY-mRFP fluorescence release was reduced up to ~50% after 72 hours of incubation with HP-thiolated siRNA nanoparticles (**Figure 4.7**) showing a greater effect than either polyplexes with non-thiolated, HP/siRNA H (~40%) (

Figure 4.6) or Lipofectamine 2000 (~40%) (**Figure 4.10**). This strongly suggests that the use of thiolated siRNA polyplexes is important for effectively downregulating the fluorescence release. An increase in inhibition effect of fluorescence release was also observed by increasing the incubation time of SH-siRNA from ~30% at 24 hours to ~50% at 72 hours (**Figure 4.7**), while none of the scrambled siRNA treatments produced any inhibition, hence confirming the fact that delivery of non-targeted siRNA does not cause a functional effect on cells.

The commercially available Lipofectamine 2000 complexed to thiol-modified siRNA was analysed for degranulation inhibition and cytotoxicity effects. That analysis showed that even ~40% degranulation inhibition, the cell viability was observed around 80% (**Figure 4.10**). A possible explanation for this toxicity may be that cationic lipids possess high cationic charge density which can cause immediate and severe membrane disruption resulting in cellular cytotoxicity (230). This result suggested that the reduction in fluorescence release with Lipofectamine 2000 polyplex

is occur partially due to a decrease in cells number and not from a gene silencing effect caused by siRNA.

Analysis of the degranulation inhibition revealed low efficiency with cross-linked complex using non-thiolated siRNA but this efficacy is greatly improved from 15% to 35% by using thiol-modified siRNA. Additionally, none of thiolated and non-thiolated siRNA nanoparticles showed any toxic effects on NPY-mRFP RBL-2H3 cells.

Therefore, we can conclude that the complexation of the thiol-modified siRNA and homopolymer became easier than non-thiolated siRNA, possibly related to different factors that control HP-thiolated siRNA nanoparticles to better activity than non-thiolated one. The particle size, surface charge and chemical bonding between the delivery agent and nucleic acid played a significant role. It is expected that the intracellular release of siRNA due to highly reductive environment present within the cells either in the endosomal or cytoplasmic compartments.

4.4 Conclusion

In this chapter, we concluded that mouse anti-DNP IgE and BSA-DNP cooperatively mediate optimal degranulation of NPY-mRFP RBL-2H3 cells and this event can be significantly decreased when RBL-2H3 cells are treated with thiolated and non-thiolated siRNA using HP and HP:CP2k polymers. Moreover, by using homopolymer-siRNA nanoparticles, degranulation levels are significantly reduced with thiol-modified siRNA treated cells thereby indicating efficiency of thiol-modified Syk inhibitors. Additionally, none of the tested PAA-siRNA nanoparticles showed significant toxicity even at the highest concentration tested. The efficiency and low cytotoxicity of this thiolated cross-linking reaction make it a promising candidate for *in vivo* siRNA delivery study in future.

Chapter 5

5 Validation of siRNA duplexes activity at mRNA and protein level

5.1 Introduction

While the unique specificity of nucleic acid therapeutics is attractive, one of the major challenges beyond the design of stable molecules, is actually the delivery and activity of siRNA to the intracellular site of action and achieving gene silencing. We hypothesized that siRNA mediated by RNAi mechanism could knockdown Syk mRNA and inhibit degranulation in basophils. Therefore, in this chapter I decided to confirm the results obtained by degranulation inhibition assays that suggest that PAA-siRNA nanoparticles effectively transfected and was able to downregulate the release of pro-inflammatory mediators and NPY-mRFP fluorescent protein (in our study) from basophils. Quantitative RT-PCR and Western blot studies were carried out where NPY-mRFP RBL-2H3 cells had been incubated with Syk-targeted siRNA and corresponding scrambled siRNA as a negative control. At 12, 24, 48 and 72 hours post-transfection, qRT-PCR was performed to assess gene silencing efficiency of siRNA polyplexes at mRNA level, whereas Western blotting was performed at 72 hours post-transfection to analyse knock-down at the protein level.

The main aims of this chapter include comparing the silencing efficiency at mRNA and protein level of thiolated and non-thiolated siRNA in polyplexes using mixtures of homopolymer (HP) and PEG-copolymer (CP). The polyplex itself is cross-linked but here the siRNA was additionally either disulphide linked or not disulphide linked into the polyplex.

5.2 Results

5.2.1 Validation of Syk gene expression by quantitative real-time PCR

Tyrosine protein kinase (Syk) is an enzyme encoded by the Syk gene. Activation of this enzyme is the first detectable signalling response resulting from binding of antigen to immunoreceptor and resulting in stimulation of inflammatory cells. Syk-targeted siRNAs were tested to verify their ability to silence the targeted gene in the cellular environment. A RT-PCR experiment was used in order to quantify the effect of knock-down on the target, using reference genes for data normalization. This technique allows the amplification and simultaneous quantification of a targeted mRNA after reverse transcription of the transcriptome.

Because of the availability of numerous Master Mixes on the market, specific and sensitive SYBR Green Master Mix need to be optimal for further PCR experiments in order to produce reliable high-quality PCR data (231). Melting curve was used for identification of nonspecific amplicons (232).

Before the selection of KAPA SYBR® FAST qPCR Master Mix Bio-Rad iCycler™, we had selected four reagents to evaluate for PCR (iQ™ SYBR® Green Supermix Bio-Rad, SsoAdvanced™ Universal SYBR® Green Supermix Bio-Rad, GoTaq® qPCR Master Mix Promega and KAPA SYBR® FAST qPCR Master Mix). Each sample was measured in triplicates. Of these products, KAPA SYBR® FAST Master Mix showed sharp and specific melting curves and hence selected for all further quantitative RT-PCR experiments which were carried out following the manufacturer's instructions (**Figure 5.1**).

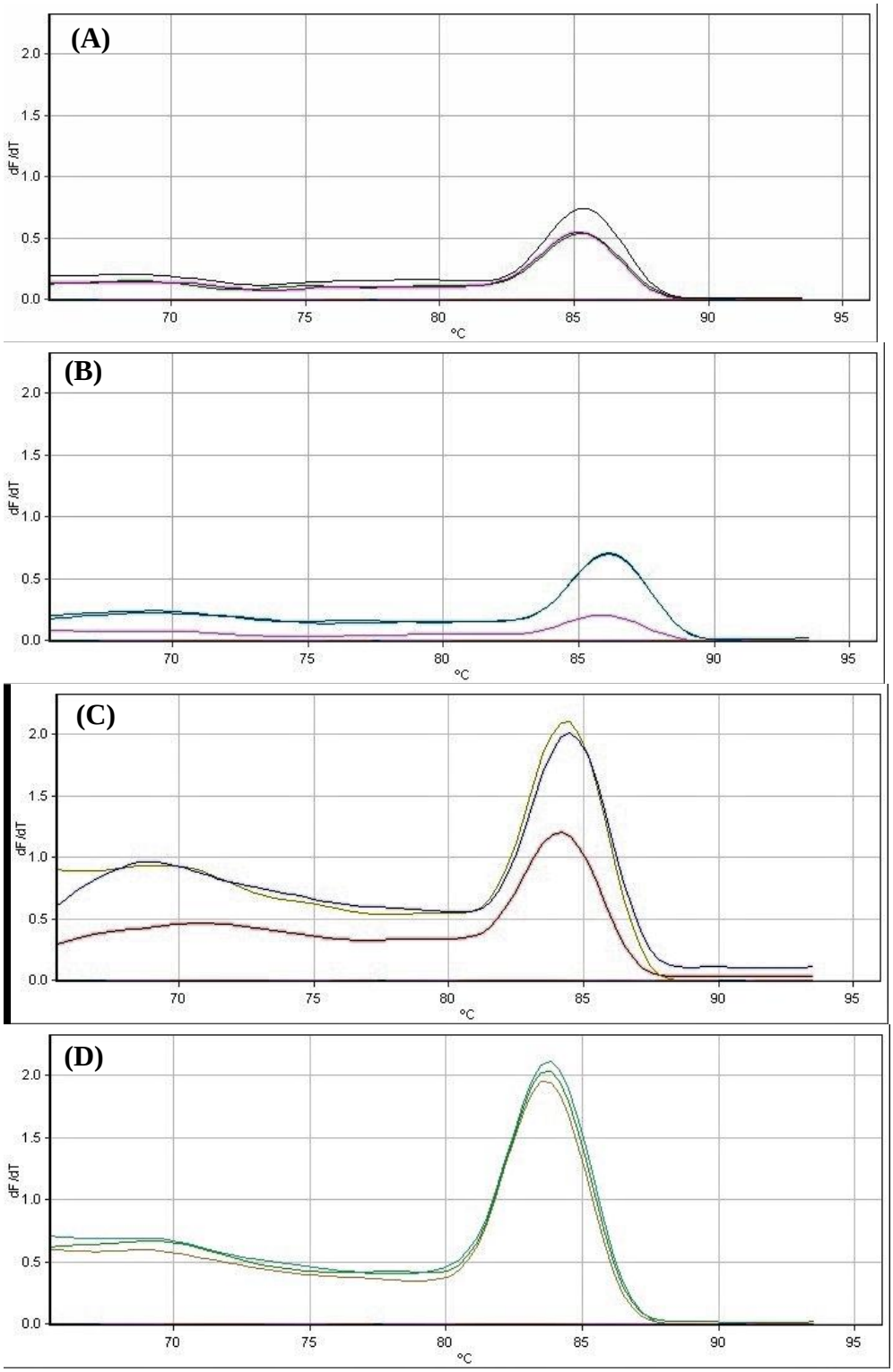

Figure 5.1 Melting curve plots of four PCR reagents performed on RBL cell lysate. (A) iQ™ SYBR® Green Supermix Bio-Rad, **(B)** SsoAdvanced™ Universal SYBR® Green Supermix Bio-Rad, **(C)** GoTaq® qPCR Master Mix Promega and **(D)** KAPA SYBR® FAST qPCR Master Mix.

To evaluate the siRNA delivery efficiency of cross-linked (HP-CP) and HP>10 KDa-siRNA polyplexes, Syk gene silencing studies were carried out using NPY-mRFP RBL-2H3 cells expressing the Syk gene. HP>10kDa and cross-linked siRNA polyplexes (polymer mixture of HP>10kDa and CP2k) were used for the knockdown experiments as optimized from the physicochemical and biological characterisation performed in ***Chapters 3*** and ***4***. All polyplexes were prepared at pH 6.5 and 30 mM NaCl solution containing either Syk-targeted siRNA or scrambled siRNA as a non-targeting control siRNA to clearly distinguish between specific and non-specific side effects of the siRNA activity.

HP/siRNA polyplexes were prepared at a RU/Nt ratio of 2.5:1 using either thiolated or non-thiolated siRNA. HP-CP/siRNA polyplexes were prepared at RU/Nt ratio of 2.5:1 and HP:CP ratio of 1:1 using non-thiolated siRNA, whereas the polyplexes were prepared at RU/Nt ratio of 4:1 and HP:CP ratio of 2:1 using thiol-modified siRNA.

For real time PCR, RNA extraction and cDNA synthesis were performed as detailed in materials and methods (***chapter 2***). To ascertain knock down efficiency of these duplexes by real time PCR, gene expression was quantified in unknown samples treated with either gene specific siRNA or a scrambled control and levels were normalised to the house keeping gene, Ggt1.

5.2.2 Effect of siRNA concentration on silencing efficiency

Knockdown ability of PAA-siRNA polyplexes is shown in

Figure 5.2, with the plot of percent gene expression of Syk mRNA across five different siRNA concentrations ranging from 50- 500 nM. The relative gene expression was analysed according to the Pfaffl method (180) by normalisation with

a reference gene (Ggt1) and comparison with the non-treated cells which defined as $2^{-\Delta\Delta Ct}$, where

$\Delta\Delta Ct = \Delta Ct$ of gene of interest - ΔCt of reference gene

A percent gene expression value close to 100 refers to no change in mRNA expression, lower and higher values refer to reduction in gene expression and overexpression, respectively. According to the data, an increase in knockdown effect for Syk expression was observed by increasing siRNA concentration from 50 to 300 nM. Syk silencing effect of around ~75 % was obtained when 300 nM of siRNA was delivered to RBL cells in comparison to scrambled siRNA. Hence, the inhibition of Syk expression was specific and depended on the concentration of the siRNA. On the contrary, overexpression of Syk mRNA occurred after treatment with high siRNA concentrations (400 nM and 500 nM in scrambled and Syk-targeted siRNA). Semizarov *et al.* reported that high concentrations of siRNA (extracellular concentration) induced the stress and apoptotic genes, resulting in off-target responses (209). This might result from an off-target effect from overloaded siRNA inside cells. Moreover, the scrambled sequence siRNA shows upregulation at high concentrations in comparison with targeted siRNA, which might be the off-target effect from the non-specificity of this sequence or increased polymer concentration (

Figure 5.2).

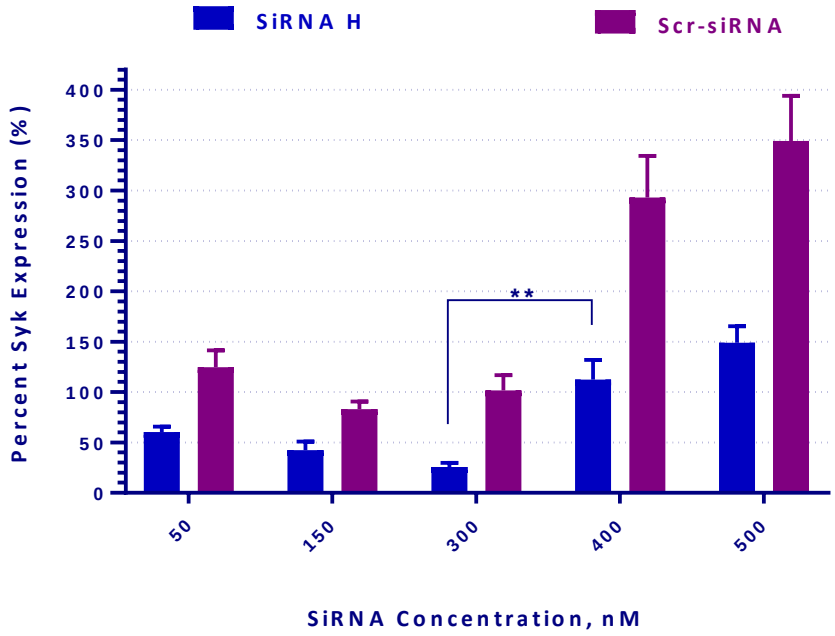

Figure 5.2 Percent of Syk mRNA expression in NPY-mRFP RBL-2H3 cells treated with HP/SH- siRNA. RBL cells were incubated with thiolated siRNA polyplexes using homopolymer at a fixed RU/Nt (2.5:1) in the presence of scrambled thiolated siRNA at different siRNA concentrations (50, 150, 300, 400 and 500 nM) 48 hours post transfection. After treatment, the RBL cells were collected to perform RNA extraction followed by cDNA synthesis and real-time PCR. The relative Syk gene expression was normalised with the untreated cells. mRNA expression of Ggt1 was used for normalization. Error bars show standard deviation. The statistical analysis used in this study was one-way ANOVA with Tukey's multiple comparison test, $p < 0.01$ (**). The data are representative of 2 separate experiments, in which each condition was analysed in triplicate per experiment.

5.2.2.1 Knockdown efficiency of HP/siRNA complexes on mRNA expression

Quantitative RT-PCR can compare the levels of mRNA transcripts in cell lysates and can lead to more a more direct assay of siRNA function, since siRNA acts on target mRNA. RT-PCR was used to examine the Syk expression in basophils that were incubated with HP-siRNA and cross-linked siRNA polyplexes for 12, 24, 48 and 72 hours at a final concentration of 300 nM. NPY-mRFP RBL-2H3 cells were transfected with Syk-targeted duplexes (thiolated and non-thiolated) by means of a PEGylated

(CP) and/or non-PEGylated PAA (HP). As shown in **Figure 5.3** and **Figure 5.4** when compared to scrambled control, thiolated and non-thiolated duplexes reduced the mRNA level of the targeted gene after 48 hours polyplexes exposure, albeit to different degrees. After 48 hours polyplexes exposure, the silencing efficiency was ~80% for thiolated siRNA using HP, and ~40% for non-thiolated siRNA. Compared to non-thiolated siRNA, Syk mRNA was significantly reduced with using thiol-modified siRNA at 24 hours polyplex exposure. With using thiolated and non-thiolated siRNA, no significant decrease in Syk expression with short incubation time (12 hours). In addition, overexpression of Syk mRNA has been noticed with incubation time longer than 48 hours (**Figure 5.3**). These results suggest that the Syk mRNA was successfully downregulated in an enhanced manner by using thiol-modified siRNA.

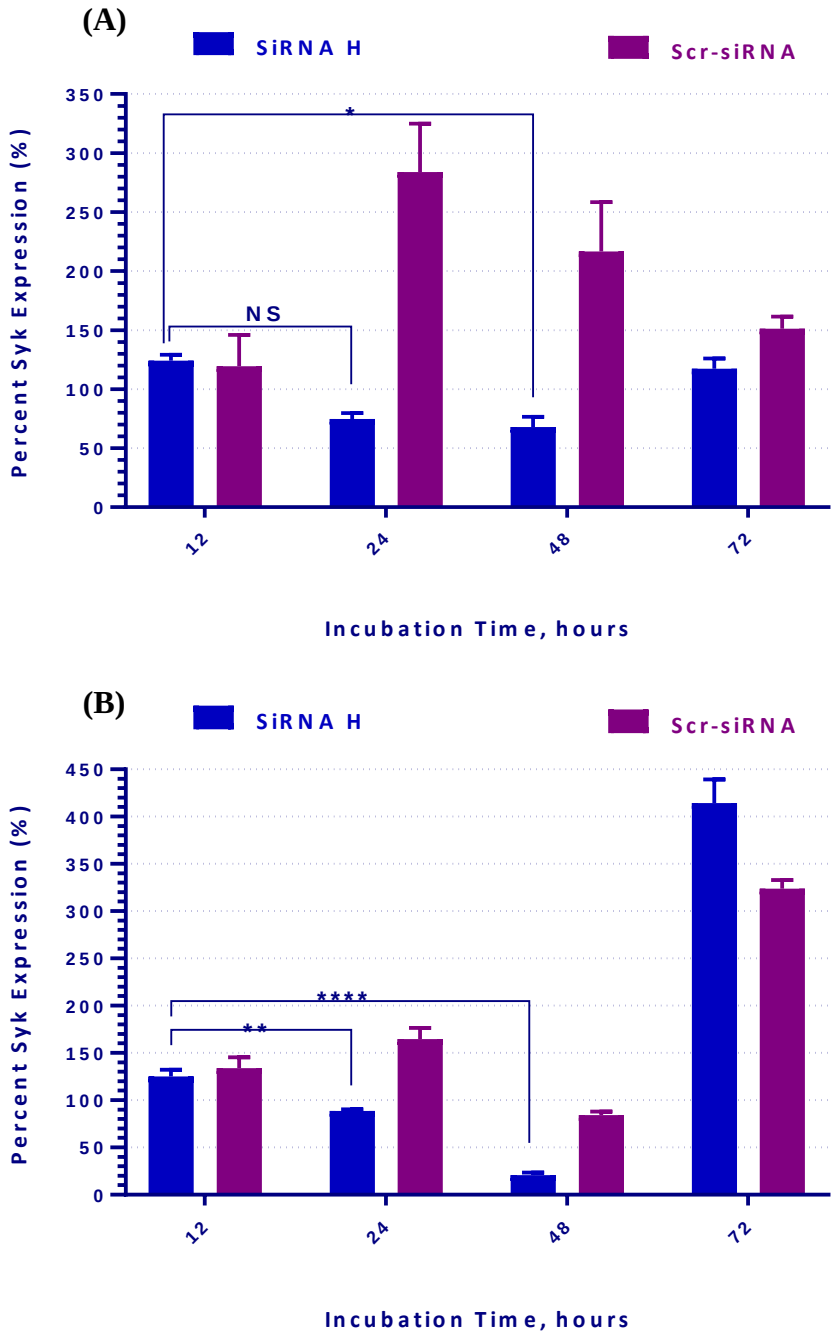

Figure 5.3 RT-PCR analysis for the Syk mRNA expression in NPY-mRFP RBL-2H3 cells treated with HP-siRNA polyplexes using (A) non-thiolated siRNA and (B) thiol-modified siRNA. RBL cells were incubated with non-thiolated and thiolated siRNA polyplexes using homopolymer at a fixed RU/Nt (2.5:1) in the presence of scrambled siRNA. After treatment, the RBL cells were collected to perform RNA extraction followed by cDNA synthesis and real-time PCR. The relative Syk gene expression was normalised with the untreated cells. mRNA expression of Ggt1 was used for normalization. Error bars show standard deviation. The statistical analysis used in this study was one-way ANOVA with Tukey's multiple comparison test, NS: not significant; $p = 0.045$ (*); $p = 0.006$ (**); $p < 0.0001$ (****). Statistical comparisons of scrambled SH-siRNAs were significant at 12-72 hours incubation time and hence all of these comparisons have been omitted for clarity.

5.2.2.2 Knockdown efficiency of HP-CP/siRNA complexes on mRNA expression

Figure 5.4 show the inhibition of Syk expression of cross-linked/siRNA polyplexes at RU/Nt ratio (2.5:1) and HP:CP ratio (1:1) for thiolated siRNA and RU/Nt ratio (4:1) and HP:CP ratio (2:1) for non-thiolated siRNA at incubation time ranging from 12-72 hours. Results showed that the knockdown ability of thiolated and non-thiolated siRNA duplexes as a percent of relative Syk mRNA expression was significantly increased with 48 hours incubation time, in normalisation with Ggt1 reference gene. In addition, a significant reduction in Syk mRNA transcript level using thiol-modified siRNA has been also noticed at 24 hours polyplexes exposure, in comparison with short incubation time (12 hours). However, upregulation of Syk mRNA level (~400%) has been observed with long exposure to polyplexes (72 hours).

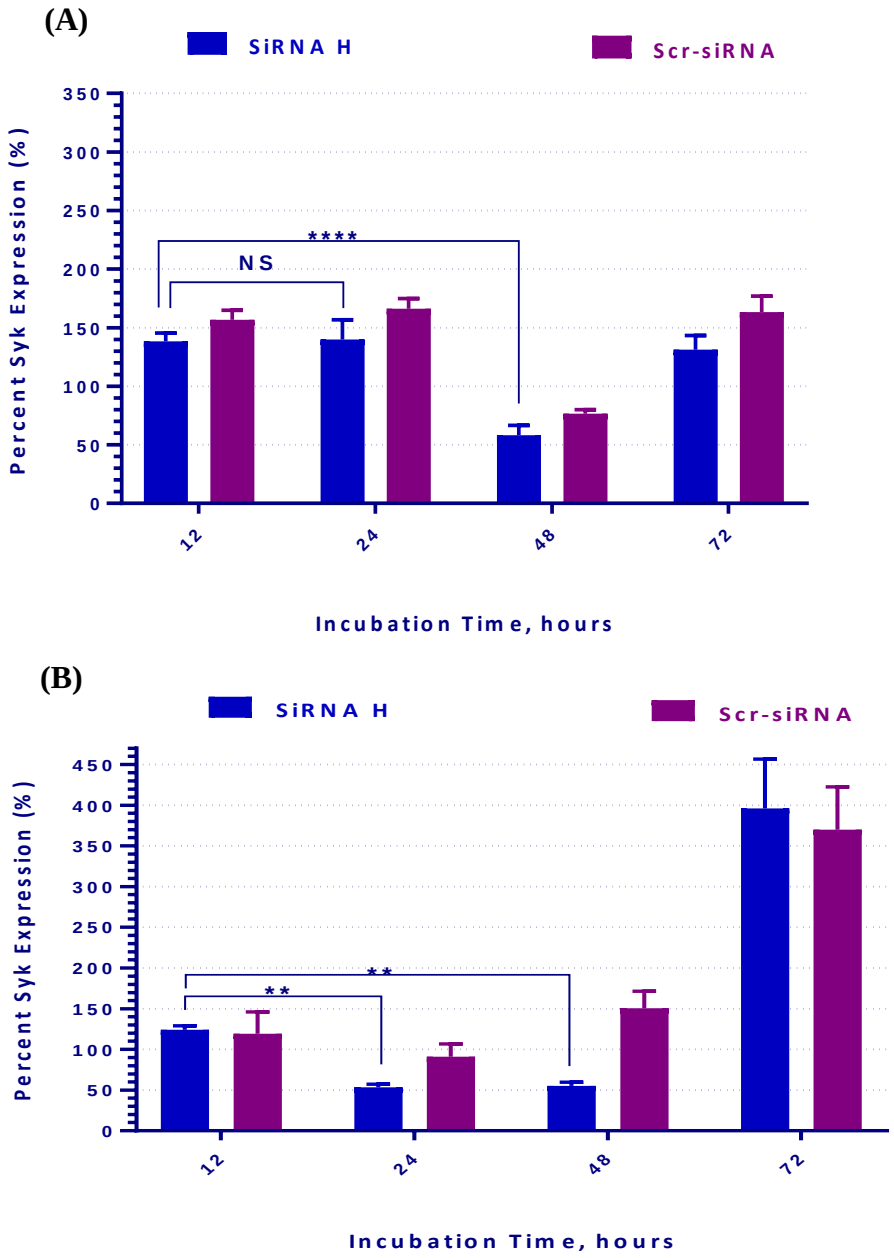

Figure 5.4 RT-PCR analysis for the Syk mRNA expression in NPY-mRFP RBL-2H3 cells treated with cross-linked/siRNA polyplexes using (A) non-thiolated siRNA and (B) thiol-modified siRNA. RBL cells were incubated with non-thiolated and thiolated siRNA polyplexes using a mixture of HP and CP at a fixed RU/Nt ratio (2.5:1) and HP:CP ratio (1:1) for non-thiolated siRNA and RU/Nt ratio (4:1) and HP:CP ratio (2:1) for thiolated siRNA based on physico-chemical characterisation, in comparison with scrambled siRNA. After treatment, the RBL cells were collected to perform RNA extraction followed by cDNA synthesis and real-time PCR. The relative Syk gene expression was normalised with the untreated cells. mRNA expression of Ggt1 was used for normalization. Error bars show standard deviation. Also, there was a significant difference between syk-targeted and scrambled siRNA treated cells for syk silencing efficiency comparisons; these results have been omitted for clarity. The statistical analysis used in this study was one-way ANOVA with Tukey's multiple comparison test, NS: not significant; $p = 0.002$ (**); $p < 0.0001$ (****).

5.2.3 Validation of Syk protein expression by Western blot

We performed protein expression analysis as a complementary step to the gene expression analysis. As shown above, Syk gene knockdown efficiency was achieved by reverse transcribing RNA into cDNA using RT-PCR and the level was analysed using quantitative real-time PCR. To assess whether these changes in mRNA expression are mirrored at the protein level, Syk protein expression was analysed with the immunological/biochemical methods of dot blot and Western blotting.

5.2.3.1 BCA protein quantification assay

In order to calculate the concentration and amount of proteins in RBL cell lysate, the total protein in the collected samples was quantified using a BCA protein assay. In this assay, a standard curve of absorbance vs protein concentration was produced as seen in Error! Reference source not found.. Based on the linear equation obtained from the tandard curve, the concentration of protein (µg/µl) was calculated for the samples and the total amount of protein obtained from each sample was also calculated as shown in **Table 5.1**.

Sample	Concentration of protein (mg/mL)
HP/siRNA H	0.65
HP/siRNA H (SCR)	0.68
Untreated cell lysate	0.67
HP/SH siRNA	0.5
HP/SH siRNA (SCR)	0.57
Untreated cell lysate	0.69
HP-CP/siRNA H	0.62
HP-CP/siRNA H (SCR)	0.61
Untreated cell lysate	0.55
HP-CP/SH siRNA	0.69
HP-CP/SH siRNA (SCR)	0.64
Untreated cell lysate	0.7

Table 5.1 Protein concentrations of each sample based on the equation derived from the standard curve of absorbance according to BCA assay.

5.2.3.2 Dot Blot Analysis

Dot blot is a simple and fast technique to check the binding specificity of target antigen using a primary antibody specific for the antigen of choice. The aim of this method is to find the best dilutions of primary and secondary antibodies which give a signal with the target protein, but not with an irrelevant control protein used (BSA) at the same concentration.

The nitrocellulose membrane is treated in the same manner as a Western blot but since no separation is present the antibody is the only tool to determine presence of a given protein. Dot blot was performed by obtaining an aliquot of RBL cell lysate and a negative control sample (BSA).

Using 3 doubling dilutions from the initial sample concentration of 0.5 µg/ml, results of RBL cell lysate dot blot has shown that all samples contain detectable levels of Syk and GAPDH proteins, except the lowest concentration with 1:4000 diluted secondary antibody(**Figure 5.5**). However, there is a visible trend of decrease in detection with reducing lysate concentration. The negative control of BSA shows no signal at all. Therefore, the specific binding of primary antibodies used appears to be very suitable, as confirmed by the absence of non-specific binding to other proteins.

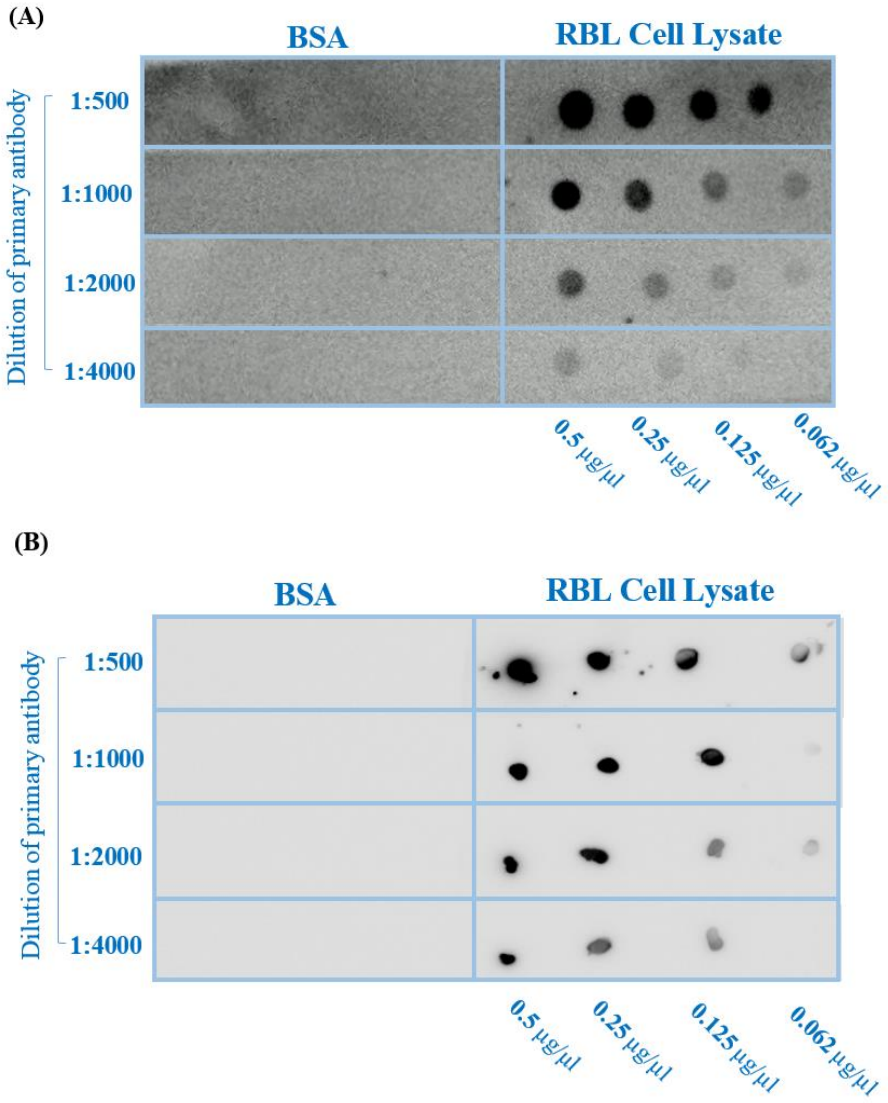

Figure 5.5 Dot blot performed on RBL cell lysate and control BSA for detection of syk protein. Four concentrations of cell lysate and BSA were prepared: 0.5, 0.25, 0.125 and 0.062 µg/µl, respectively. BSA was used as a negative control. Samples are arranged from left to right in order of decreasing concentrations of BSA and RBL cell lysate. Nitrocellulose membranes were incubated with **(A)** purified anti-Syk antibody or **(B)** GAPDH loading control monoclonal antibody followed by anti-mouse IgG (whole molecule)-peroxidase antibody.

Before the selection of GAPDH loading control monoclonal primary antibody, we had run a dot blot using anti-β-Actin monoclonal antibody produced in mouse (Bio-Rad) as a positive control but the non-specific binding of the primary antibody used seemed to be very high (**Figure 5.6**). This is most likely caused by non-specific binding to other proteins in the lysate. Similar trends can be seen when using the same primary

antibody in Western blot where the antibody shows multiple bands even when running the samples on an SDS PAGE.

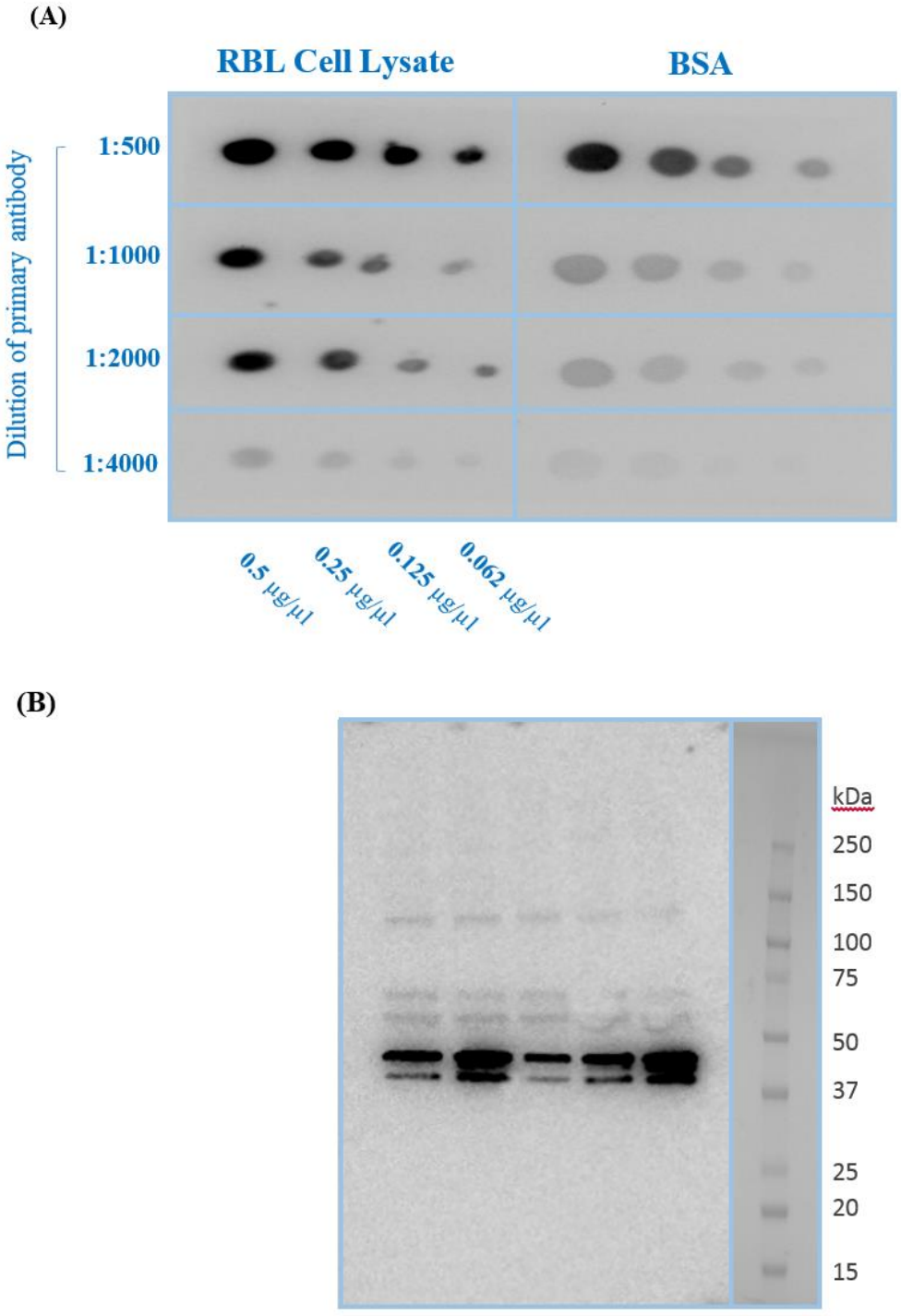

Figure 5.6 Detection of β-Actin protein from RBL cell lysate. (A) Dot blot of RBL cell lysate and control BSA. Four concentrations of cell lysate and BSA were prepared: 0.5, 0.25, 0.125 and 0.062 µg/µl, respectively. BSA was used as a negative control. Samples are arranged from left to right in order of decreasing concentrations of BSA and RBL cell lysate. **(B)** Western blot detection of β-Actin protein using anti-β-Actin monoclonal antibody produced in mouse followed by anti-mouse IgG (whole molecule)-peroxidase antibody. The molecular weight markers are indicated on the right.

5.2.3.3 Detection of Syk silencing at protein level by Western blot

The efficiency of Syk gene silencing using PAA/SH-siRNA nanoparticles at protein level was analysed by Western blot. The main purpose of the Western blot was to confirm the silencing of Syk in RBL cells and to compare the silencing with expression of another protein (GAPDH) used as a negative control.

Protein was extracted from cells at 48 and 72 hours after incubation with 300 nM thiolated Syk-targeted siRNA/PAA nanoparticles and thiolated scrambled siRNA/PAA nanoparticles and untreated cells were used as control. After protein extraction, the total amount was quantified by a BCA protein assay and equal amounts of protein were separated by SDS-PAGE. Following the western blotting, ImageJ was used to visualize and analyse Syk protein expression.

As observed in**Figure 5.7**, the RBL cell line exhibited a reduction in total cellular Syk protein band intensity to approximately 30% of the negative control in response to treatment with 300 nM of Syk-targeted thiol-modified siRNA complexed with homopolymer after 72 hours incubation of nanoparticles and in comparison with cells treated with scrambled siRNA loaded nanoparticles (~75% of untreated cells). Transfection with HP/siRNA (300 nM) for 48 hour was an exception as it did not decrease the cellular Syk protein level. Since the Syk band was the lightest in the cells treated with Syk-silencing siRNA complexed with a homopolymer nanoparticles at 300 nM and after 72 hours post transfection relative to the scrambled siRNA sequence, these results confirm that Syk silencing siRNA was effective in down-regulation protein expression and degranulation. Because the results were promising, we decided to evaluate the reduction of Syk following treatment of RBL cells with HP-CP/SH-siRNA (HP-CP/siRNA) nanoparticles.

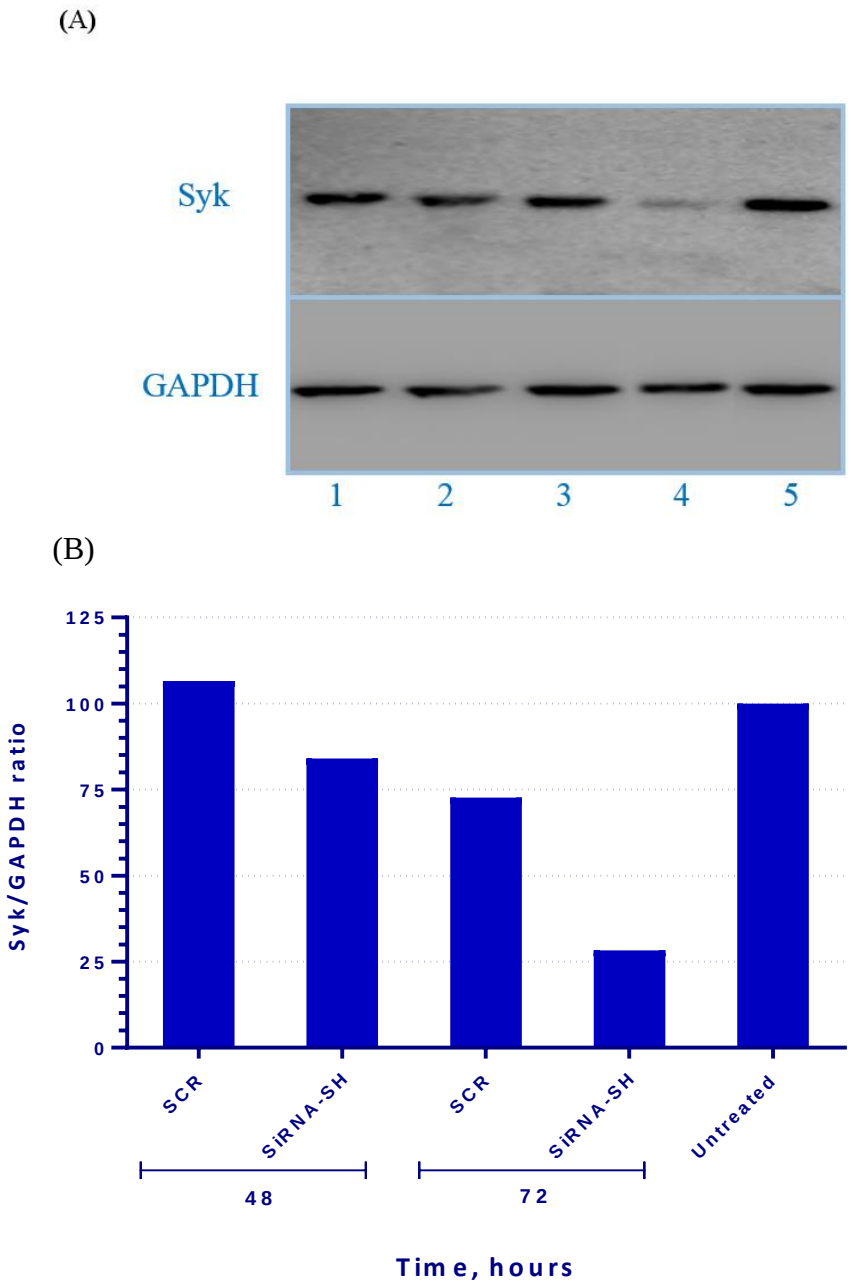

Figure 5.7 Detection of Syk silencing in RBL cell lysate using HP/SH-siRNA nanoparticles by Western blot. Bands 1=SCR, 2=SiRNA-SH, 3=SCR, 4=SiRNA-SH and 5=untreated cells. RBL cells transfected with HP/SH-siRNA complexes were lysed after 48 and 72 hours. Lysate of untreated cells expressing Syk was also included to compare the level of Syk protein between lanes. **(A)** Western blot detection of Syk and GAPDH proteins using anti-Syk monoclonal antibody and GAPDH loading control monoclonal antibody, respectively followed by anti-mouse IgG (whole molecule)-peroxidase antibody. **(B)** Normalised intensity of the proteins bands for detecting the level of Syk protein inhibition. This experiment was done only once and thus mean and standard deviation values are not represented. n=1.

RBL cells did not decrease the total cellular Syk protein level in response to treatment with 300 nM of thiol- modified siRNA where PEGylated copolymer and homopolymer were the delivery vector. RBL cells which did not receive any siRNA treatment were also included in this experiment to compare the total cellular Syk protein level with those cells that were treated with SH-siRNA. We observed that cells treated with HP-CP/SH-siRNA did not appear to have reduced Syk protein levels. Also as seen in**Figure 5.8,** the cells which were treated with scrambled SH-siRNA had a higher cellular Syk protein level when compared to those treated with HP-CP/SH-siRNA after 48 and 72 hours of nanoparticles incubation. This comparison added to our conclusion that the treatment with 300 nM of HP-CP/SH-siRNA nanoparticles did not decrease Syk protein levels in RBL cells. Apparently the amount of Syk expressed in the cells treated with scrambled SH-siRNA is higher than that treated with Syk-targeted SH-siRNA, which might result from an off-target effect of this sequence due to some residual binding.

(A)

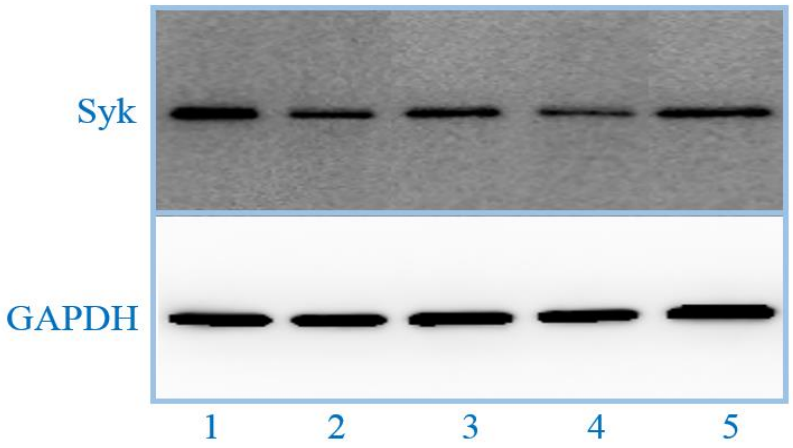

(B)

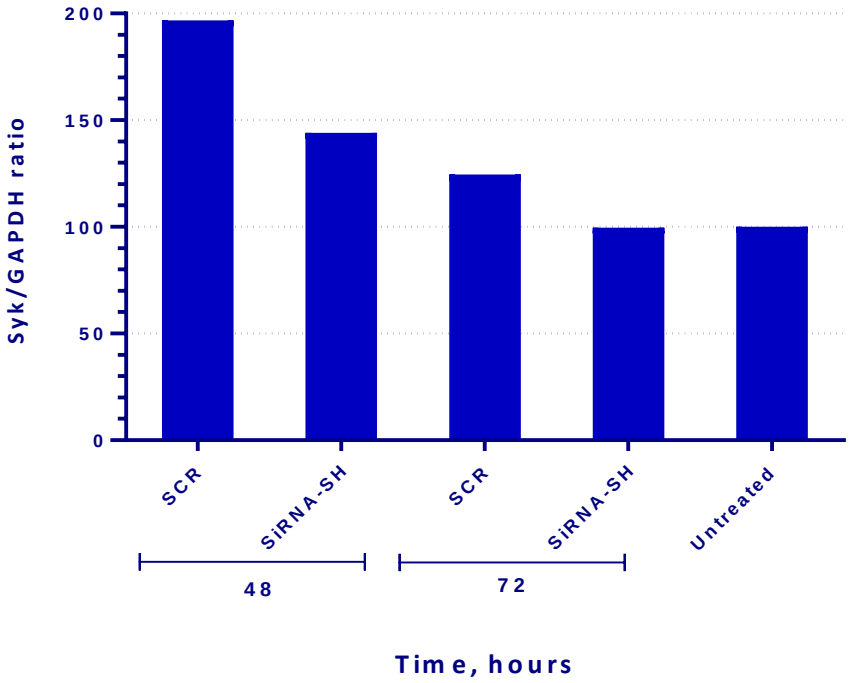

Figure 5.8 Detection of Syk silencing in RBL cell lysate using HP-CP/SH-siRNA nanoparticles by western blot. Bands 1=SCR, 2=SiRNA-SH, 3=SCR, 4=SiRNA-SH and 5=untreated cells. RBL cells transfected with HP-CP/SH-siRNA complexes were lysed after 48 and 72 hours. Lysate of untreated cells expressing Syk was also included to compare the level of Syk protein between lanes. **(A)** Western blot detection of Syk and GAPDH proteins using anti-Syk monoclonal antibody and GAPDH loading control monoclonal antibody, respectively followed by anti-mouse IgG (whole molecule)-peroxidase antibody. **(B)** Relative intensity of the proteins bands for detecting the level of Syk protein inhibition. This experiment was done only once and thus mean and standard deviation values are not represented. n=1.

5.3 Discussion

In ***chapter 4***, it was shown that Syk-targeted siRNA effectively reduced degranulation comparable to scrambled siRNA and untreated cells. However, the degranulation assay as a reporter system revealed that the use of homopolymer as a delivery vector had much higher efficiency compared to homopolymer-copolymer mixture. Consequently, it was essential to confirm if this downregulation in degranulation relates to direct gene silencing efficiency of homopolymer-based nanoparticles. In this chapter, we have used quantitative RT-PCR and western blot to study the knockdown of Syk gene and protein present in RBL cells. This study included gene silencing of Syk-targeted thiolated and non-thiolated siRNA based complexes.

The results from the quantitative RT-PCR suggest that the use of thiol-modified siRNA with HP-based nanoparticles improved Syk gene silencing efficiency 48 hours after nanoparticle exposure. However, the improvement in Syk gene silencing for HP-CP/SH-siRNA nanoparticles was not as expected.

The positive charge of HP/siRNA complexes can result in reducing aggregation and facilitating cellular membrane uptake, confirming the importance of producing discrete positively charged nanoparticles to produce optimal results (116). Whereas, the possible reason for the underperformance of cross-linked HP-CP/siRNA complexes compared to HP-based complexes, is that the low surface charge density of HP-CP/siRNA complexes because of the presence of PEG layer may act as a steric barrier around nanoparticles and make it difficult for the nanoparticle to approach cell surfaces and thus, reduced cellular membrane interaction and consequent cellular uptake. The surface characteristics and the nature of PEG chains (length, density and conformation) influence cell-surface interaction and hence cellular uptake and internalisation (116, 233, 234). Moreover, the low performance of HP-CP/siRNA

nanoparticles was also attributed to incomplete condensation of siRNA using this delivery system (**Figure 3.6**).

The better performance of homopolymer also suggested by a comparative study involving the packing of miRNA and siRNA with PAA polymer system (117). Similarly, the presence of PEG on gold nanoparticle surface reduced cellular uptake and subsequent intracellular localization of these nanoparticles. The highest uptake and internalization was observed for non-PEGylated gold nanoparticles (235). Moreover, presence of high density and high molecular weight PEG reduces protein adsorption and shields the nanoparticle surface from directly interacting with the cell surface, which leads to lower cellular uptake and subsequent cellular internalisation compared to non-PEGylated nanoparticles (46, 234, 236).

Rackstraw *et al.* also compared a PEGylated polymer with a non-PEGylated PAA polymer with similar backbone (MBA-DMEDA). Homopolymer demonstrated best results in a luciferase assay and this was attributed to its strong positive charge with low aggregation which is important to produce discrete well-condensed complexes (116). This is consistent with our observations with homopolymer that showed optimal results at mRNA and protein levels.

However, two studies showed that the use of cationic polymers self-assembled with hydrophilic moiety (PEG) can result in well condensed complexes with increased nucleic acid protection from nuclease degradation due to the formation of PEG layer around the nanoparticle (73, 237), but this modification did not increase the stability of nanoparticles (237). These findings suggests that the relative ratio of copolymer to homopolymer could be high and thus influenced on cell-surface interaction.

Based on the results observed after quantitatively studying Syk silencing, a 300 nM thiol-modified siRNA dose was selected to demonstrate qualitative Syk silencing after

a 48 and 72 hours polyplex incubation in RBL cells (**Figure 5.7** and **Figure 5.8**). The 72 hours transfection period was adopted to check if we could further decrease the cellular Syk levels. As seen from the results it can be concluded that the 72 hours transfection with siRNA provided more satisfactory data when compared to the 48 hours transfection with siRNA. Thus it can be stated that the siRNA takes 72 hours to effectively down regulate the cellular protein levels. The transfection efficiencies were compared between homopolymer and homopolymer-copolymer/SH-siRNA nanoparticles.

As observed in Western blot results, HP/SH-siRNA nanoparticles had a better transfection efficiency at protein level and were able to reduce ~75 % of cellular Syk when compared to the HP-CP/SH-siRNA nanoparticles at 72 hours post-transfection. Although preliminary results of RT-PCR and degranulation inhibition appeared promising that siRNA significantly inhibited fluorescence release and Syk mRNA 48 hours and 72 hours post transfection respectively, no silencing activity was observed in cells treated with HP-CP/SH-siRNA nanoparticles at protein level. There are four possible explanations for the lack of detection for Syk knockdown with HP-CP/SH-siRNA nanoparticles:

I. The HP-CP complexes did not form stable complexes. This may occur due to the presence of traces of DTT in the purified copolymer which would affect the formation of stabilizing disulphide bonds, leading to less stable nanoparticles.
II. A study by Narz, 2007 reported that the background of untransfected cells can prevent analysis of gene-silencing especially in hard-to-transfect cell lines (238). They demonstrate two strategies for the enrichment of siRNA-transfected cells: Firstly, for cell suspensions the transfected cells are separated

from untransfected by antibody-coated magnetic particles. Secondly, for adherent cells the siRNA is co-transfected with a plasmid that expresses a eukaryotic antibiotic resistance gene. However, both techniques are limited by the initial transfection rates.

III. A study by Tschaharganeh, 2007 reported the importance of using non-targeted siRNA to ensure that functional cellular changes are only due to target-specific effects and not due to off-target effects (239). In this case, the western blot results showed that the cells treated with targeted HP-CP/SH-siRNA had a lower cellular Syk protein level when compared to those treated with scrambled SH-siRNA after 48 and 72 hours of nanoparticle incubation. This could be because the untransfected cells contain small amounts of Syk protein and/or large amounts of GAPDH protein and this affects the relative expression for the protein of interest, as the relative Syk protein expression relies on normalisation with reference GAPDH protein. In addition, the Syk and GAPDH gene expression can vary according to the experimental condition.

IV. RT-PCR results showed overexpression of Syk mRNA with incubation time (post transfection) longer than 48 hours. This was in line with Western blot results that also revealed increased level of Syk protein with HP-CP/SH-siRNA nanoparticles at 48 and 72 hours incubation time.

V. Western blot assay was not a quantitative technique and it was difficult to detect differences in the expression levels of Syk protein. Whereas, quantitative RT-PCR can compare the levels of mRNA transcripts in cell lysates and could lead to a more direct assay of siRNA function, since siRNA did act on target mRNA.

In general, a thiol-modified siRNA had better activity than non-thiolated one, although a western blot assay was unable to show knockdown in Syk expression with HP-CP/SH-siRNA nanoparticles.

5.4 Conclusion

By using homopolymer-siRNA nanoparticles, Syk mRNA and protein are significantly reduced with thiol-modified siRNA treated cells thereby indicating efficiency of thiol-modified Syk inhibitors. Whereas, HP-CP/SH-siRNA complexes, with 45 % Syk gene reduction efficiency at mRNA level, yield almost no silencing activity at protein level.

The low performance of the HP-CP/SH-siRNA nanoparticles was attributed to the low surface charge and shielding effect of PEG on the complex, which reduced binding with cell membrane and subsequent silencing efficiency of the complexes.

Chapter 6

6 General discussion

The principal aim of the present work was focused on characterization and evaluation of the newly developed thiol crosslinked polyamidoamine-siRNA (PAA-siRNA) nanoparticles that can used for the treatment of allergic diseases (IgE-mediated allergy, Type I) through inhibition of Syk gene signalling downstream of degranulation in RBL-2H3 NPY-mRFP cell line.

PEGylated (CP) and non-PEGylated (HP) linear chain cationic polyamidoamine (PAA) polymers that have thiol-crosslinkable groups were used for the formulation of the PAA-siRNA nanoparticles. The rationale for cross-linked polymeric system is to increase nucleic acid loading and *in vivo* stability of nanoparticles, reduce toxicity by increasing biodegradability (240) and to control the release of cargo in response to specific stimuli (241, 242).

PEG is also important *in vivo* to prolong circulation time by avoiding non-specific uptake by phagocytic cells. The presence of PEG shields the surface charge of the nanoparticles and reduces the adsorption of proteins like opsonins thereby delaying the clearance by

reticulo-endothelial system (RES) (46). Hence, PEGylation is desirable for systemic *in vivo* delivery of nanoparticles. Moreover, the presence of PEG is important to reduce interparticulate aggregation, thus increasing colloidal stability of nanoparticles (138).

This work includes description the physicochemical and biological characterisations of the nanoparticles produced with the HP-CP mixture, compared with the cationic homopolymer (HP) using thiolated and non-thiolated siRNAs.

This thesis includes: (i) characterization of the physicochemical properties of PAA-siRNA complexes, such as binding ability and size; (ii) investigation of the degranulation inhibition and cytotoxicity induced by the PAA-siRNA complexes in a model reporter system; (iii) evaluation of the gene silencing effect of thiol crosslinked PAA-siRNA complexes with Western blot and RT-PCR methods.

The HP-siRNA complexes are formed by mixing a non-PEGylated cationic homopolymer with thiolated or non-thiolated siRNA, whereas the HP-CP/siRNA polyplexes are formed by mixing a non-PEGylated cationic homopolymer and a PEGylated cationic copolymer with thiolated or non-thiolated siRNA. The thiol group (SH) from the reduced copolymer and thiol-modified siRNA reacts with the thiopyridine from the homopolymer (HP) to form disulphide bonds. These disulphide bridges formed in the PAA-siRNA complexes between the homopolymer and the co-polymer prevents disassembly of the nanostructure and hence provides stability to the nanoparticles in physiological medium. The relative proportion of HP and CP to siRNA is also important in achieving the correct level of surface PEGylation without adversely affecting the compaction of the polyplexes.

In order to obtain maximum siRNA incorporation into the nanoparticle, it was expected that the nanoparticle preparation medium should be at optimal pH and ionic concentration. Previous studies have used a variety of conditions. Chitosan nanoparticles are prepared routinely in acidic medium to facilitate chitosan solubility (243). Jones *et al*. prepared PAA-DNA nanoparticles in 15 mM PBS (100), whereas a comparative study involving the packing of different nucleic acids (pDNA, ODNs and

siRNA) with the crosslinked PAA polymer system was prepared in 5 mM NaCl by Danish *et al* (140).

Hence, the optimal salt concentrations and pH required for the maximal PAA-siRNA interaction for these set of linear polyamidoamine polymers was determined by agarose gel electrophoresis as 30 mM NaCl and pH 6.5. The low salt concentration causes a drastic decrease in the aggregation, providing an additional probability to control size of the polyplex, whereas the pH of the dilute solution affects the conformational freedom of the polymer binding. At acidic pH, protonation increases the positive charges on the polymer which repel each other and hence, the polymer assumes a more rigid conformation. By increasing the pH to a more basic condition or by addition of salt, the repulsion of the charges is reduced and the polymers attain a more flexible conformation.

In ***Chapter 3***, I investigated the possibility of utilizing thiol-modified siRNA to achieve an improvement in physicochemical characterisation of crosslinked PAA nanoparticles.

The formation and stability of polyplexes largely depends on electrostatic interactions and these are low because of the small size of siRNA and consequently the small number of charges present per duplex (181). The poor complexation of the nanoparticles is a major barrier especially when cationic linear polyamidoamine polymers are used as siRNA delivery vehicle because the polyamidoamine is linear which decreases the association with siRNA. Therefore, many reports describe new strategies that have been developed to improve cationic polymer/siRNA complexation either by enhancing the cationic charges of polymers or by cross-linking reactions. The polymer/siRNA complexation can improved by increasing positive charge of polymers, but this will produce positive charge-mediated cytotoxicity (244). On the

other hand, enhancing the anionic charge of siRNA represents an efficient strategy to improve polymer/siRNA interaction (185, 186). Park *et al.* reported that cationic polymer/siRNA complexation could be improved by using a thiol-modified siRNA at the 5′ end of sense and anti-sense strands (245). Disulphide cross-linked PEI with a low Mw of 800 Da can efficiently bind and condense plasmid DNA with lower *in vitro* toxicity and higher transfection efficiency compared with PEI of 25 kDa Mw (205). Thiamine pyrophosphate (TPP) is also used to increase chitosan/ siRNA complexation due to salt formation between phosphates of TPP and amines of chitosan, thus improving chitosan water solubility. Moreover, amines of TPP also increase the electrostatic interaction with siRNA and thereby improving the silencing efficiency (246). However, the addition of a third binding agent adds complexity for nanoparticle optimization (247).

In comparison with these reported strategies, we developed a new formulation approach to increase PAA-mediated complexation of siRNA and thereby increasing the transfection efficiency. The thiol aliphatic group was introduced at the 5'-terminus on the antisense strand of siRNA to allow the formation of disulphide linkages after PAA/siRNA interaction. Electrostatic forces between oppositely charged PAA and siRNA lead to the formation of loose complexes, then the compact and well condensed complexes were subsequently formed via crosslinking of the thiol-thiopyridine groups. In addition to increasing PAA/siRNA complexation, thiol crosslinked nanoparticles are redox-responsive and hence release siRNA only in a highly reductive environment.

The concept of a disulphide based cross-linked system is based upon when a short cross-linking homopolymer (HP) is attached with PEGylated copolymer (CP) via cleavable disulphide linkages to acquire the bioreducible characteristics. A disulphide

linkage can be developed by reacting two thiol (-SH) groups such as short cross-linking homopolymer (HP) containing thiopyridyl activated groups attached with a PEG-PAA-PEG copolymer (CP) having already reduced -SH groups. Mixing the polymers results in the spontaneous formation of stable, mono-disperse and small cross-linked polyplexes when brought closer with nucleic acids. The concept of such cross-linking system is previously reported by Garnett *et al* (134). However, this concept of cross-linking system based on linear PAA nanoparticles have not been described yet for thiolated-siRNA gene delivery.

The gel electrophoresis showed that non-thiolated siRNA was unable to tightly bind HP and HP-CP polymers as evidenced by the siRNA and free polymer migration in electrophoresis even at low RU/Nt ratio. Compared to non-thioated siRNA, the gel retardation assay for HP-CP/SH-siRNA polyplexes revealed full retardation at a higher RU/Nt ratio with no free polymer, indicating that SH-siRNA could be effectively and tightly condensed by the HP-CP blend.

The mean particle size, determined by DLS, was found to be smaller at all ratios prepared with thiolated siRNA than mean sizes of non-thiolated based nanoparticles, indicating that the presence of thiolated siRNA led to the transformation from loose complexes to tight complexes. Taken together, good condensation, small particle size, selective intracellular release and minimum free components should make these nanoparticles suitable for *in vitro* and *in vivo* applications.

In ***Chapter 4***, we examined the use of NPY-mRFP RBL-2H3 cell line as an *in vitro* model for rat basophilic degranulation upon IgE and antigen stimulation, to be used for pharmacological screening of new therapeutics to regulate basophil activity.

The RBL-2H3 cell line has mostly been used for studying the IgE-FcεRI interactions and the intracellular pathways leading to degranulation. Many studies using the RBL-

2H3 cell line have primarily been screening studies of new drug candidates with anti-allergic and/or anti-inflammatory properties (248-250). A common approach to study basophils is to sensitize the cells with immunoglobulin (Ig) E antibodies, that cross-link and thereby activate the FcεRI receptor in the cellular membrane. Activation of the FcεRI receptor will up-regulate the synthesis and stimulate the secretion of intracellular mediators of basophils. Interestingly, Azouz *et al*. have used NPY-mRFP as a reporter for the quantitative assessment of exocytosis in rat basophilic cell line, RBL-2H3 (251).

The NPY-mRFP degranulation inhibition assay is then used as an alternative to the β-hexosaminidase assay to assess the functional activity of PAA/siRNA nanoparticles. It is faster than the β-hexosaminidase assay and there is also no need to buy additional reagents, such as substrate or stop solutions for the β-hexosaminidase assay, or luciferase assay reagents, which are expensive. In addition, enzymatic assays such as the β-hexosaminidase assay and luciferase assay are very time-sensitive, and it can be more difficult to obtain consistent results with these assays. Another advantage over the β-hexosaminidase assay is that impurities in allergen extracts may interfere with the β-hexosaminidase released from the cells. Allergen extracts may also directly cleave the assay substrate themselves, as we found in several crude pollen extracts, such as oak pollen extract, even in the absence of cells. The NPY-mRFP assay won't be affected by this problem, although some intrinsically fluorescent allergen extracts may increase background fluorescence measurements (176).

As with all assays, the NPY-mRFP assay consistency is dependent on the competence of the scientist carrying out the assay. Similar to the β-hexosaminidase assay, care must be taken to avoid taking up cells with the pipette tip when transferring the supernatants. Some cell transfer is unavoidable, but inconsistent pipetting may cause

variable results. Also, it is possible that cells can detach after treatment with certain stimuli. For example, treatment of RBL cells with the calcium ionophore A23187 may cause detachment by downregulating the integrin VLA-4 (252). As a result, increased fluorescence in the supernatant may be due to an increased transfer of detached cells, rather than, or in addition to, degranulated NPY-mRFP fusion protein, unless an extra centrifugation of filtration step is added to remove any cells in the supernatant.

In the second part of ***Chapter 4***, the cytotoxicity and efficiency of crosslinked PAA/siRNA nanoparticles in inhibition of NPY-mRFP fluorescence release were evaluated.

The HP/siRNA nanoparticles were able to downregulate fluorescence release by 40% at a high concentration of siRNA H (300 nM), whereas the HP-CP/siRNA nanoparticles was not able to knockdown more than 15% of fluorescence release at the same concentration (300 nM).

After using thiol-modified siRNA,HP/SH-siRNA and HP-CP/SH-siRNA polyplexes could efficiently downregulate fluorescence release in a sequence-specific manner, which was comparable to the efficacy of Lipofectamine 2000.

As can be seen in the cytotoxicity assay, thiol-mediated siRNA delivered through PAA into RBL cells did not show any toxicity when compared with untreated cells, whereas Lipofectamine 2000 lipoplexes were significantly more toxic.

Commercial transfection reagents that are optimized for *in vitro* siRNA delivery generally work in the concentration range of 10-50 nM siRNA concentration [e.g. Peptide based N-TER (Sigma), Liposome based Lipofectamine® RNAiMAX (Life Technologies),Cationic Polymer based INTERFERin®-HTS (Polyplus Transfection)].

Polyethylenimine (PEI) is a synthetic cationic polymer used as a gold standard for DNA transfection. Although all forms of PEI are able to form complexes with siRNA, it has been reported that only certain forms of PEI are capable of efficiently delivering siRNA [e.g. linear 22 kDa jetPEI® (Polyplus-Transfection), branched 10 kDa PEI obtained from gel-filtration chromatography of 25kDa PEI (72). These two unmodified forms of PEI have relatively low toxicity and exhibit a working range of 50-100 nM. Several chemical modifications have been made on PEI to increase the efficacy and reduce toxicity. For example, disulphide cross-linked polyethyleneimine resulted in effective knock-down of pro-proliferative Akt1 mRNA and protein at 75 nM siRNA concentration (253). Similarly, pyridylthiourea-grafted polyethylenimine was effective at 10 nM siRNA concentration due to the enhanced buffering capacity and hydrophobic nature of the pyridylthiourea-group (254). Moreover, imidazole-grafted-PEI showed slightly better knock-down efficiency than commercial transfection reagent (50-100 nM siRNA concentrations). Imidazole-grafting increased the endosomal escape and partially converted primary and secondary amines to secondary and tertiary amines, hence reducing the toxicity (255).

Chitosan-siRNA nanoparticles also work in the similar range of siRNA concentration (50-125 nM) (256). For example, thiolated glycol chitosan showed effective *in vitro* knock-down of TNF-α mRNA at 100 nM siRNA concentration with effective suppression of inflammation and bone erosion in mice, which was comparable to the effect of methotrexate, anti-rheumatic drug (191).

Hence, it can be generalized that the siRNA concentration widely used in literature is between 10-150 nM. The PAA-siRNA nanoparticles required 300 nM to show significant gene-knockdown activity. This requirement for a high siRNA concentration may occur due to the low transfection efficiency RBL-2H3 cells (257)

or due to moderate *in vitro* uptake of cross-linked HP-CP nanoparticles which are sterically stabilised with reduced interaction with the cell membrane (117). Improvements in cellular uptake might enhance the knockdown efficiency of these PAA-siRNA nanoparticles. The drawback of using high siRNA concentration is that it may induce off-target effects and cytotoxicity (258), in addition to the cost of siRNA synthesis and chemical modification.

In ***Chapter 5***, Western blotting and RT-PCR were be carried out to confirm whether the 300 nM dose selected for siRNA was sufficient to induce Syk silencing at mRNA and protein level.

A study by MacGlashan suggested that the half-life of Syk mRNA in basophils is 3.5 hours, which is higher than that of IL-4 or FcεRI-α mRNA (~2 h), but somewhat lower than FcεRI-β mRNA (8 h) (259). However, in our study, the optimal silencing at Syk mRNA level was obtained at 48 hours postransfection.

The qRT-PCR study suggested that 80 % Syk mRNA silencing was observed with HP/SH-siRNA nanoparticles at a RU/Nt ratio of (2.5:1). At the same ratio, HP/siRNA nanoparticles successfully reduced Syk mRNA to 65 % of the untreated control levels at 48 hours. No improvement in silencing of Syk mRNA level was observed for HP-CP based nanoparticles by using thiolated siRNA. Thiolated and non-thiolated siRNA showed 45 % Syk mRNA silencing efficiency at 48 hours incubation period for HP-CP.

The effectiveness and low cytotoxicity of this new carrier make it a promising candidate for future *in vivo* siRNA delivery studies in disease models.

In our study, Syk protein and mRNA levels were relatively concordant for HP/SH-siRNA complexes, where gene silencing experiments at protein level showed that at a RU/Nt ratio of (2.5:1), of Syk protein expression was reduced by by treatment with

HP/SH-siRNA complexes, whereas no reduction in expression of Syk protein was observed using 300 nM HP-CP/SH-siRNA nanoparticles at a RU/Nt ratio of 4:1 and HP:CP ratio of 2:1. This value does not correspond with the degranulation inhibition and PCR results, most likely due to the instability of the Syk protein under the experimental conditions, thereby making the data unreliable. Youssef *et al.* suggested that the Syk protein would be unstable in basophils, with calculated half-life of less than 15 minutes (260). However, another published study showed that Syk protein is highly stable for more than 12 hours in human peripheral blood basophils (259). This study suggested that the low Syk expression in basophils in comparison to other types of leukocytes, does not result from protein or mRNA stability. Alternatively, it results from regulation at the transcription level.

Future perspectives

Thiol cross-linked PAA-siRNA nanoparticles have great advantage to develop effective and safe siRNA delivery system due to the presence of thiol in the polymeric backbone. These thiols allow crosslinking between the polymeric chains which increased nanoparticle stability in physiological medium, which in turn would allow these nanoparticles to survive *in vivo* conditions which is lacking in the non-crosslinked systems. The bioreducible properties should allow the selective release of nucleic acid in the intracellular environment and hence be useful for *in vivo* siRNA delivery. In this project, we have used a formulation limited to a particular set of PAA polymer mono-block polymer (HP) and PEGylated tri-block polymer (CP2k) with a defined chain length (11 kDa), degree of pendant sulphydry groups (22 % of the PAA repeating units), and PEG chain length (1.7 kDa) on both sides of central PAA unit with reasonable success to deliver siRNA at *in vitro* level. Hence, there is a still need to compare the effect of the varying molecular weight of PEG molecules and different chain lengths of the central PAA units in the formulation and subsequently on gene silencing. Development of a targeted system by covalent coupling of ligands to one of the polymer components would also facilitate the uptake of siRNA efficiently resulting successful receptor mediated cellular internalization and hopefully, more efficient knockdown effects. Incorporation of membrane disrupting peptides can increase the endosomal escape (261). Very limited data is available for the bio-distribution of siRNA polyplexes, hence pharmacokinetics and bio-distribution studies of the cross-linked siRNA complexes would also play an additional part in the strategy to understand the potential of PAA nanoparticles for clinical use.

References

1. National Institute of Health – Clinical Trials.gov. NCT01591044. 2013. Available at: https://clinicaltrials.gov/ct2/show/NCT01591044?term=R343&cond=Allergy&rank=1.
2. Tatum E. Molecular biology, nucleic acids, and the future of medicine. Cell Ther Transplant. 2009;1:e.000042.01.
3. Wigler M, Silverstein S, Lee LS, Pellicer A, Cheng Y, Axel R. Transfer of purified herpes virus thymidine kinase gene to cultured mouse cells. Cell. 1977;11(1):223-32.
4. Anderson WF, Killos L, Sanders-Haigh L, Kretschmer PJ, Diacumakos EG. Replication and expression of thymidine kinase and human globin genes microinjected into mouse fibroblasts. Proceedings of the National Academy of Sciences of the United States of America. 1980;77(9):5399-403.
5. Eglitis MA, Kantoff P, Gilboa E, Anderson WF. Gene expression in mice after high efficiency retroviral-mediated gene transfer. Science (New York, NY). 1985;230(4732):1395-8.
6. Rosenberg SA, Aebersold P, Cornetta K, Kasid A, Morgan RA, Moen R, et al. Gene transfer into humans--immunotherapy of patients with advanced melanoma, using tumor-infiltrating lymphocytes modified by retroviral gene transduction. The New England journal of medicine. 1990;323(9):570-8.
7. Pathak A, Patnaik S, Gupta KC. Recent trends in non-viral vector-mediated gene delivery. Biotechnology journal. 2009;4(11):1559-72.
8. Raemdonck K, Martens TF, Braeckmans K, Demeester J, De Smedt SC. Polysaccharide-based nucleic acid nanoformulations. Advanced drug delivery reviews. 2013;65(9):1123-47.
9. Pushpendra S, Arvind, P., and Anil, B.,. Pushpendra, S., Arvind, P., and Anil, B., Nucleic Acids as Therapeutics, in From Nucleic Acids Sequences to Molecular Medicine, V.A. Erdmann and J. Barciszewski, Editors. 2012, Springer-Verlag: Berlin. p. 19-45.
10.Hannon GJ. RNA interference. Nature. 2002;418(6894):244-51.
11.Lytle JR, Yario TA, Steitz JA. Target mRNAs are repressed as efficiently by microRNA-binding sites in the 5' UTR as in the 3' UTR. Proceedings of the National Academy of Sciences of the United States of America. 2007;104(23):9667-72.
12.Pecot CV, Calin GA, Coleman RL, Lopez-Berestein G, Sood AK. RNA interference in the clinic: challenges and future directions. Nature reviews Cancer. 2011;11(1):59-67.
13.Whitehead KA, Langer R, Anderson DG. Knocking down barriers: advances in siRNA delivery. Nature reviews Drug discovery. 2009;8(2):129-38.
14.Manfredsson FP, Lewin AS, Mandel RJ. RNA knockdown as a potential therapeutic strategy in Parkinson's disease. Gene therapy. 2006;13(6):517-24.
15.Jacque JM, Triques K, Stevenson M. Modulation of HIV-1 replication by RNA interference. Nature. 2002;418(6896):435-8.
16.Kaiser PK, Symons RC, Shah SM, Quinlan EJ, Tabandeh H, Do DV, et al. RNAi-based treatment for neovascular age-related macular degeneration by Sirna-027. American journal of ophthalmology. 2010;150(1):33-9.e2.
17.Czech MP, Aouadi M, Tesz GJ. RNAi-based therapeutic strategies for metabolic disease. Nature reviews Endocrinology. 2011;7(8):473-84.
18.Xu H, Wilcox D, Nguyen P, Voorbach M, Smith H, Brodjian S, et al. Hepatic knockdown of stearoyl-CoA desaturase 1 via RNA interference in obese mice decreases lipid content and changes fatty acid composition. Frontiers in bioscience : a journal and virtual library. 2007;12:3781-94.
19.Hibbitt O, Agkatsev S, Owen C, Cioroch M, Seymour L, Channon K, et al. RNAi-mediated knockdown of HMG CoA reductase enhances gene expression from physiologically regulated low-density lipoprotein receptor therapeutic vectors in vivo. Gene therapy. 2012;19(4):463-7.

20.Courties G, Presumey J, Duroux-Richard I, Jorgensen C, Apparailly F. RNA interference-based gene therapy for successful treatment of rheumatoid arthritis. Expert opinion on biological therapy. 2009;9(5):535-8.
21.Dillon CP, Sandy P, Nencioni A, Kissler S, Rubinson DA, Van Parijs L. RNAI AS AN EXPERIMENTAL AND THERAPEUTIC TOOL TO STUDY AND REGULATE PHYSIOLOGICAL AND DISEASE PROCESSES. Annual Review of Physiology. 2004;67(1):147-73.
22.Jackson AL, Bartz SR, Schelter J, Kobayashi SV, Burchard J, Mao M, et al. Expression profiling reveals off-target gene regulation by RNAi. Nature biotechnology. 2003;21(6):635-7.
23.Persengiev SP, Zhu X, Green MR. Nonspecific, concentration-dependent stimulation and repression of mammalian gene expression by small interfering RNAs (siRNAs). RNA (New York, NY). 2004;10(1):12-8.
24.Elbashir SM, Harborth J, Lendeckel W, Yalcin A, Weber K, Tuschl T. Duplexes of 21-nucleotide RNAs mediate RNA interference in cultured mammalian cells. Nature. 2001;411(6836):494-8.
25.Maguire AM, Simonelli F, Pierce EA, Pugh ENJ, Mingozzi F, Bennicelli J, et al. Safety and Efficacy of Gene Transfer for Leber's Congenital Amaurosis. New England Journal of Medicine. 2008;358(21):2240-8.
26.Elbashir SM, Harborth J, Weber K, Tuschl T. Analysis of gene function in somatic mammalian cells using small interfering RNAs. Methods (San Diego, Calif). 2002;26(2):199-213.
27.Lee NS, Dohjima T, Bauer G, Li H, Li MJ, Ehsani A, et al. Expression of small interfering RNAs targeted against HIV-1 rev transcripts in human cells. Nat Biotechnol. 2002;20(5):500-5.
28.Wilson JA, Jayasena S, Khvorova A, Sabatinos S, Rodrigue-Gervais IG, Arya S, et al. RNA interference blocks gene expression and RNA synthesis from hepatitis C replicons propagated in human liver cells. Proc Natl Acad Sci U S A. 2003;100(5):2783-8.
29.Jiang M, Milner J. Selective silencing of viral gene expression in HPV-positive human cervical carcinoma cells treated with siRNA, a primer of RNA interference. Oncogene. 2002;21(39):6041-8.
30.Shlomai A, Shaul Y. Inhibition of hepatitis B virus expression and replication by RNA interference. Hepatology. 2003;37(4):764-70.
31.Kitaura J, Song J, Tsai M, Asai K, Maeda-Yamamoto M, Mocsai A, et al. Evidence that IgE molecules mediate a spectrum of effects on mast cell survival and activation via aggregation of the FcεRI. Proceedings of the National Academy of Sciences. 2003;100(22):12911-6.
32.Wilda M, Fuchs U, Wossmann W, Borkhardt A. Killing of leukemic cells with a BCR/ABL fusion gene by RNA interference (RNAi). Oncogene. 2002;21(37):5716-24.
33.Wu H, Hait WN, Yang JM. Small interfering RNA-induced suppression of MDR1 (P-glycoprotein) restores sensitivity to multidrug-resistant cancer cells. Cancer Res. 2003;63(7):1515-9.
34.Nagy P, Arndt-Jovin DJ, Jovin TM. Small interfering RNAs suppress the expression of endogenous and GFP-fused epidermal growth factor receptor (erbB1) and induce apoptosis in erbB1-overexpressing cells. Exp Cell Res. 2003;285(1):39-49.
35.Cioca DP, Aoki Y, Kiyosawa K. RNA interference is a functional pathway with therapeutic potential in human myeloid leukemia cell lines. Cancer Gene Ther. 2003;10(2):125-33.
36.Zhang L, Yang N, Mohamed-Hadley A, Rubin SC, Coukos G. Vector-based RNAi, a novel tool for isoform-specific knock-down of VEGF and anti-angiogenesis gene therapy of cancer. Biochem Biophys Res Commun. 2003;303(4):1169-78.
37.Caplen NJ, Taylor JP, Statham VS, Tanaka F, Fire A, Morgan RA. Rescue of polyglutamine-mediated cytotoxicity by double-stranded RNA-mediated RNA interference. Hum Mol Genet. 2002;11(2):175-84.

38.Xia H, Mao Q, Paulson HL, Davidson BL. siRNA-mediated gene silencing in vitro and in vivo. Nat Biotechnol. 2002;20(10):1006-10.
39.Song E, Lee SK, Wang J, Ince N, Ouyang N, Min J, et al. RNA interference targeting Fas protects mice from fulminant hepatitis. Nat Med. 2003;9(3):347-51.
40.Karlas A, Machuy N, Shin Y, Pleissner KP, Artarini A, Heuer D, et al. Genome-wide RNAi screen identifies human host factors crucial for influenza virus replication. Nature. 2010;463(7282):818-22.
41.Higuchi Y, Kawakami S, Hashida M. Strategies for in vivo delivery of siRNAs: recent progress. BioDrugs : clinical immunotherapeutics, biopharmaceuticals and gene therapy. 2010;24(3):195-205.
42.Oh Y-K, Park TG. siRNA delivery systems for cancer treatment. Advanced drug delivery reviews. 2009;61(10):850-62.
43.Takahashi Y, Nishikawa M, Takakura Y. Nonviral vector-mediated RNA interference: its gene silencing characteristics and important factors to achieve RNAi-based gene therapy. Advanced drug delivery reviews. 2009;61(9):760-6.
44.Wang J, Lu Z, Wientjes MG, Au JL. Delivery of siRNA therapeutics: barriers and carriers. The AAPS journal. 2010;12(4):492-503.
45.Santel A, Aleku M, Keil O, Endruschat J, Esche V, Fisch G, et al. A novel siRNA-lipoplex technology for RNA interference in the mouse vascular endothelium. Gene therapy. 2006;13(16):1222-34.
46.Alexis F, Pridgen E, Molnar LK, Farokhzad OC. Factors Affecting the Clearance and Biodistribution of Polymeric Nanoparticles. Molecular Pharmaceutics. 2008;5(4):505-15.
47.Zhen G, Hinton TM, Muir BW, Shi S, Tizard M, McLean KM, et al. Glycerol monooleate-based nanocarriers for siRNA delivery in vitro. Mol Pharm. 2012;9(9):2450-7.
48.Raymond FR, Ho H-A, Peytavi R, Bissonnette L, Boissinot M, Picard FJ, et al. Detection of target DNA using fluorescent cationic polymer and peptide nucleic acid probes on solid support. BMC Biotechnology. 2005;5:10-.
49.Dai S. CHAPTER 21 Natural Cationic Polymers for Advanced Gene and Drug Delivery. Cationic Polymers in Regenerative Medicine: The Royal Society of Chemistry; 2015. p. 557-82.
50.Rozema DB, Lewis DL, Wakefield DH, Wong SC, Klein JJ, Roesch PL, et al. Dynamic PolyConjugates for targeted in vivo delivery of siRNA to hepatocytes. Proceedings of the National Academy of Sciences of the United States of America. 2007;104(32):12982-7.
51.Xu C-f, Wang J. Delivery systems for siRNA drug development in cancer therapy. Asian Journal of Pharmaceutical Sciences. 2015;10(1):1-12.
52.Rensen PC, van Leeuwen SH, Sliedregt LA, van Berkel TJ, Biessen EA. Design and synthesis of novel N-acetylgalactosamine-terminated glycolipids for targeting of lipoproteins to the hepatic asialoglycoprotein receptor. Journal of medicinal chemistry. 2004;47(23):5798-808.
53.Biessen EAL, Beuting DM, Roelen HCPF, van de Marel GA, Van Boom JH, Van Berkel TJC. Synthesis of Cluster Galactosides with High Affinity for the Hepatic Asialoglycoprotein Receptor. Journal of medicinal chemistry. 1995;38(9):1538-46.
54.Kanasty R, Dorkin JR, Vegas A, Anderson D. Delivery materials for siRNA therapeutics. Nat Mater. 2013;12(11):967-77.
55.Lee H, Lytton-Jean AKR, Chen Y, Love KT, Park AI, Karagiannis ED, et al. Molecularly Self-Assembled Nucleic Acid Nanoparticles for Targeted In Vivo siRNA Delivery. Nature nanotechnology. 2012;7(6):389-93.
56.Tseng YC, Mozumdar S, Huang L. Lipid-based systemic delivery of siRNA. Advanced drug delivery reviews. 2009;61(9):721-31.
57.Hatakeyama H, Ito E, Akita H, Oishi M, Nagasaki Y, Futaki S, et al. A pH-sensitive fusogenic peptide facilitates endosomal escape and greatly enhances the gene silencing of siRNA-

containing nanoparticles in vitro and in vivo. Journal of controlled release : official journal of the Controlled Release Society. 2009;139(2):127-32.
58.Tam YYC, Chen S, Cullis PR. Advances in Lipid Nanoparticles for siRNA Delivery. Pharmaceutics. 2013;5(3):498-507.
59.Sahay G, Querbes W, Alabi C, Eltoukhy A, Sarkar S, Zurenko C, et al. Efficiency of siRNA delivery by lipid nanoparticles is limited by endocytic recycling. Nat Biotech. 2013;31(7):653-8.
60.Love KT, Mahon KP, Levins CG, Whitehead KA, Querbes W, Dorkin JR, et al. Lipid-like materials for low-dose, in vivo gene silencing. Proceedings of the National Academy of Sciences. 2010;107(5):1864-9.
61.Akinc A, Zumbuehl A, Goldberg M, Leshchiner ES, Busini V, Hossain N, et al. A combinatorial library of lipid-like materials for delivery of RNAi therapeutics. Nature biotechnology. 2008;26(5):561-9.
62.Khan A, Benboubetra M, Sayyed PZ, Ng KW, Fox S, Beck G, et al. Sustained polymeric delivery of gene silencing antisense ODNs, siRNA, DNAzymes and ribozymes: in vitro and in vivo studies. Journal of drug targeting. 2004;12(6):393-404.
63.Katas H, Cevher E, Alpar HO. Preparation of polyethyleneimine incorporated poly(d,l-lactide-co-glycolide) nanoparticles by spontaneous emulsion diffusion method for small interfering RNA delivery. International Journal of Pharmaceutics. 2009;369(1):144-54.
64.Nafee N, Taetz S, Schneider M, Schaefer UF, Lehr CM. Chitosan-coated PLGA nanoparticles for DNA/RNA delivery: effect of the formulation parameters on complexation and transfection of antisense oligonucleotides. Nanomedicine : nanotechnology, biology, and medicine. 2007;3(3):173-83.
65.Patil Y, Panyam J. Polymeric nanoparticles for siRNA delivery and gene silencing. Int J Pharm. 2009;367(1-2):195-203.
66.Murata N, Takashima Y, Toyoshima K, Yamamoto M, Okada H. Anti-tumor effects of anti-VEGF siRNA encapsulated with PLGA microspheres in mice. Journal of controlled release : official journal of the Controlled Release Society. 2008;126(3):246-54.
67.Gonzalez H, Hwang SJ, Davis ME. New class of polymers for the delivery of macromolecular therapeutics. Bioconjugate chemistry. 1999;10(6):1068-74.
68.Pun SH, Bellocq NC, Liu A, Jensen G, Machemer T, Quijano E, et al. Cyclodextrin-Modified Polyethylenimine Polymers for Gene Delivery. Bioconjugate chemistry. 2004;15(4):831-40.
69.Hwang SJ, Bellocq NC, Davis ME. Effects of structure of beta-cyclodextrin-containing polymers on gene delivery. Bioconjugate chemistry. 2001;12(2):280-90.
70.Popielarski SR, Mishra S, Davis ME. Structural Effects of Carbohydrate-Containing Polycations on Gene Delivery. 3. Cyclodextrin Type and Functionalization. Bioconjugate chemistry. 2003;14(3):672-8.
71.Davis ME. The First Targeted Delivery of siRNA in Humans via a Self-Assembling, Cyclodextrin Polymer-Based Nanoparticle: From Concept to Clinic. Molecular Pharmaceutics. 2009;6(3):659-68.
72.Hobel S, Aigner A. Polyethylenimine (PEI)/siRNA-mediated gene knockdown in vitro and in vivo. Methods in molecular biology (Clifton, NJ). 2010;623:283-97.
73.Katayose S, Kataoka K. Remarkable increase in nuclease resistance of plasmid DNA through supramolecular assembly with poly(ethylene glycol)-poly(L-lysine) block copolymer. Journal of pharmaceutical sciences. 1998;87(2):160-3.
74.Ragelle H, Vandermeulen G, Preat V. Chitosan-based siRNA delivery systems. Journal of controlled release : official journal of the Controlled Release Society. 2013;172(1):207-18.
75.Meade BR, Dowdy SF. Exogenous siRNA delivery using peptide transduction domains/cell penetrating peptides. Advanced drug delivery reviews. 2007;59(2-3):134-40.

76.Deshayes S, Heitz A, Morris MC, Charnet P, Divita G, Heitz F. Insight into the Mechanism of Internalization of the Cell-Penetrating Carrier Peptide Pep-1 through Conformational Analysis. Biochemistry. 2004;43(6):1449-57.
77.Simeoni F, Morris MC, Heitz F, Divita G. Insight into the mechanism of the peptide-based gene delivery system MPG: implications for delivery of siRNA into mammalian cells. Nucleic acids research. 2003;31(11):2717-24.
78.Fire A, Xu S, Montgomery MK, Kostas SA, Driver SE, Mello CC. Potent and specific genetic interference by double-stranded RNA in Caenorhabditis elegans. Nature. 1998;391(6669):806-11.
79.Svenson S. Dendrimers as versatile platform in drug delivery applications. European journal of pharmaceutics and biopharmaceutics : official journal of Arbeitsgemeinschaft fur Pharmazeutische Verfahrenstechnik eV. 2009;71(3):445-62.
80.Lin C, Blaauboer C-J, Timoneda MM, Lok MC, van Steenbergen M, Hennink WE, et al. Bioreducible poly(amido amine)s with oligoamine side chains: Synthesis, characterization, and structural effects on gene delivery. Journal of Controlled Release. 2008;126(2):166-74.
81.Maiti PK, Çağın T, Lin S-T, Goddard WA. Effect of Solvent and pH on the Structure of PAMAM Dendrimers. Macromolecules. 2005;38(3):979-91.
82.Tomalia DA, Naylor AM, Goddard WA. Starburst Dendrimers: Molecular-Level Control of Size, Shape, Surface Chemistry, Topology, and Flexibility from Atoms to Macroscopic Matter. Angewandte Chemie International Edition in English. 1990;29(2):138-75.
83.Tomalia DA. The dendritic state. Materials Today. 2005;8(3):34-46.
84.Bielinska AU, Chen C, Johnson J, Baker JR, Jr. DNA complexing with polyamidoamine dendrimers: implications for transfection. Bioconjugate chemistry. 1999;10(5):843-50.
85.Kukowska-Latallo JF, Bielinska AU, Johnson J, Spindler R, Tomalia DA, Baker JR. Efficient transfer of genetic material into mammalian cells using Starburst polyamidoamine dendrimers. Proceedings of the National Academy of Sciences of the United States of America. 1996;93(10):4897-902.
86.Tomlinson E, Rolland AP. Controllable gene therapy pharmaceutics of non-viral gene delivery systems. Journal of Controlled Release. 1996;39(2):357-72.
87.Tang MX, Redemann CT, Szoka FC, Jr. In vitro gene delivery by degraded polyamidoamine dendrimers. Bioconjugate chemistry. 1996;7(6):703-14.
88.Luo D, Haverstick K, Belcheva N, Han E, Saltzman WM. Poly(ethylene glycol)-Conjugated PAMAM Dendrimer for Biocompatible, High-Efficiency DNA Delivery. Macromolecules. 2002;35(9):3456-62.
89.Ranucci E, Ferruti P. Block copolymers containing poly(ethylene glycol) and poly(amido-amine) or poly(amido-thioether-amine) segments. Macromolecules. 1991;24(13):3747-52.
90.Hill IR, Garnett MC, Bignotti F, Davis SS. In vitro cytotoxicity of poly(amidoamine)s: relevance to DNA delivery. Biochimica et biophysica acta. 1999;1427(2):161-74.
91.Malik N, Evagorou EG, Duncan R. Dendrimer-platinate: a novel approach to cancer chemotherapy. Anti-cancer drugs. 1999;10(8):767-76.
92.Malik N, Wiwattanapatapee R, Klopsch R, Lorenz K, Frey H, Weener JW, et al. Dendrimers: relationship between structure and biocompatibility in vitro, and preliminary studies on the biodistribution of 125I-labelled polyamidoamine dendrimers in vivo. Journal of controlled release : official journal of the Controlled Release Society. 2000;65(1-2):133-48.
93.Haensler J, Szoka FC, Jr. Polyamidoamine cascade polymers mediate efficient transfection of cells in culture. Bioconjugate chemistry. 1993;4(5):372-9.
94.Danusso F, Ferruti P. Synthesis of tertiary amine polymers. Polymer. 1970;11(2):88-113.
95.Ferruti P, Ranucci E, Bignotti F, Sartore L, Bianciardi P, Marchisio MA. Degradation behaviour of ionic stepwise polyaddition polymers of medical interest. Journal of Biomaterials Science, Polymer Edition. 1995;6(9):833-44.

96.Ferruti P, Marchisio MA, Duncan R. Poly (amido-amine) s: Biomedical Applications. Macromolecular Rapid Communications. 2002;23(5-6):332-55.
97.Ferruti P, Barbucci R. Linear amino polymers: Synthesis, protonation and complex formation. Polymerization Reactions. Berlin, Heidelberg: Springer Berlin Heidelberg; 1984. p. 55-92.
98.Barbucci R, Ferruti P, Improta C, Delfini M, Segre AL, Conti F. Protonation studies of multifunctional polymers with a poly(amido-amine) structure. Polymer. 1978;19(11):1329-34.
99.Richardson S, Ferruti P, Duncan R. Poly(amidoamine)s as potential endosomolytic polymers: evaluation in vitro and body distribution in normal and tumour-bearing animals. Journal of drug targeting. 1999;6(6):391-404.
100. Jones NA, Hill IRC, Stolnik S, Bignotti F, Davis SS, Garnett MC. Polymer chemical structure is a key determinant of physicochemical and colloidal properties of polymer–DNA complexes for gene delivery. Biochimica et Biophysica Acta (BBA) - Gene Structure and Expression. 2000;1517(1):1-18.
101. Lin C, Engbersen JFJ. Effect of chemical functionalities in poly(amido amine)s for non-viral gene transfection. Journal of Controlled Release. 2008;132(3):267-72.
102. Griffiths PC, Paul A, Khayat Z, Wan K-W, King SM, Grillo I, et al. Understanding the Mechanism of Action of Poly(amidoamine)s as Endosomolytic Polymers: Correlation of Physicochemical and Biological Properties. Biomacromolecules. 2004;5(4):1422-7.
103. Stolnik S, Illum L, Davis SS. Long circulating microparticulate drug carriers. Advanced drug delivery reviews. 1995;16(2):195-214.
104. Torchilin VP, Trubetskoy VS. Which polymers can make nanoparticulate drug carriers long-circulating? Advanced drug delivery reviews. 1995;16(2):141-55.
105. Tabata Y, Ikada Y. Effect of the size and surface charge of polymer microspheres on their phagocytosis by macrophage. Biomaterials. 1988;9(4):356-62.
106. Ogris M, Brunner S, Schuller S, Kircheis R, Wagner E. PEGylated DNA/transferrin-PEI complexes: reduced interaction with blood components, extended circulation in blood and potential for systemic gene delivery. Gene therapy. 1999;6(4):595-605.
107. Dash PR, Read ML, Fisher KD, Howard KA, Wolfert M, Oupicky D, et al. Decreased binding to proteins and cells of polymeric gene delivery vectors surface modified with a multivalent hydrophilic polymer and retargeting through attachment of transferrin. The Journal of biological chemistry. 2000;275(6):3793-802.
108. Zhang X, Pan SR, Hu HM, Wu GF, Feng M, Zhang W, et al. Poly(ethylene glycol)-block-polyethylenimine copolymers as carriers for gene delivery: effects of PEG molecular weight and PEGylation degree. Journal of biomedical materials research Part A. 2008;84(3):795-804.
109. Plank C, Mechtler K, Szoka FC, Jr., Wagner E. Activation of the complement system by synthetic DNA complexes: a potential barrier for intravenous gene delivery. Human gene therapy. 1996;7(12):1437-46.
110. Kakizawa Y, Kataoka K. Block copolymer micelles for delivery of gene and related compounds. Advanced drug delivery reviews. 2002;54(2):203-22.
111. Lungwitz U, Breunig M, Blunk T, Gopferich A. Polyethylenimine-based non-viral gene delivery systems. European journal of pharmaceutics and biopharmaceutics : official journal of Arbeitsgemeinschaft fur Pharmazeutische Verfahrenstechnik eV. 2005;60(2):247-66.
112. Kwon GS, Kataoka K. Block copolymer micelles as long-circulating drug vehicles. Advanced drug delivery reviews. 1995;16(2):295-309.
113. Oupický D, Koňák Č, Ulbrich K, Wolfert MA, Seymour LW. DNA delivery systems based on complexes of DNA with synthetic polycations and their copolymers. Journal of Controlled Release. 2000;65(1):149-71.

114. Sung SJ, Min SH, Cho KY, Lee S, Min YJ, Yeom YI, et al. Effect of polyethylene glycol on gene delivery of polyethylenimine. Biological & pharmaceutical bulletin. 2003;26(4):492-500.
115. Rackstraw BJ, Martin AL, Stolnik S, Roberts CJ, Garnett MC, Davies MC, et al. Microscopic Investigations into PEG−Cationic Polymer-Induced DNA Condensation. Langmuir. 2001;17(11):3185-93.
116. Rackstraw BJ, Stolnik S, Davis SS, Bignotti F, Garnett MC. Development of multicomponent DNA delivery systems based upon poly(amidoamine)–PEG co-polymers. Biochimica et Biophysica Acta (BBA) - Gene Structure and Expression. 2002;1576(3):269-86.
117. Anthiya S. Development of miRNA-mimics nanoparticles for the treatment of brain tumours. School of Pharmacy, University of Nottingham. 2016.
118. You Y-Z, Manickam DS, Zhou Q-H, Oupický D. Reducible poly(2-dimethylaminoethyl methacrylate): Synthesis, cytotoxicity, and gene delivery activity. Journal of controlled release : official journal of the Controlled Release Society. 2007;122(3):217-25.
119. Read ML, Singh S, Ahmed Z, Stevenson M, Briggs SS, Oupicky D, et al. A versatile reducible polycation-based system for efficient delivery of a broad range of nucleic acids. Nucleic acids research. 2005;33(9):e86.
120. Lin C, Zhong Z, Lok MC, Jiang X, Hennink WE, Feijen J, et al. Random and block copolymers of bioreducible poly(amido amine)s with high- and low-basicity amino groups: study of DNA condensation and buffer capacity on gene transfection. Journal of controlled release : official journal of the Controlled Release Society. 2007;123(1):67-75.
121. Adami RC, Rice KG. Metabolic stability of glutaraldehyde cross-linked peptide dna condensates. Journal of pharmaceutical sciences. 1999;88(8):739-46.
122. Csaba N, Köping-Höggård M, Alonso MJ. Ionically crosslinked chitosan/tripolyphosphate nanoparticles for oligonucleotide and plasmid DNA delivery. International Journal of Pharmaceutics. 2009;382(1):205-14.
123. Deng JZ, Sun YX, Wang HY, Li C, Huang FW, Cheng SX, et al. Poly(beta-amino amine) cross-linked PEIs as highly efficient gene vectors. Acta biomaterialia. 2011;7(5):2200-8.
124. Jordan PA, Gibbins JM. Extracellular disulfide exchange and the regulation of cellular function. Antioxidants & redox signaling. 2006;8(3-4):312-24.
125. Townsend DM, Tew KD, Tapiero H. The importance of glutathione in human disease. Biomedicine & pharmacotherapy = Biomedecine & pharmacotherapie. 2003;57(3-4):145-55.
126. Reynolds A, Laurie C, Mosley RL, Gendelman HE. Oxidative stress and the pathogenesis of neurodegenerative disorders. International review of neurobiology. 2007;82:297-325.
127. Huber WW, Parzefall W. Thiols and the chemoprevention of cancer. Current opinion in pharmacology. 2007;7(4):404-9.
128. Wu G, Fang Y-Z, Yang S, Lupton JR, Turner ND. Glutathione Metabolism and Its Implications for Health. The Journal of Nutrition. 2004;134(3):489-92.
129. Saito G, Swanson JA, Lee K-D. Drug delivery strategy utilizing conjugation via reversible disulfide linkages: role and site of cellular reducing activities. Advanced drug delivery reviews. 2003;55(2):199-215.
130. Cavallaro G, Campisi M, Licciardi M, Ogris M, Giammona G. Reversibly stable thiopolyplexes for intracellular delivery of genes. Journal of controlled release : official journal of the Controlled Release Society. 2006;115(3):322-34.
131. Hoon Jeong J, Christensen LV, Yockman JW, Zhong Z, Engbersen JF, Jong Kim W, et al. Reducible poly(amido ethylenimine) directed to enhance RNA interference. Biomaterials. 2007;28(10):1912-7.
132. Oishi M, Hayama T, Akiyama Y, Takae S, Harada A, Yamasaki Y, et al. Supramolecular Assemblies for the Cytoplasmic Delivery of Antisense Oligodeoxynucleotide: Polyion

Complex (PIC) Micelles Based on Poly(ethylene glycol)-SS-Oligodeoxynucleotide Conjugate. Biomacromolecules. 2005;6(5):2449-54.
133. Pichon C, LeCam E, Guerin B, Coulaud D, Delain E, Midoux P. Poly[Lys-(AEDTP)]: a cationic polymer that allows dissociation of pDNA/cationic polymer complexes in a reductive medium and enhances polyfection. Bioconjugate chemistry. 2002;13(1):76-82.
134. Garnett Martin C, Ferruti P, Ranucci E, Suardi Marco A, Heyde M, Sleat R. Sterically stabilized self-assembling reversibly cross-linked polyelectrolyte complexes with nucleic acids for environmental and medical applications. Biochemical Society Transactions. 2009;37(4):713-6.
135. Oupicky D, Carlisle RC, Seymour LW. Triggered intracellular activation of disulfide crosslinked polyelectrolyte gene delivery complexes with extended systemic circulation in vivo. Gene therapy. 2001;8(9):713-24.
136. Ferruti P. Poly(amidoamine)s: Past, present, and perspectives. Journal of Polymer Science Part A: Polymer Chemistry. 2013;51(11):2319-53.
137. Ranucci E, Ferruti P, Suardi MA, Manfredi A. Poly(amidoamine)s with 2-Dithiopyridine Side Substituents as Intermediates to Peptide–Polymer Conjugates. Macromolecular Rapid Communications. 2007;28(11):1243-50.
138. Rackstraw BJ, Stolnik S, Davis SS, Bignotti F, Garnett MC. Development of multicomponent DNA delivery systems based upon poly(amidoamine)-PEG co-polymers. Biochimica et biophysica acta. 2002;1576(3):269-86.
139. Aljaeid B. Formulation of novel cross-linked sterically stabilised polyplexes with polyethylene glycol for DNA delivery:. School of Pharmacy, University of Nottingham;. 2012.
140. Danish M. Formulation and characterization of self-assembling, bioreducible cross-linked siRNA polyplexes:. School of Pharmacy, University of Nottingham;. 2014.
141. Zioncheck TF, Harrison ML, Geahlen RL. Purification and characterization of a protein-tyrosine kinase from bovine thymus. Journal of Biological Chemistry. 1986;261(33):15637-43.
142. Mocsai A, Ruland J, Tybulewicz VL. The SYK tyrosine kinase: a crucial player in diverse biological functions. Nature reviews Immunology. 2010;10(6):387-402.
143. Latour S, Zhang J, Siraganian RP, Veillette A. A unique insert in the linker domain of Syk is necessary for its function in immunoreceptor signalling. The EMBO Journal. 1998;17(9):2584-95.
144. de Castro RO. Regulation and Function of Syk Tyrosine Kinase in Mast Cell Signaling and Beyond. Journal of Signal Transduction. 2011;2011.
145. Siraganian RP, Zhang J, Suzuki K, Sada K. Protein tyrosine kinase Syk in mast cell signaling. Molecular immunology. 2002;38(16-18):1229-33.
146. Tohyama Y, Yamamura H. Protein Tyrosine Kinase, Syk: A Key Player in Phagocytic Cells. The Journal of Biochemistry. 2009;145(3):267-73.
147. Mócsai A, Ruland J, Tybulewicz VLJ. The SYK tyrosine kinase: a crucial player in diverse biological functions. Nature reviews Immunology. 2010;10(6):387-402.
148. Faccio R, Teitelbaum SL, Fujikawa K, Chappel J, Zallone A, Tybulewicz VL, et al. Vav3 regulates osteoclast function and bone mass. Nature medicine. 2005;11(3):284-90.
149. Yamada T, Fujieda S, Yanagi S, Yamamura H, Inatome R, Sunaga H, et al. Protein-tyrosine kinase Syk expressed in human nasal fibroblasts and its effect on RANTES production. Journal of immunology (Baltimore, Md : 1950). 2001;166(1):538-43.
150. Coopman PJ, Do MT, Barth M, Bowden ET, Hayes AJ, Basyuk E, et al. The Syk tyrosine kinase suppresses malignant growth of human breast cancer cells. Nature. 2000;406(6797):742-7.
151. Underhill DM, Goodridge HS. The many faces of ITAMs. Trends in immunology. 2007;28(2):66-73.

152. Sanderson MP, Lau CW, Schnapp A, Chow CW. Syk: a novel target for treatment of inflammation in lung disease. Inflammation & allergy drug targets. 2009;8(2):87-95.
153. Fuller GLJ, Williams JAE, Tomlinson MG, Eble JA, Hanna SL, Pöhlmann S, et al. The C-type lectin receptors CLEC-2 and Dectin-1, but not DC-SIGN, signal via a novel YXXL-dependent signalling cascade. The Journal of biological chemistry. 2007;282(17):12397-409.
154. Lau C, Castellanos P, Ranev D, Wang X, Chow CW. HRV signaling in airway epithelial cells is regulated by ITAM-mediated recruitment and activation of Syk. Protein and peptide letters. 2011;18(5):518-29.
155. Deindl S, Kadlecek TA, Brdicka T, Cao X, Weiss A, Kuriyan J. Structural basis for the inhibition of tyrosine kinase activity of ZAP-70. Cell. 2007;129(4):735-46.
156. Tsang E, Giannetti AM, Shaw D, Dinh M, Tse JKY, Gandhi S, et al. Molecular Mechanism of the Syk Activation Switch. Journal of Biological Chemistry. 2008;283(47):32650-9.
157. Cheng AM, Rowley B, Pao W, Hayday A, Bolen JB, Pawson T. Syk tyrosine kinase required for mouse viability and B-cell development. Nature. 1995;378(6554):303-6.
158. Turner M, Mee PJ, Costello PS, Williams O, Price AA, Duddy LP, et al. Perinatal lethality and blocked B-cell development in mice lacking the tyrosine kinase Syk. Nature. 1995;378(6554):298-302.
159. Lu Y, Wang W, Mao H, Hu H, Wu Y, Chen BG, et al. Antibody-mediated platelet phagocytosis by human macrophages is inhibited by siRNA specific for sequences in the SH2 tyrosine kinase, Syk. Cell Immunol. 2011;268(1):1-3.
160. Cheng S, Coffey G, Zhang XH, Shaknovich R, Song Z, Lu P, et al. SYK inhibition and response prediction in diffuse large B-cell lymphoma. Blood. 2011;118(24):6342-52.
161. Buchner M, Baer C, Prinz G, Dierks C, Burger M, Zenz T, et al. Spleen tyrosine kinase inhibition prevents chemokine- and integrin-mediated stromal protective effects in chronic lymphocytic leukemia. Blood. 2010;115(22):4497-506.
162. Matsuda M, Park JG, Wang DC, Hunter S, Chien P, Schreiber AD. Abrogation of the Fc gamma receptor IIA-mediated phagocytic signal by stem-loop Syk antisense oligonucleotides. Molecular biology of the cell. 1996;7(7):1095-106.
163. Stenton GR, Ulanova M, Dery RE, Merani S, Kim MK, Gilchrist M, et al. Inhibition of allergic inflammation in the airways using aerosolized antisense to Syk kinase. Journal of immunology (Baltimore, Md : 1950). 2002;169(2):1028-36.
164. HAYLER J LD, H B. Novel 2,6- disubstituted purines – the synthesis of potent and selective inhibitors of the protein tyrosine kinase syk. Drugs Future. 2002;27:280.
165. Riccaboni M, Bianchi I, Petrillo P. Spleen tyrosine kinases: biology, therapeutic targets and drugs. Drug discovery today. 2010;15(13-14):517-30.
166. Costello PS, Turner M, Walters AE, Cunningham CN, Bauer PH, Downward J, et al. Critical role for the tyrosine kinase Syk in signalling through the high affinity IgE receptor of mast cells. Oncogene. 1996;13(12):2595-605.
167. Kepley CL, Youssef L, Andrews RP, Wilson BS, Oliver JM. Syk deficiency in nonreleaser basophils. Journal of Allergy and Clinical Immunology. 1999;104(2):279-84.
168. Matsubara S, Koya T, Takeda K, Joetham A, Miyahara N, Pine P, et al. Syk activation in dendritic cells is essential for airway hyperresponsiveness and inflammation. American journal of respiratory cell and molecular biology. 2006;34(4):426-33.
169. Matsubara S, Li G, Takeda K, Loader JE, Pine P, Masuda ES, et al. Inhibition of Spleen Tyrosine Kinase Prevents Mast Cell Activation and Airway Hyperresponsiveness. American Journal of Respiratory and Critical Care Medicine. 2006;173(1):56-63.
170. Yamamoto N, Takeshita K, Shichijo M, Kokubo T, Sato M, Nakashima K, et al. The orally available spleen tyrosine kinase inhibitor 2-[7-(3,4-dimethoxyphenyl)-imidazo[1,2-c]pyrimidin-5-ylamino]nicotinamide dihydrochloride (BAY 61-3606) blocks antigen-induced

airway inflammation in rodents. The Journal of pharmacology and experimental therapeutics. 2003;306(3):1174-81.
171. Holgate ST, Polosa R. Treatment strategies for allergy and asthma. Nature Reviews Immunology. 2008;8:218.
172. Passante E, Frankish N. The RBL-2H3 cell line: its provenance and suitability as a model for the mast cell. Inflammation research : official journal of the European Histamine Research Society [et al]. 2009;58(11):737-45.
173. Barsumian EL, Isersky C, Petrino MG, Siraganian RP. IgE-induced histamine release from rat basophilic leukemia cell lines: isolation of releasing and nonreleasing clones. European journal of immunology. 1981;11(4):317-23.
174. Passante E, Ehrhardt C, Sheridan H, Frankish N. In vitro inhibition of rat basophilic leukaemia mast cell (RBL-2H3) degranulation by novel indane compounds. Inflamm Res. 2008;57 Suppl 1:S15-6.
175. Kim CH, Lee T, Oh I, Nam KW, Kim KH, Oh KB, et al. Mast cell stabilizing effect of (-)-Elema-1,3,11(13)-trien-12-ol and thujopsene from Thujopsis dolabrata is mediated by down-regulation of interleukin-4 secretion in antigen-induced RBL-2H3 cells. Biological & pharmaceutical bulletin. 2013;36(3):339-45.
176. Daniel W. Development of high-throughput, humanised rat basophilic leukaemia reporter systems for assessment of allergic sensitisation. School of Pharmacy, University of Nottingham. 2014.
177. Sanderson MP, Gelling SJ, Rippmann JF, Schnapp A. Comparison of the anti-allergic activity of Syk inhibitors with optimized Syk siRNAs in FcεRI-activated RBL-2H3 basophilic cells. Cellular Immunology. 2010;262(1):28-34.
178. Tatemoto K, Carlquist M, Mutt V. Neuropeptide Y--a novel brain peptide with structural similarities to peptide YY and pancreatic polypeptide. Nature. 1982;296(5858):659-60.
179. Azouz NP, Matsui T, Fukuda M, Sagi-Eisenberg R. Decoding the regulation of mast cell exocytosis by networks of Rab GTPases. Journal of immunology (Baltimore, Md : 1950). 2012;189(5):2169-80.
180. Pfaffl MW. A new mathematical model for relative quantification in real-time RT-PCR. Nucleic acids research. 2001;29(9):e45.
181. Ghildiyal M, Zamore PD. Small silencing RNAs: an expanding universe. Nat Rev Genet. 2009;10(2):94-108.
182. Gabrielson NP, Lu H, Yin L, Kim KH, Cheng J. A cell-penetrating helical polymer for siRNA delivery to mammalian cells. Molecular therapy : the journal of the American Society of Gene Therapy. 2012;20(8):1599-609.
183. Zheng N, Song Z, Liu Y, Zhang R, Zhang R, Yao C, et al. Redox-responsive, reversibly-crosslinked thiolated cationic helical polypeptides for efficient siRNA encapsulation and delivery. Journal of controlled release : official journal of the Controlled Release Society. 2015;205:231-9.
184. Breunig M, Hozsa C, Lungwitz U, Watanabe K, Umeda I, Kato H, et al. Mechanistic investigation of poly(ethylene imine)-based siRNA delivery: disulfide bonds boost intracellular release of the cargo. Journal of controlled release : official journal of the Controlled Release Society. 2008;130(1):57-63.
185. Lee SJ, Huh MS, Lee SY, Min S, Lee S, Koo H, et al. Tumor-homing poly-siRNA/glycol chitosan self-cross-linked nanoparticles for systemic siRNA delivery in cancer treatment. Angewandte Chemie (International ed in English). 2012;51(29):7203-7.
186. Namgung R, Kim WJ. A highly entangled polymeric nanoconstruct assembled by siRNA and its reduction-triggered siRNA release for gene silencing. Small (Weinheim an der Bergstrasse, Germany). 2012;8(20):3209-19.

187. Mok H, Lee SH, Park JW, Park TG. Multimeric small interfering ribonucleic acid for highly efficient sequence-specific gene silencing. Nat Mater. 2010;9(3):272-8.
188. Al-Qadi S, Alatorre-Meda M, Zaghloul EM, Taboada P, Remunán-López C. Chitosan–hyaluronic acid nanoparticles for gene silencing: The role of hyaluronic acid on the nanoparticles' formation and activity. Colloids and Surfaces B: Biointerfaces. 2013;103:615-23.
189. Liao ZX, Ho YC, Chen HL, Peng SF, Hsiao CW, Sung HW. Enhancement of efficiencies of the cellular uptake and gene silencing of chitosan/siRNA complexes via the inclusion of a negatively charged poly(gamma-glutamic acid). Biomaterials. 2010;31(33):8780-8.
190. Ravina M, Cubillo E, Olmeda D, Novoa-Carballal R, Fernandez-Megia E, Riguera R, et al. Hyaluronic acid/chitosan-g-poly(ethylene glycol) nanoparticles for gene therapy: an application for pDNA and siRNA delivery. Pharmaceutical research. 2010;27(12):2544-55.
191. Lee SJ, Lee A, Hwang SR, Park JS, Jang J, Huh MS, et al. TNF-alpha gene silencing using polymerized siRNA/thiolated glycol chitosan nanoparticles for rheumatoid arthritis. Molecular therapy : the journal of the American Society of Gene Therapy. 2014;22(2):397-408.
192. Osada K, Christie RJ, Kataoka K. Polymeric micelles from poly(ethylene glycol)–poly(amino acid) block copolymer for drug and gene delivery. Journal of the Royal Society Interface. 2009;6(Suppl 3):S325-S39.
193. Garnett MC. Gene-delivery systems using cationic polymers. Critical reviews in therapeutic drug carrier systems. 1999;16(2):147-207.
194. Dautzenberg H. Polyelectrolyte Complex Formation in Highly Aggregating Systems. 1. Effect of Salt: Polyelectrolyte Complex Formation in the Presence of NaCl. Macromolecules. 1997;30(25):7810-5.
195. Perry S, Li Y, Priftis D, Leon L, Tirrell M. The Effect of Salt on the Complex Coacervation of Vinyl Polyelectrolytes. Polymers. 2014;6(6):1756.
196. Scientific T. Crosslinking Technical Handbook.
197. Kabanov AV, Astafyeva IV, Chikindas ML, Rosenblat GF, Kiselev VI, Severin ES, et al. DNA interpolyelectrolyte complexes as a tool for efficient cell transformation. Biopolymers. 1991;31(12):1437-43.
198. Priftis D, Tirrell M. Phase behaviour and complex coacervation of aqueous polypeptide solutions. Soft Matter. 2012;8(36):9396-405.
199. Wan KW, Malgesini B, Verpilio I, Ferruti P, Griffiths PC, Paul A, et al. Poly(amidoamine) salt form: effect on pH-dependent membrane activity and polymer conformation in solution. Biomacromolecules. 2004;5(3):1102-9.
200. Wan K-W, Malgesini B, Verpilio I, Ferruti P, Griffiths PC, Paul A, et al. Poly(amidoamine) Salt Form: Effect on pH-Dependent Membrane Activity and Polymer Conformation in Solution. Biomacromolecules. 2004;5(3):1102-9.
201. Jere D, Kim JE, Arote R, Jiang HL, Kim YK, Choi YJ, et al. Akt1 silencing efficiencies in lung cancer cells by sh/si/ssiRNA transfection using a reductable polyspermine carrier. Biomaterials. 2009;30(8):1635-47.
202. Wiradharma N, Khan M, Tong YW, Wang S, Yang Y-Y. Self-assembled Cationic Peptide Nanoparticles Capable of Inducing Efficient Gene Expression In Vitro. Advanced Functional Materials. 2008;18(6):943-51.
203. Muthiah M, Che HL, Kalash S, Jo J, Choi SY, Kim WJ, et al. Formulation of glutathione responsive anti-proliferative nanoparticles from thiolated Akt1 siRNA and disulfide-crosslinked PEI for efficient anti-cancer gene therapy. Colloids and surfaces B, Biointerfaces. 2015;126:322-7.
204. Dorsett Y, Tuschl T. siRNAs: applications in functional genomics and potential as therapeutics. Nature reviews Drug discovery. 2004;3(4):318-29.

205. Peng Q, Zhong Z, Zhuo R. Disulfide Cross-Linked Polyethylenimines (PEI) Prepared via Thiolation of Low Molecular Weight PEI as Highly Efficient Gene Vectors. Bioconjugate chemistry. 2008;19(2):499-506.
206. Brülisauer L, Gauthier MA, Leroux J-C. Disulfide-containing parenteral delivery systems and their redox-biological fate. Journal of Controlled Release. 2014;195:147-54.
207. Tatemoto K, Carlquist M, Mutt V. Neuropeptide Y[mdash]a novel brain peptide with structural similarities to peptide YY and pancreatic polypeptide. Nature. 1982;296(5858):659-60.
208. O'Brien J, Wilson I, Orton T, Pognan F. Investigation of the Alamar Blue (resazurin) fluorescent dye for the assessment of mammalian cell cytotoxicity. European journal of biochemistry. 2000;267(17):5421-6.
209. Semizarov D, Frost L, Sarthy A, Kroeger P, Halbert DN, Fesik SW. Specificity of short interfering RNA determined through gene expression signatures. Proceedings of the National Academy of Sciences of the United States of America. 2003;100(11):6347-52.
210. Choi Y, Kim MS, Hwang JK. Inhibitory effects of panduratin A on allergy-related mediator production in rat basophilic leukemia mast cells. Inflammation. 2012;35(6):1904-15.
211. Huang FH, Zhang XY, Zhang LY, Li Q, Ni B, Zheng XL, et al. Mast cell degranulation induced by chlorogenic acid. Acta pharmacologica Sinica. 2010;31(7):849-54.
212. Stone KD, Prussin C, Metcalfe DD. IgE, mast cells, basophils, and eosinophils. The Journal of allergy and clinical immunology. 2010;125(2 Suppl 2):S73-80.
213. Amin K. The role of mast cells in allergic inflammation. Respiratory medicine. 2012;106(1):9-14.
214. Passante E, Ehrhardt C, Sheridan H, Frankish N. RBL-2H3 cells are an imprecise model for mast cell mediator release. Inflammation research : official journal of the European Histamine Research Society [et al]. 2009;58(9):611-8.
215. Pinho BR, Sousa C, Valentão P, Oliveira JMA, Andrade PB. Modulation of Basophils' Degranulation and Allergy-Related Enzymes by Monomeric and Dimeric Naphthoquinones. PLoS ONE. 2014;9(2):e90122.
216. Schwarz DS, Hutvagner G, Du T, Xu Z, Aronin N, Zamore PD. Asymmetry in the assembly of the RNAi enzyme complex. Cell. 2003;115(2):199-208.
217. Khvorova A, Reynolds A, Jayasena SD. Functional siRNAs and miRNAs exhibit strand bias. Cell. 2003;115(2):209-16.
218. Kretschmer-Kazemi Far R, Sczakiel G. The activity of siRNA in mammalian cells is related to structural target accessibility: a comparison with antisense oligonucleotides. Nucleic acids research. 2003;31(15):4417-24.
219. Patzel V, Rutz S, Dietrich I, Koberle C, Scheffold A, Kaufmann SH. Design of siRNAs producing unstructured guide-RNAs results in improved RNA interference efficiency. Nature biotechnology. 2005;23(11):1440-4.
220. Turner M, Schweighoffer E, Colucci F, Di Santo JP, Tybulewicz VL. Tyrosine kinase SYK: essential functions for immunoreceptor signalling. Immunology today. 2000;21(3):148-54.
221. Wong BR, Grossbard EB, Payan DG, Masuda ES. Targeting Syk as a treatment for allergic and autoimmune disorders. Expert opinion on investigational drugs. 2004;13(7):743-62.
222. Pine PR, Chang B, Schoettler N, Banquerigo ML, Wang S, Lau A, et al. Inflammation and bone erosion are suppressed in models of rheumatoid arthritis following treatment with a novel Syk inhibitor. Clinical immunology (Orlando, Fla). 2007;124(3):244-57.
223. Moore TL, Rodriguez-Lorenzo L, Hirsch V, Balog S, Urban D, Jud C, et al. Nanoparticle colloidal stability in cell culture media and impact on cellular interactions. Chemical Society Reviews. 2015;44(17):6287-305.

224. Moghimi SM, Symonds P, Murray JC, Hunter AC, Debska G, Szewczyk A. A two-stage poly(ethylenimine)-mediated cytotoxicity: Implications for gene transfer/therapy. Molecular Therapy. 2005;11(6):990-5.
225. Neu M, Fischer D, Kissel T. Recent advances in rational gene transfer vector design based on poly(ethylene imine) and its derivatives. Journal of Gene Medicine. 2005;7(8):992-1009.
226. Ahn CH, Chae SY, Bae YH, Kim SW. Synthesis of biodegradable multi-block copolymers of poly(L-lysine) and poly(ethylene glycol) as a non-viral gene carrier. Journal of Controlled Release. 2004;97(3):567-74.
227. Mano SS, Kanehira K, Sonezaki S, Taniguchi A. Effect of Polyethylene Glycol Modification of TiO2 Nanoparticles on Cytotoxicity and Gene Expressions in Human Cell Lines. International Journal of Molecular Sciences. 2012;13(3):3703-17.
228. Choksakulnimitr S, Masuda S, Tokuda H, Takakura Y, Hashida M. In vitro cytotoxicity of macromolecules in different cell culture systems. Journal of Controlled Release. 1995;34(3):233-41.
229. Fischer D, Bieber T, Li Y, Elsasser HP, Kissel T. A novel non-viral vector for DNA delivery based on low molecular weight, branched polyethylenimine: effect of molecular weight on transfection efficiency and cytotoxicity. Pharmaceutical research. 1999;16(8):1273-9.
230. Chen DJ, Majors BS, Zelikin A, Putnam D. Structure–function relationships of gene delivery vectors in a limited polycation library. Journal of Controlled Release. 2005;103(1):273-83.
231. Yang J, Kemps-Mols B, Spruyt-Gerritse M, Anholts J, Claas F, Eikmans M. The source of SYBR green master mix determines outcome of nucleic acid amplification reactions. BMC Research Notes. 2016;9:292.
232. Ririe KM, Rasmussen RP, Wittwer CT. Product differentiation by analysis of DNA melting curves during the polymerase chain reaction. Analytical biochemistry. 1997;245(2):154-60.
233. Hu Y, Xie J, Tong YW, Wang CH. Effect of PEG conformation and particle size on the cellular uptake efficiency of nanoparticles with the HepG2 cells. Journal of controlled release : official journal of the Controlled Release Society. 2007;118(1):7-17.
234. Gref R, Luck M, Quellec P, Marchand M, Dellacherie E, Harnisch S, et al. 'Stealth' corona-core nanoparticles surface modified by polyethylene glycol (PEG): influences of the corona (PEG chain length and surface density) and of the core composition on phagocytic uptake and plasma protein adsorption. Colloids and surfaces B, Biointerfaces. 2000;18(3-4):301-13.
235. Cruje C, Chithrani D. Polyethylene Glycol Density and Length Affects Nanoparticle Uptake by Cancer Cells. Journal of Nanomedicine Research 2014;1(1):1-6.
236. Pelaz B, del Pino P, Maffre P, Hartmann R, Gallego M, Rivera-Fernández S, et al. Surface Functionalization of Nanoparticles with Polyethylene Glycol: Effects on Protein Adsorption and Cellular Uptake. ACS Nano. 2015;9(7):6996-7008.
237. Dash PR, Toncheva V, Schacht E, Seymour LW. Synthetic polymers for vectorial delivery of DNA: characterisation of polymer-DNA complexes by photon correlation spectroscopy and stability to nuclease degradation and disruption by polyanions in vitro. Journal of Controlled Release. 1997;48(2):269-76.
238. Narz F, Hübner S, Magyar S, Bielke W, Weber M, Dennig J. Enrichment strategies for siRNA-transfected cells in an untransfected background. Journal of Biotechnology. 2007;130(3):209-12.
239. Tschaharganeh D, Ehemann V, Nussbaum T, Schirmacher P, Breuhahn K. Non-specific effects of siRNAs on tumor cells with implications on therapeutic applicability using RNA interference. Pathology oncology research : POR. 2007;13(2):84-90.

240. Lin C, Zhong Z, Lok MC, Jiang X, Hennink WE, Feijen J, et al. Linear poly(amido amine)s with secondary and tertiary amino groups and variable amounts of disulfide linkages: synthesis and in vitro gene transfer properties. Journal of controlled release : official journal of the Controlled Release Society. 2006;116(2):130-7.
241. Raemdonck K, Demeester J, De Smedt S. Advanced nanogel engineering for drug delivery. Soft Matter. 2009;5(4):707-15.
242. Zhang X, Malhotra S, Molina M, Haag R. Micro- and nanogels with labile crosslinks - from synthesis to biomedical applications. Chem Soc Rev. 2015;44(7):1948-73.
243. Abdul Ghafoor Raja M, Katas H, Jing Wen T. Stability, Intracellular Delivery, and Release of siRNA from Chitosan Nanoparticles Using Different Cross-Linkers. PLoS ONE. 2015;10(6):e0128963.
244. Breunig M, Hozsa C, Lungwitz U, Watanabe K, Umeda I, Kato H, et al. Mechanistic investigation of poly(ethylene imine)-based siRNA delivery: Disulfide bonds boost intracellular release of the cargo. Journal of Controlled Release. 2008;130(1):57-63.
245. Mok H, Lee SH, Park JW, Park TG. Multimeric small interfering ribonucleic acid for highly efficient sequence-specific gene silencing. Nature Materials. 2010;9(3):272-8.
246. Rojanarata T, Opanasopit P, Techaarpornkul S, Ngawhirunpat T, Ruktanonchai U. Chitosan-Thiamine Pyrophosphate as a Novel Carrier for siRNA Delivery. Pharmaceutical research. 2008;25(12):2807.
247. Ragelle H, Vandermeulen G, Préat V. Chitosan-based siRNA delivery systems. Journal of Controlled Release. 2013;172(1):207-18.
248. Yoo JM, Park ES, Kim MR, Sok DE. Inhibitory effect of N-Acyl dopamines on IgE-mediated allergic response in RBL-2H3 cells. Lipids. 2013;48(4):383-93.
249. Granberg M, Fowler CJ, Jacobsson SO. Effects of the cannabimimetic fatty acid derivatives 2-arachidonoylglycerol, anandamide, palmitoylethanolamide and methanandamide upon IgE-dependent antigen-induced beta-hexosaminidase, serotonin and TNF alpha release from rat RBL-2H3 basophilic leukaemic cells. Naunyn-Schmiedeberg's archives of pharmacology. 2001;364(1):66-73.
250. Chung MJ, Sohng JK, Choi DJ, Park YI. Inhibitory effect of phloretin and biochanin A on IgE-mediated allergic responses in rat basophilic leukemia RBL-2H3 cells. Life sciences. 2013;93(9-11):401-8.
251. Azouz NP, Matsui T, Fukuda M, Sagi-Eisenberg R. Decoding the Regulation of Mast Cell Exocytosis by Networks of Rab GTPases. The Journal of Immunology. 2012;189(5):2169-80.
252. Wang X, Cato P, Lin HC, Li T, Wan D, Alcocer MJ, et al. Optimisation and use of humanised RBL NF-AT-GFP and NF-AT-DsRed reporter cell lines suitable for high-throughput scale detection of allergic sensitisation in array format and identification of the ECM-integrin interaction as critical factor. Molecular biotechnology. 2014;56(2):136-46.
253. Che H-L, Bae I-H, Lim KS, Song IT, Lee H, Muthiah M, et al. Suppression of post-angioplasty restenosis with an Akt1 siRNA-embedded coronary stent in a rabbit model. Biomaterials. 2012;33(33):8548-56.
254. Creusat G, Thomann JS, Maglott A, Pons B, Dontenwill M, Guerin E, et al. Pyridylthiourea-grafted polyethylenimine offers an effective assistance to siRNA-mediated gene silencing in vitro and in vivo. Journal of controlled release : official journal of the Controlled Release Society. 2012;157(3):418-26.
255. Goyal R, Bansal R, Tyagi S, Shukla Y, Kumar P, Gupta KC. 1,4-Butanediol diglycidyl ether (BDE)-crosslinked PEI-g-imidazole nanoparticles as nucleic acid-carriers in vitro and in vivo. Molecular BioSystems. 2011;7(6):2055-65.
256. Buschmann MD, Merzouki A, Lavertu M, Thibault M, Jean M, Darras V. Chitosans for delivery of nucleic acids. Advanced drug delivery reviews. 2013;65(9):1234-70.
257. . Small GTPases in Disease -2011 - Science - Part 1 - Page 198.

258. Ki KH, Park DY, Lee SH, Kim NY, Choi BM, Noh GJ. The optimal concentration of siRNA for gene silencing in primary cultured astrocytes and microglial cells of rats. Korean Journal of Anesthesiology. 2010;59(6):403-10.
259. MacGlashan D. Stability of Syk protein and mRNA in human peripheral blood basophils. Journal of Leukocyte Biology. 2016;100(3):535-43.
260. Youssef LA, Wilson BS, Oliver JM. Proteasome-dependent regulation of Syk tyrosine kinase levels in human basophils. The Journal of allergy and clinical immunology. 2002;110(3):366-73.
261. El-Sayed A, Futaki S, Harashima H. Delivery of macromolecules using arginine-rich cell-penetrating peptides: ways to overcome endosomal entrapment. The AAPS journal. 2009;11(1):13-22.

Appendix

Appendix A

DLS analysis of thiolated and non-thiolated siRNA polyplexes

Free siRNAs

I. Free non-thiolated siRNA

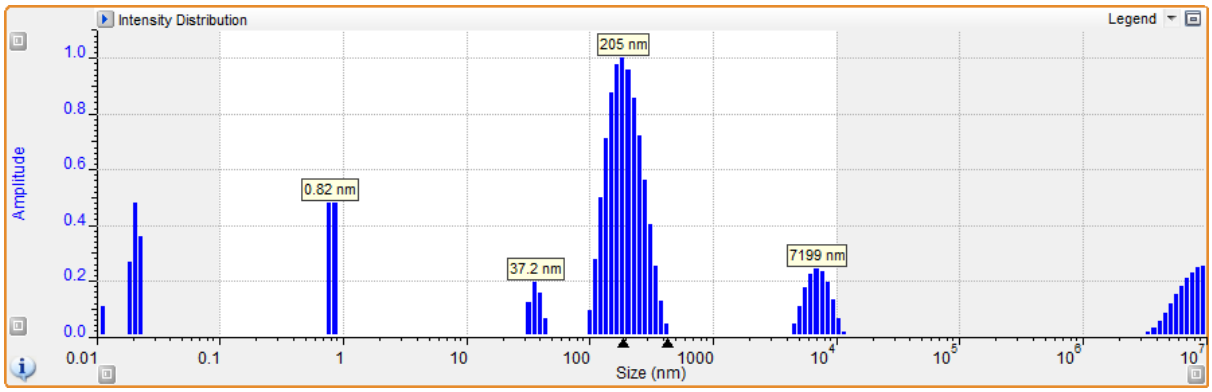

II. Free thiolated siRNA

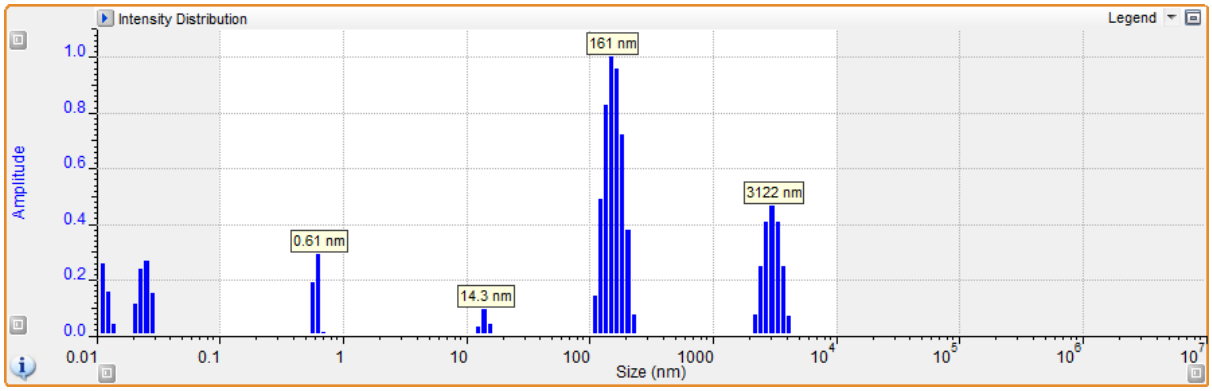

HP/siRNA nanoparticles

I. RU/Nt ratio of 0.5:1

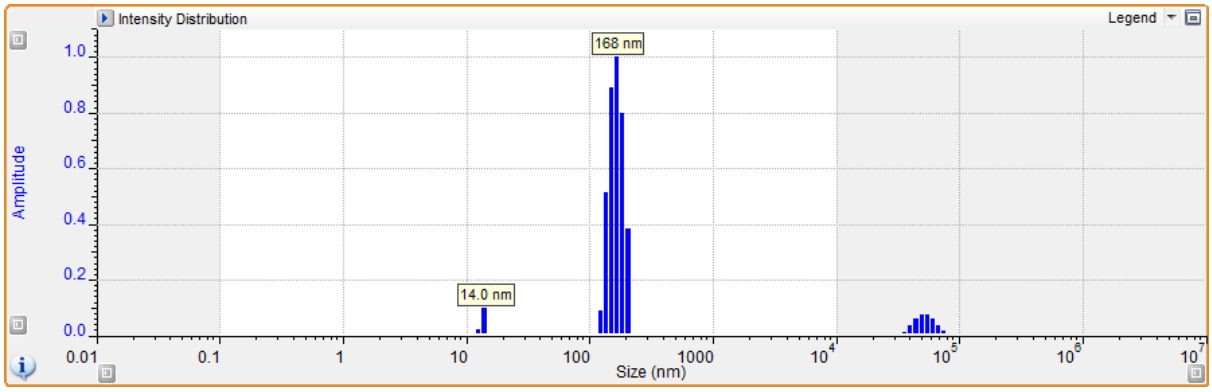

II. RU/Nt ratio of 1:1

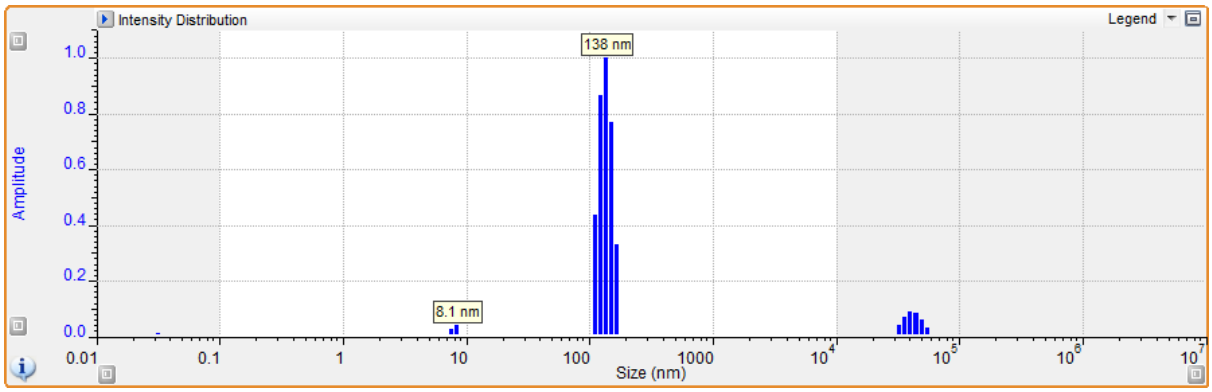

III. RU/Nt ratio of 1.5:1

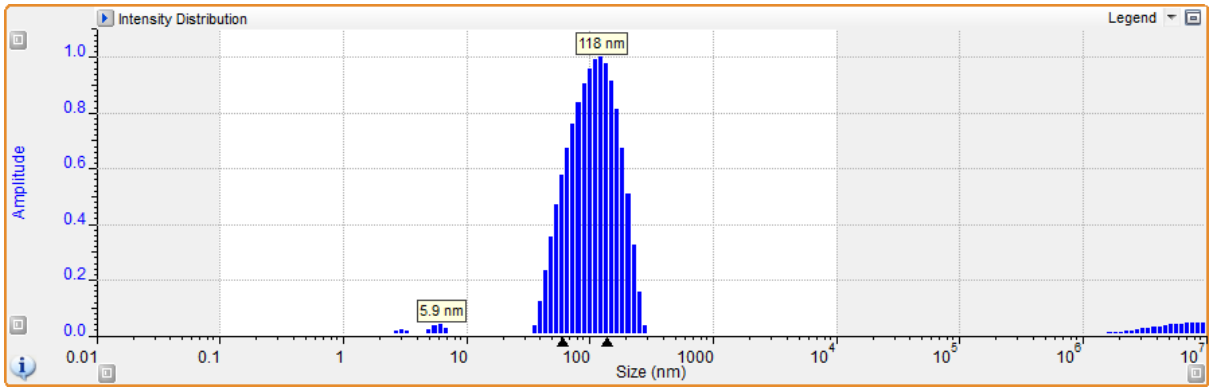

IV. RU/Nt ratio of 2:1

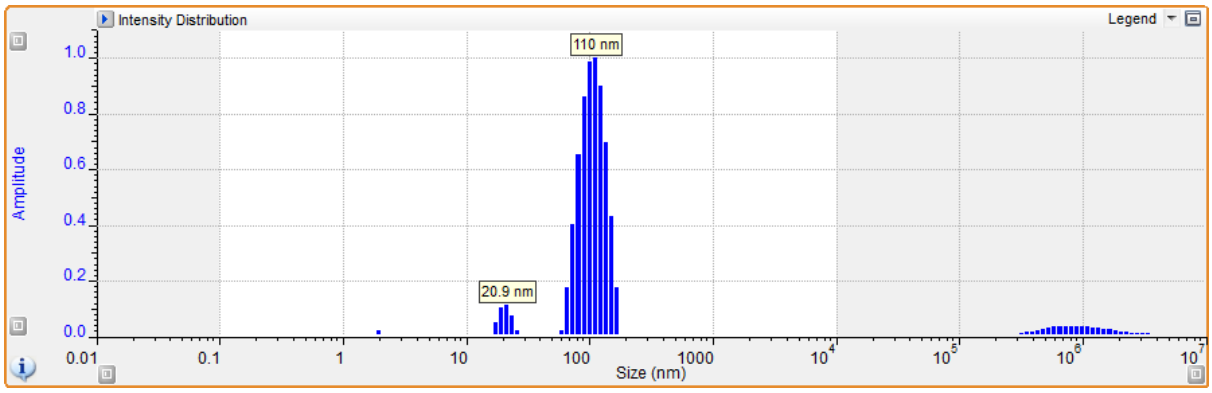

V. RU/Nt ratio of 2.5:1

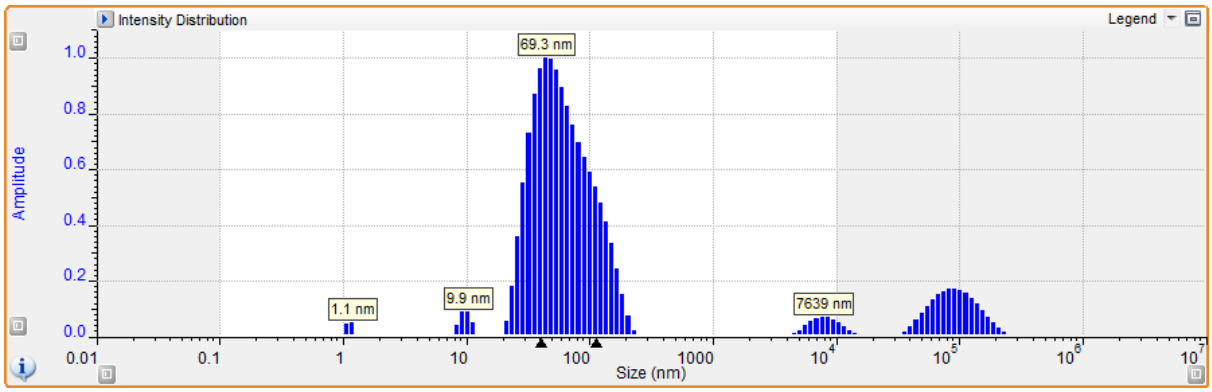

VI. RU/Nt ratio of 3:1

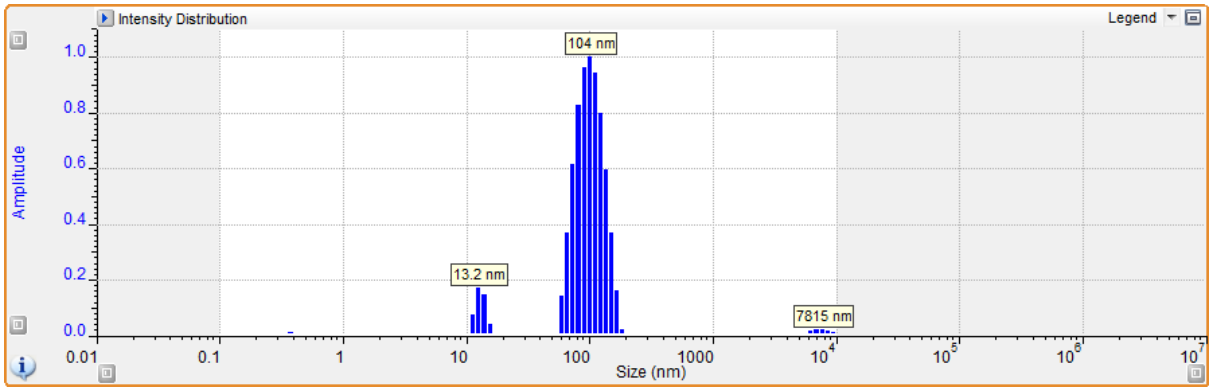

VII. RU/Nt ratio of 4:1

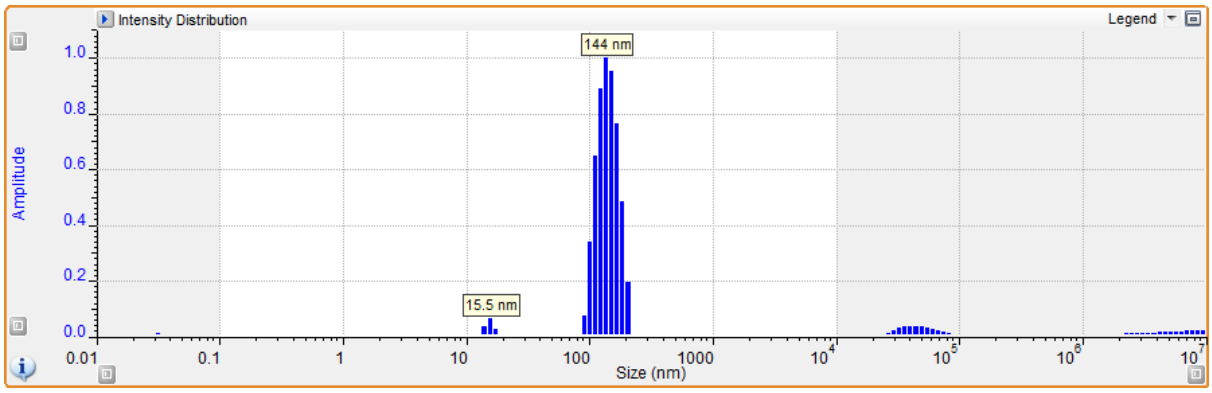

VIII. RU/Nt ratio of 5:1

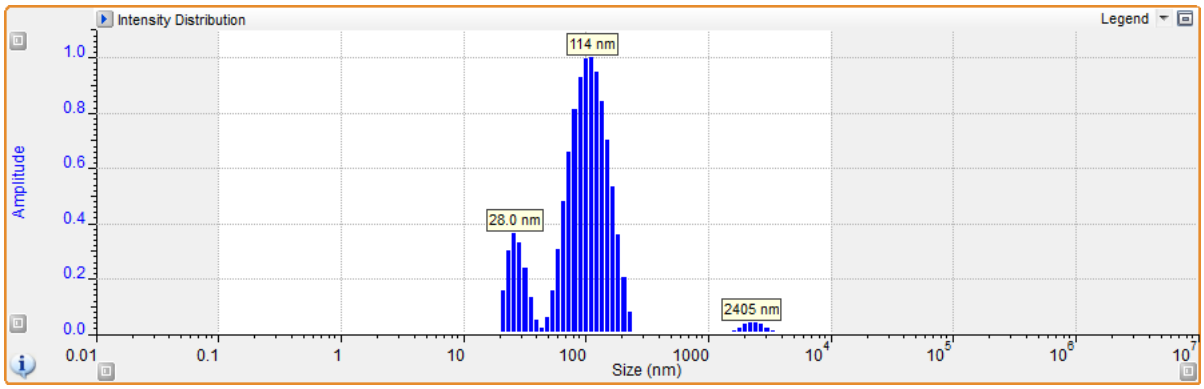

HP/SH-siRNA nanoparticles

I. RU/Nt ratio of 0.5:1

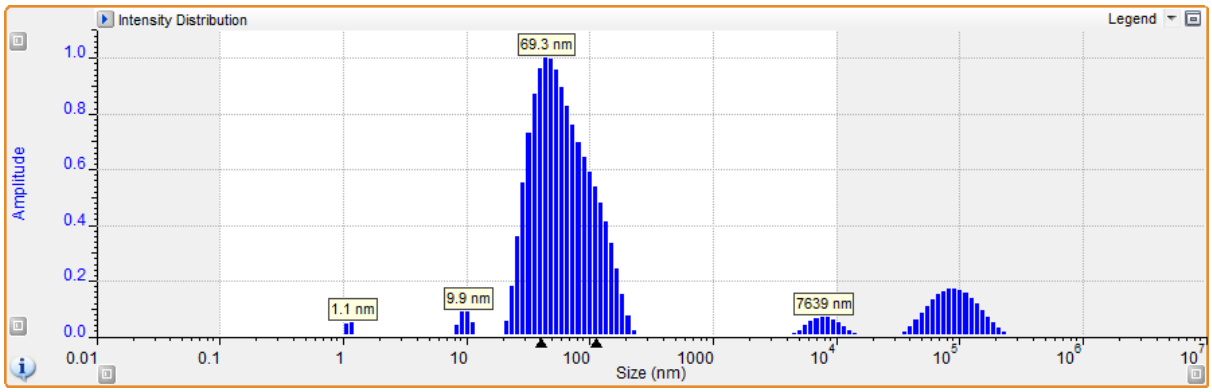

II. RU/Nt ratio of 1:1

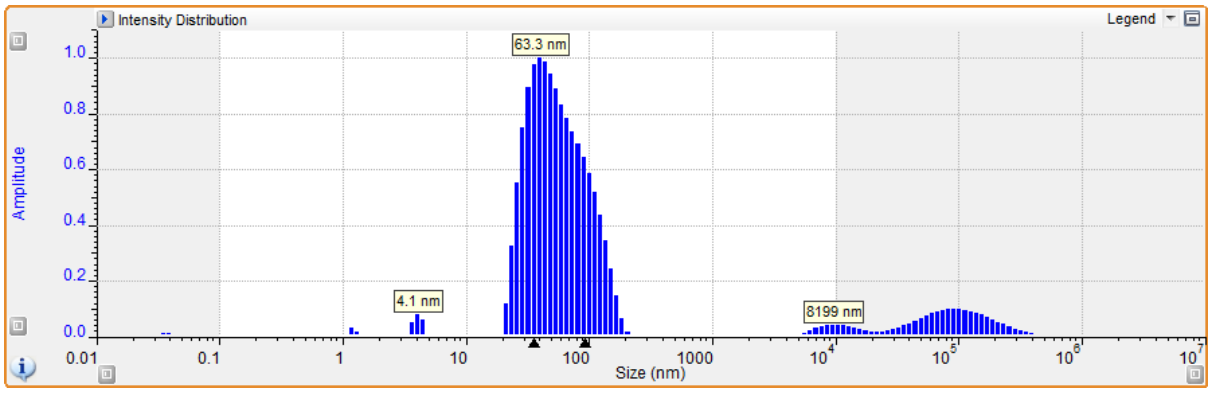

III. RU/Nt ratio of 1.5:1

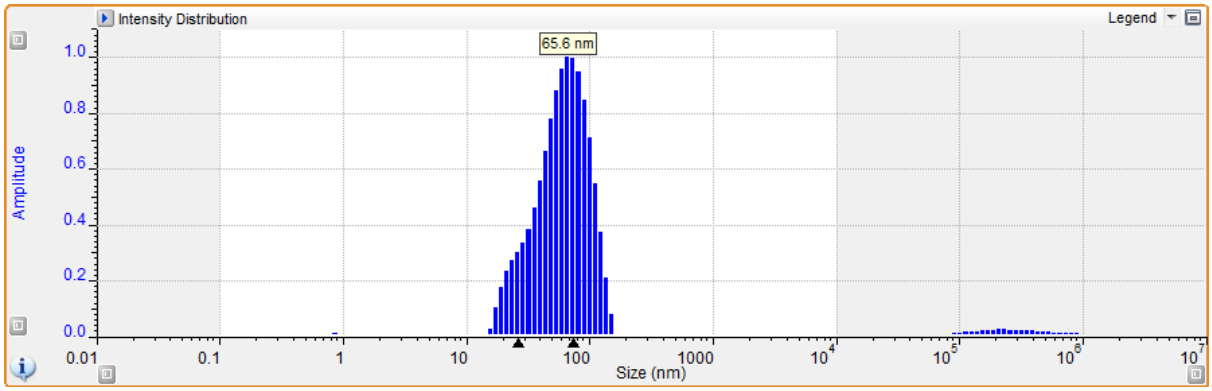

IV. RU/Nt ratio of 2:1

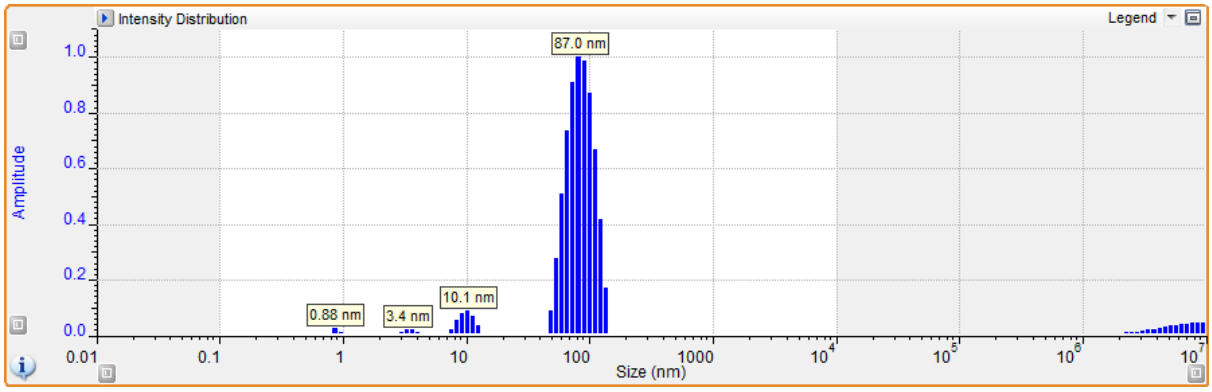

V. RU/Nt ratio of 2.5:1

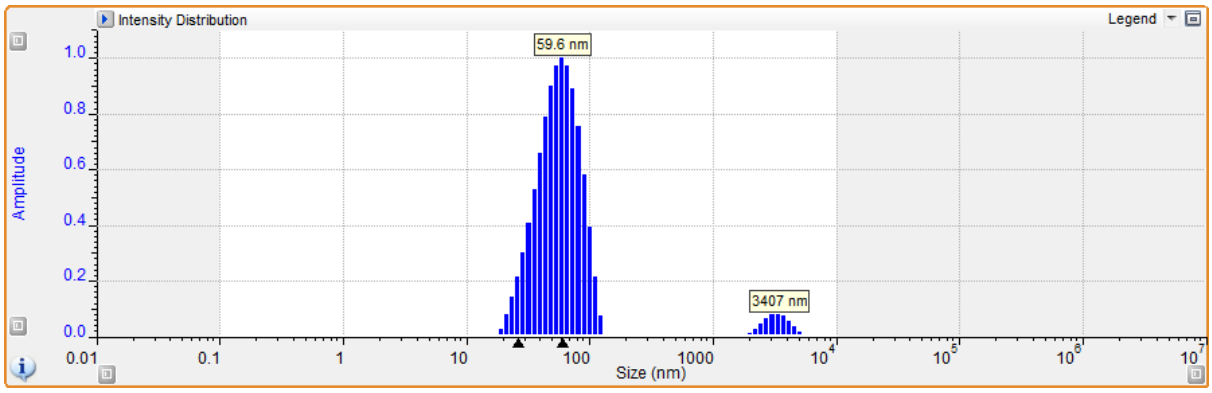

VI. RU/Nt ratio of 3:1

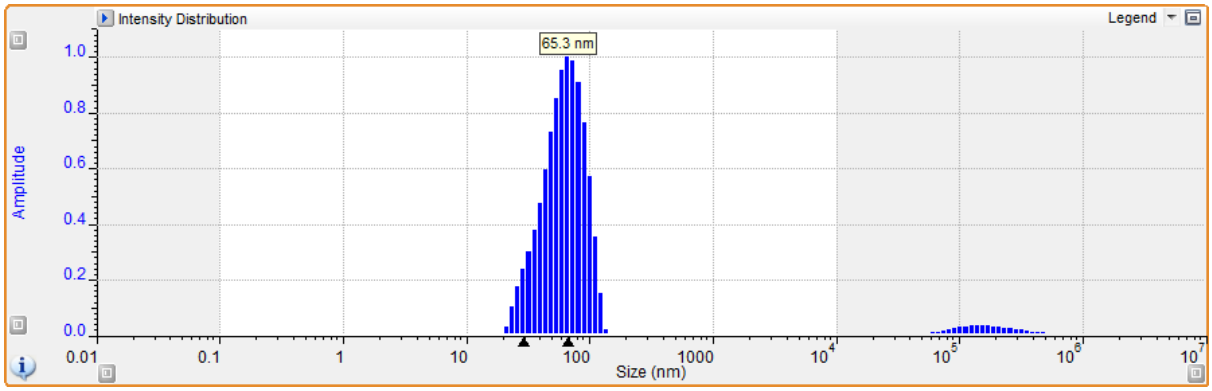

VII. RU/Nt ratio of 4:1

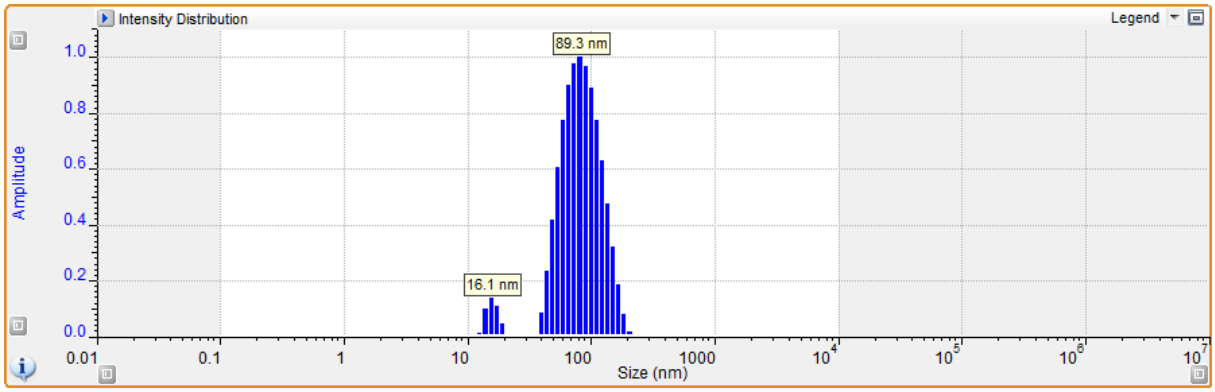

VIII. RU/Nt ratio of 5:1

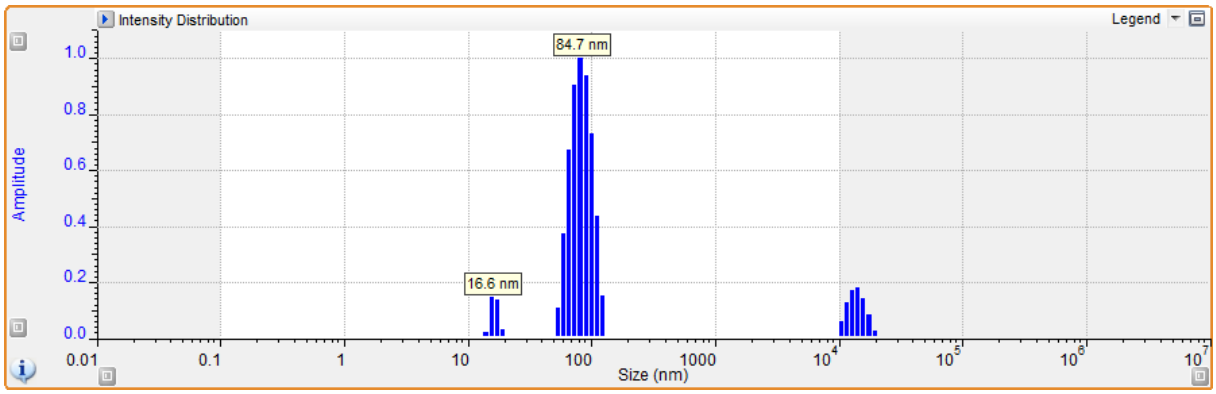

HP-CP/siRNA nanoparticles

I. RU/Nt ratio of 2.5:1 & HP:CP ratio of 1:1

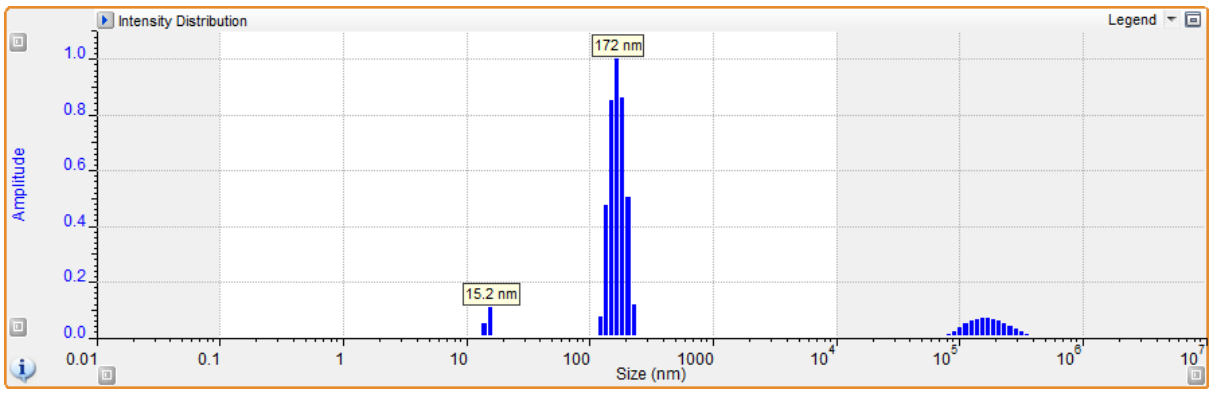

II. RU/Nt ratio of 2.5:1 & HP:CP ratio of 2:1

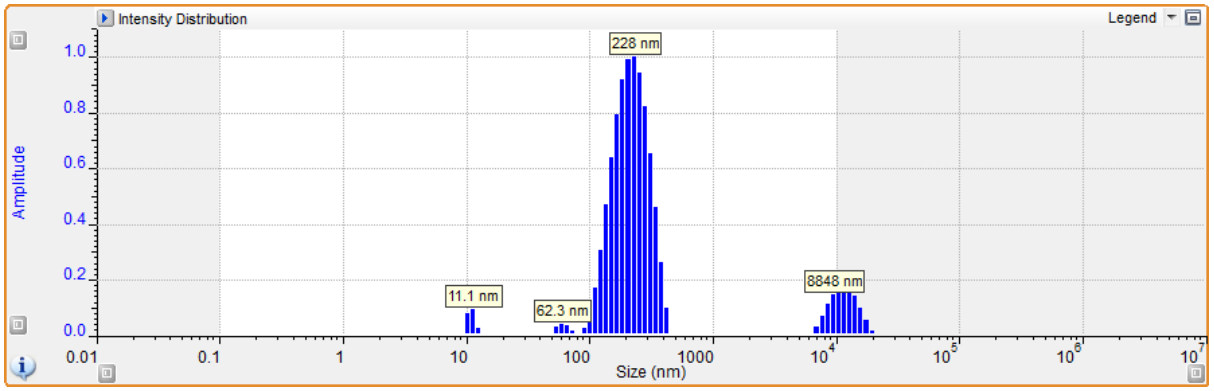

III. RU/Nt ratio of 2.5:1 & HP:CP ratio of 3:1

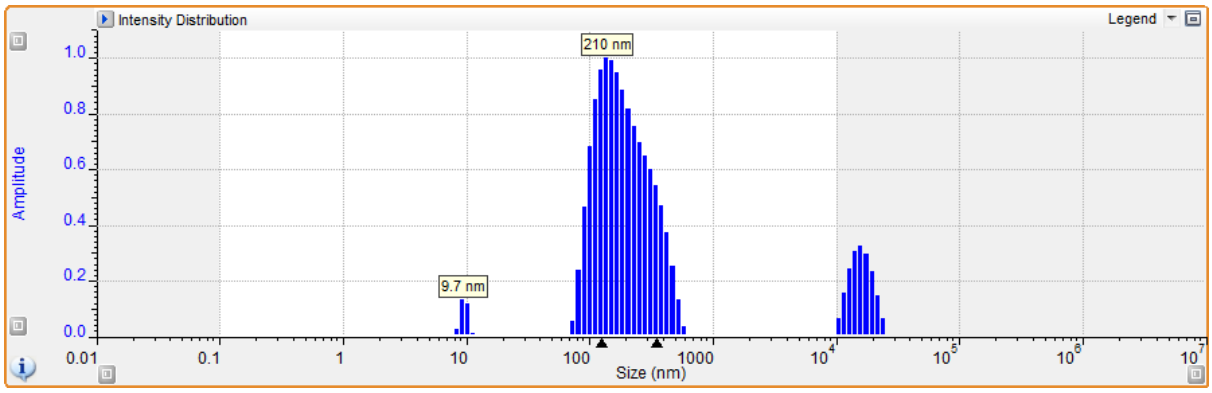

IV. RU/Nt ratio of 3:1 & HP:CP ratio of 1:1

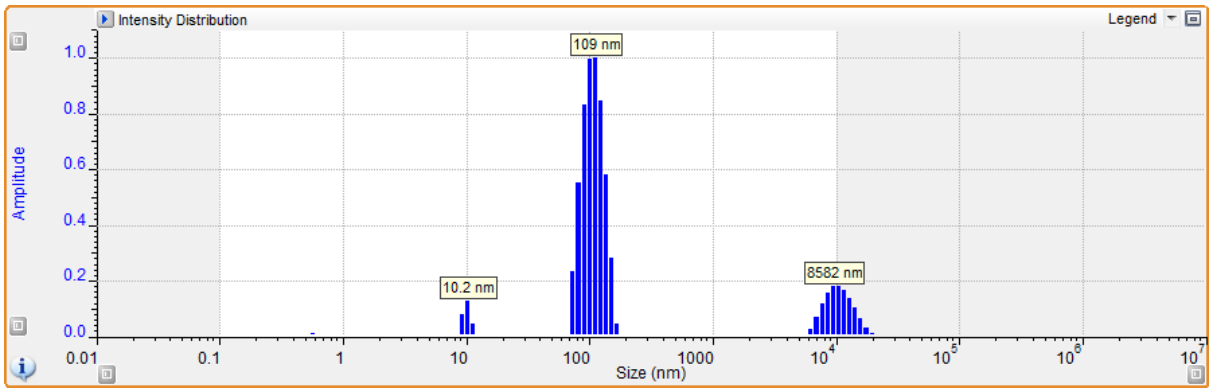

V. RU/Nt ratio of 3:1 & HP:CP ratio of 2:1

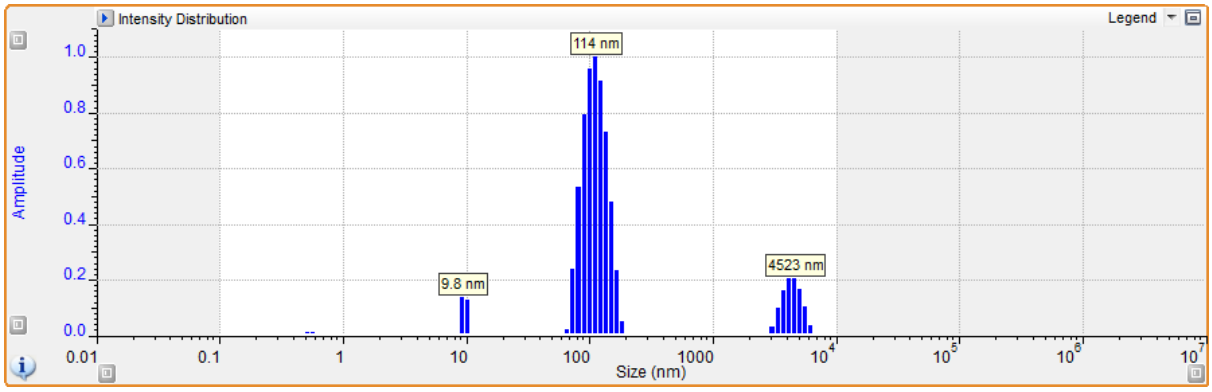

VI. RU/Nt ratio of 3:1 & HP:CP ratio of 3:1

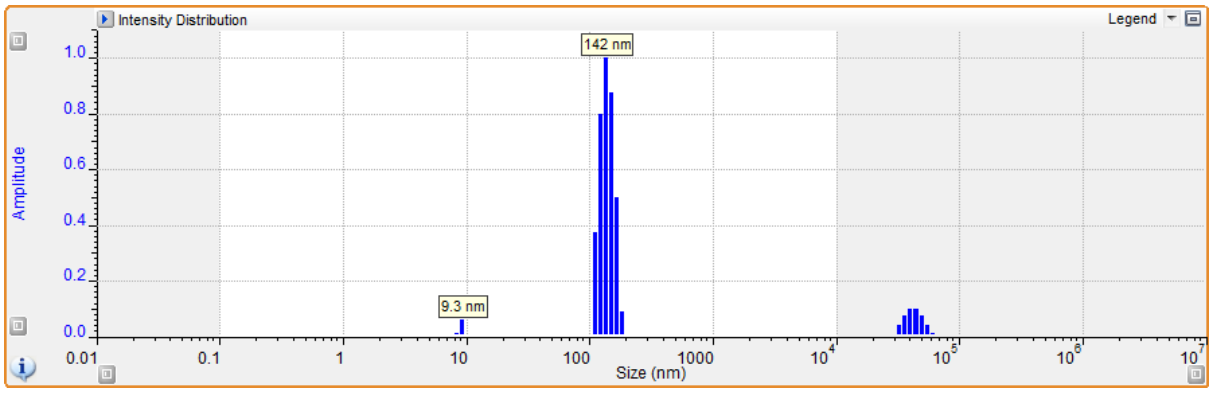

VII. RU/Nt ratio of 4:1 & HP:CP ratio of 1:1

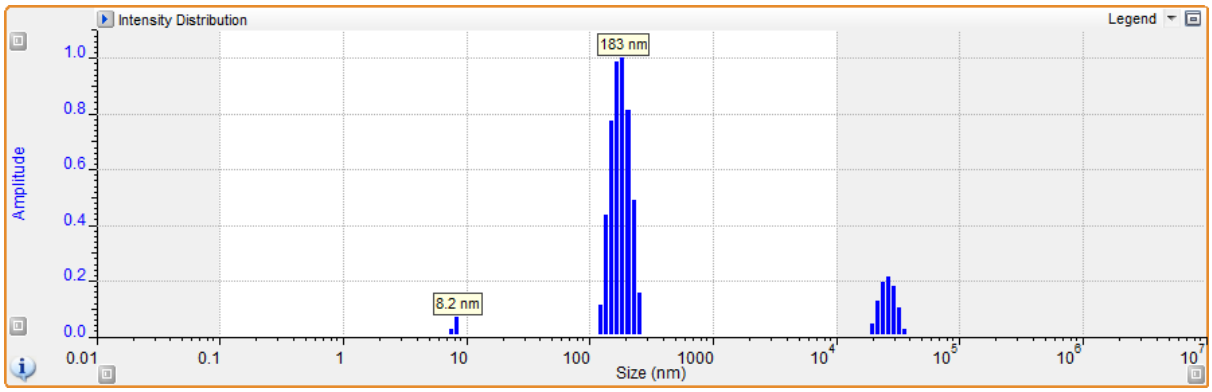

VIII. RU/Nt ratio of 4:1 & HP:CP ratio of 2:1

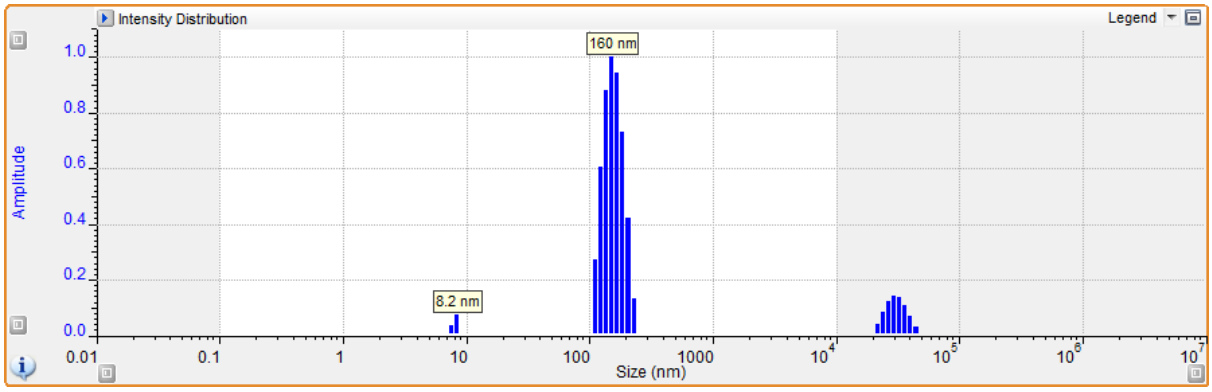

IX. RU/Nt ratio of 4:1 & HP:CP ratio of 3:1

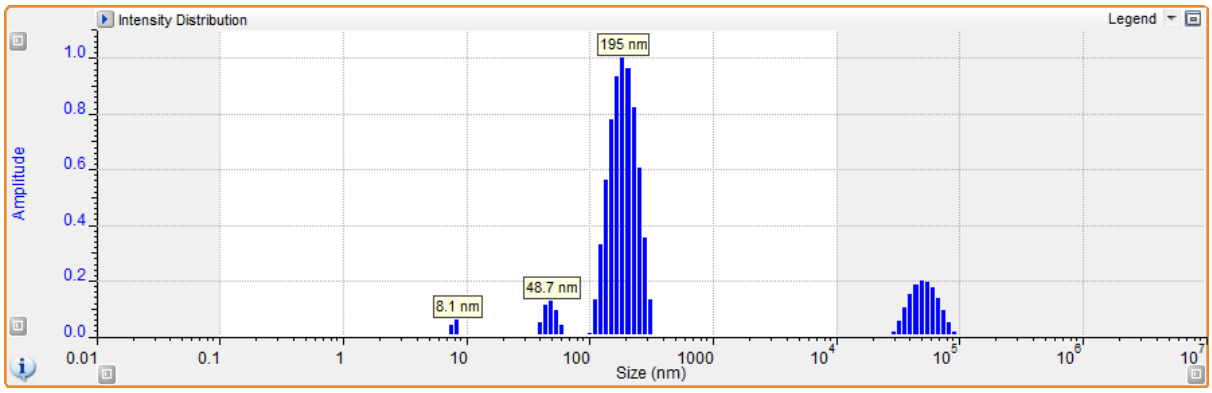

HP-CP/SH-siRNA nanoparticles

I. RU/Nt ratio of 2.5:1 & HP:CP ratio of 1:1

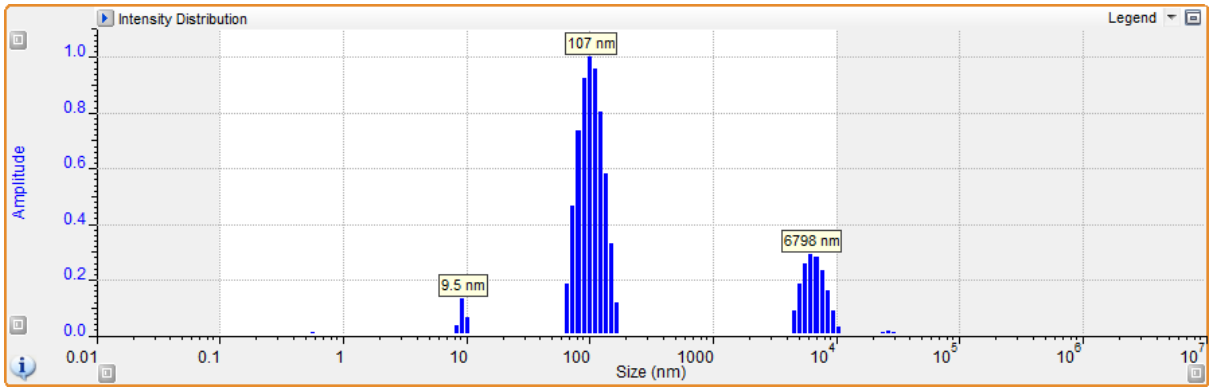

II. RU/Nt ratio of 2.5:1 & HP:CP ratio of 2:1

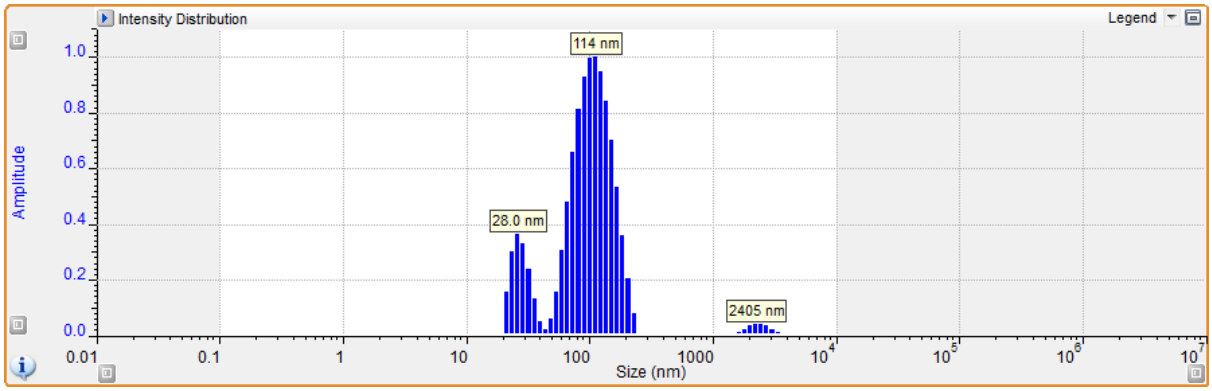

III. RU/Nt ratio of 2.5:1 & HP:CP ratio of 3:1

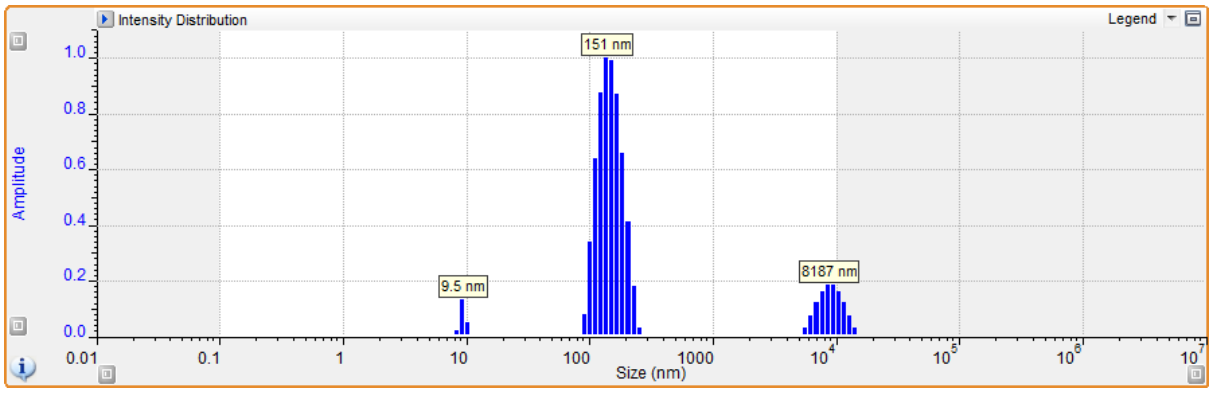

IV. RU/Nt ratio of 3:1 & HP:CP ratio of 1:1

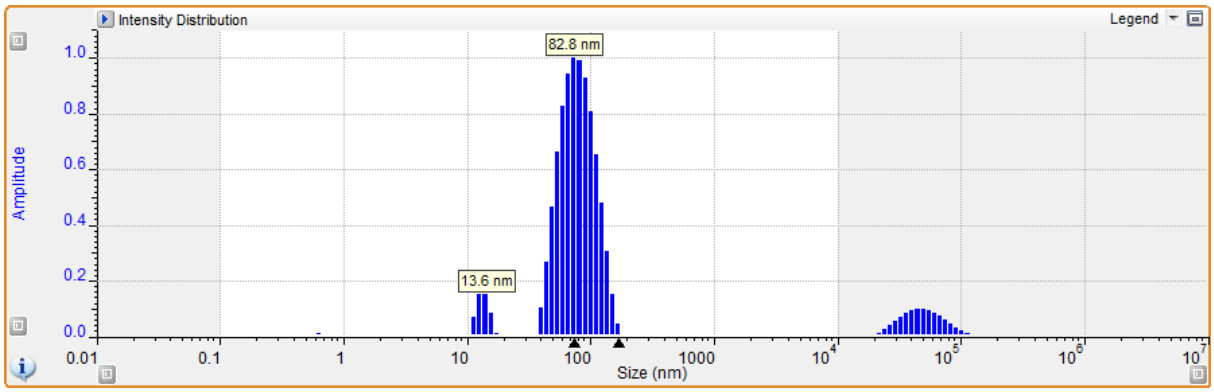

V. RU/Nt ratio of 3:1 & HP:CP ratio of 2:1

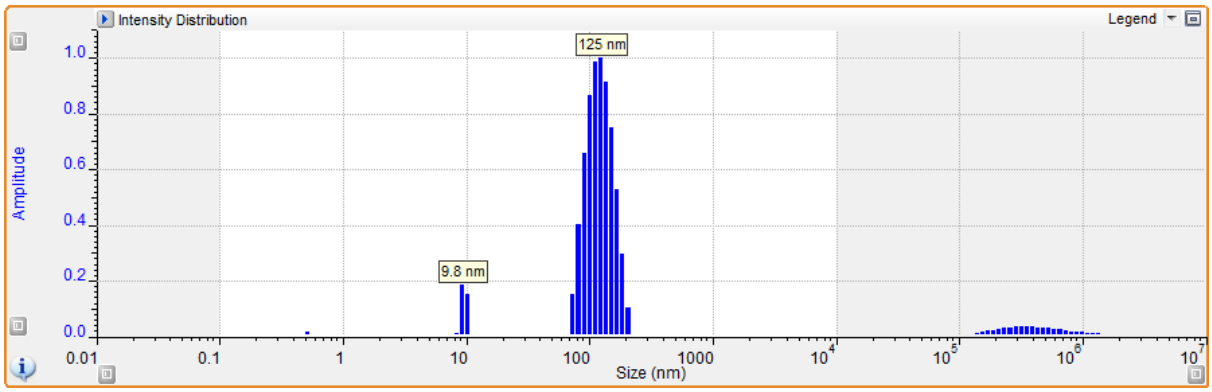

VI. RU/Nt ratio of 3:1 & HP:CP ratio of 3:1

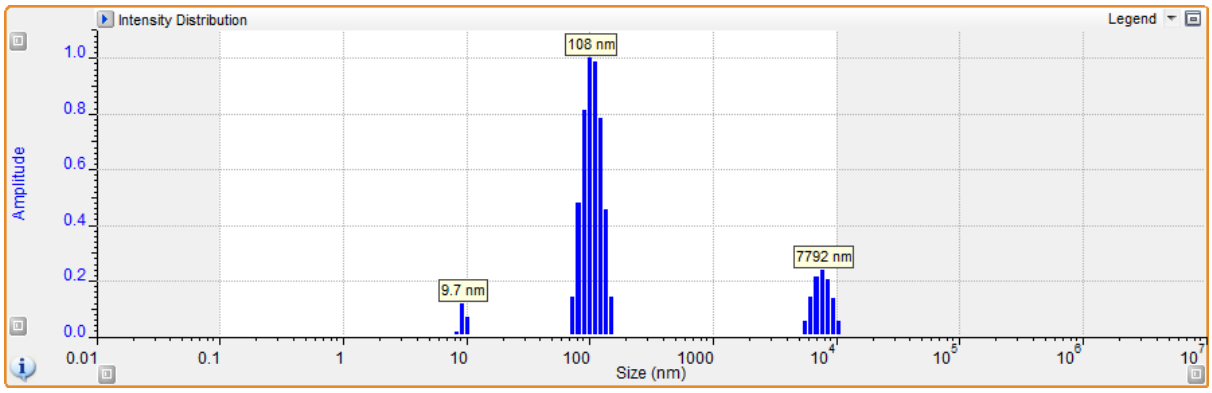

VII. RU/Nt ratio of 4:1 & HP:CP ratio of 1:1

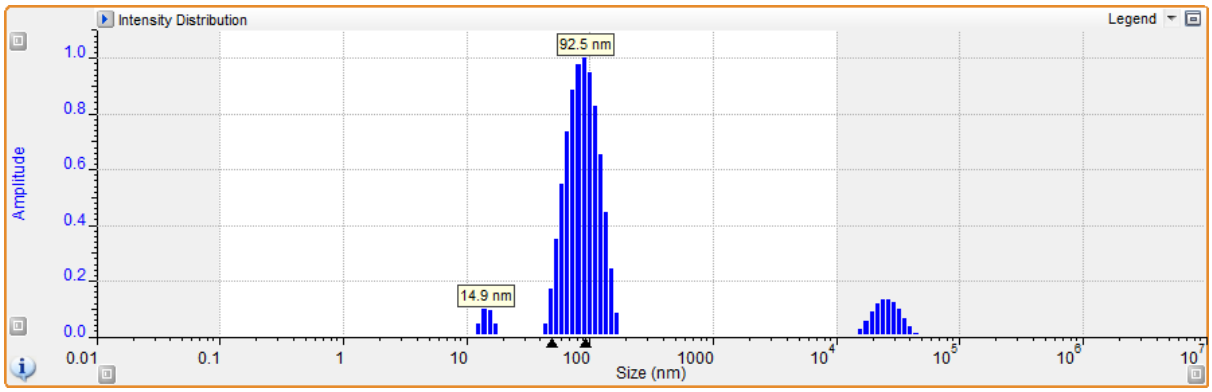

VIII. RU/Nt ratio of 4:1 & HP:CP ratio of 2:1

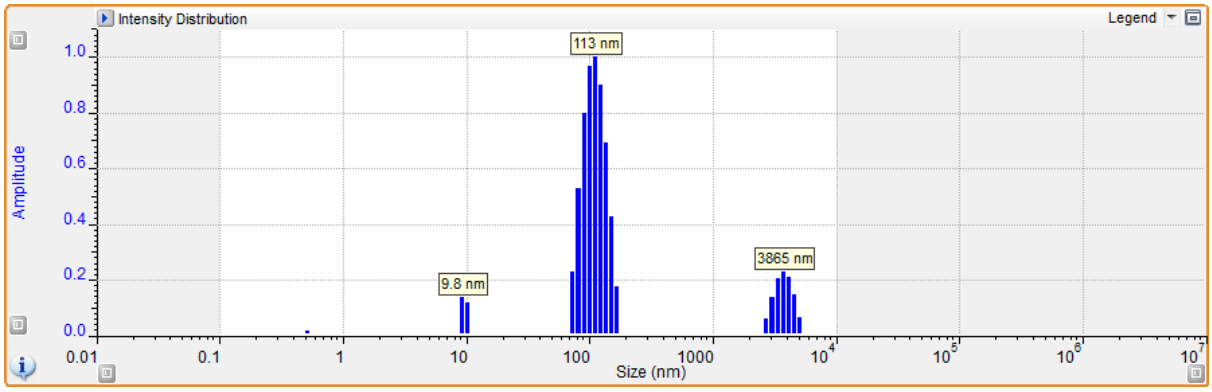

IX. RU/Nt ratio of 4:1 & HP:CP ratio of 3:1

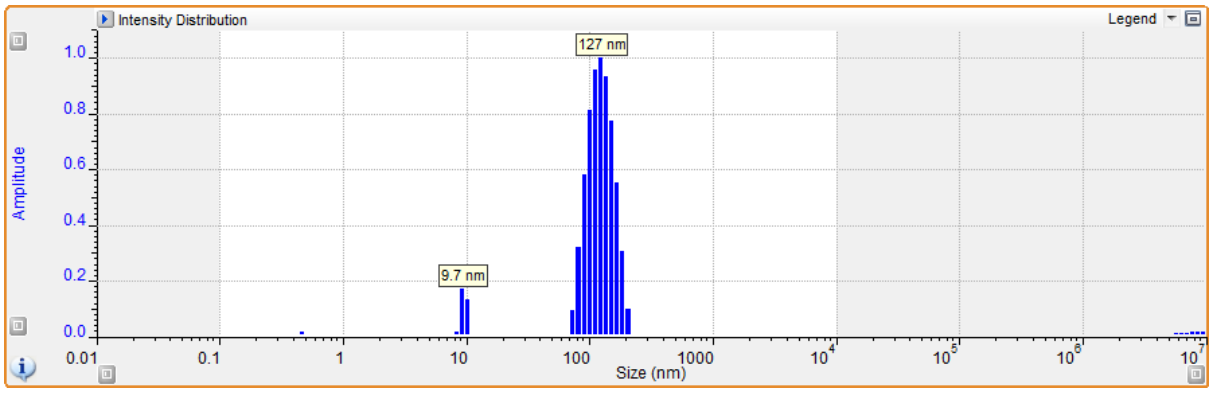

Appendix B

Melting curve analysis for Syk (targeted) and Ggt1 (reference) genes using KAPA SYBR® FAST qPCR kit master mix.

I. HP/siRNA nanoparticles

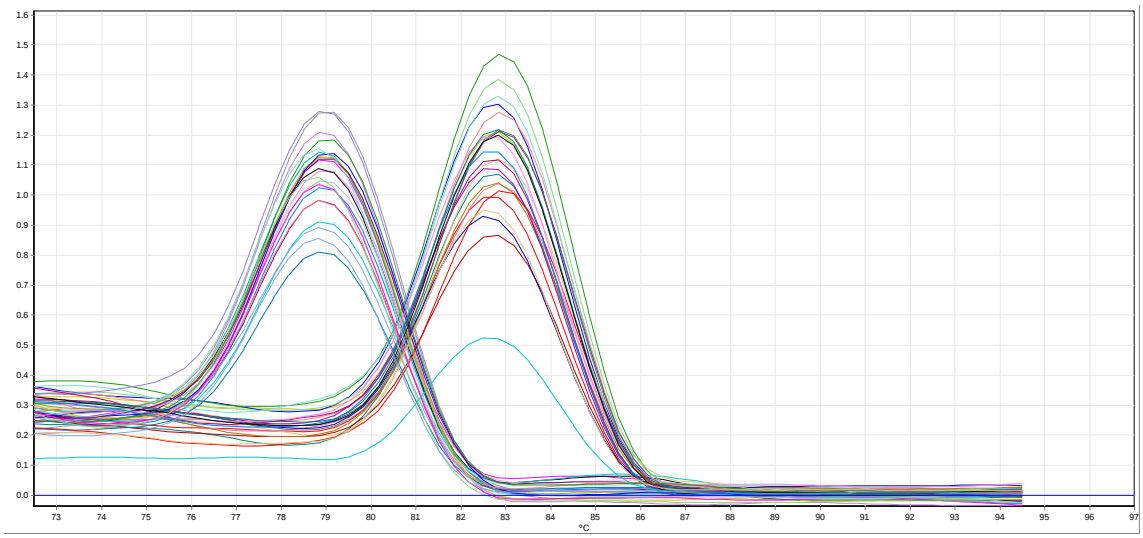

II. HP/SH-siRNA nanoparticles

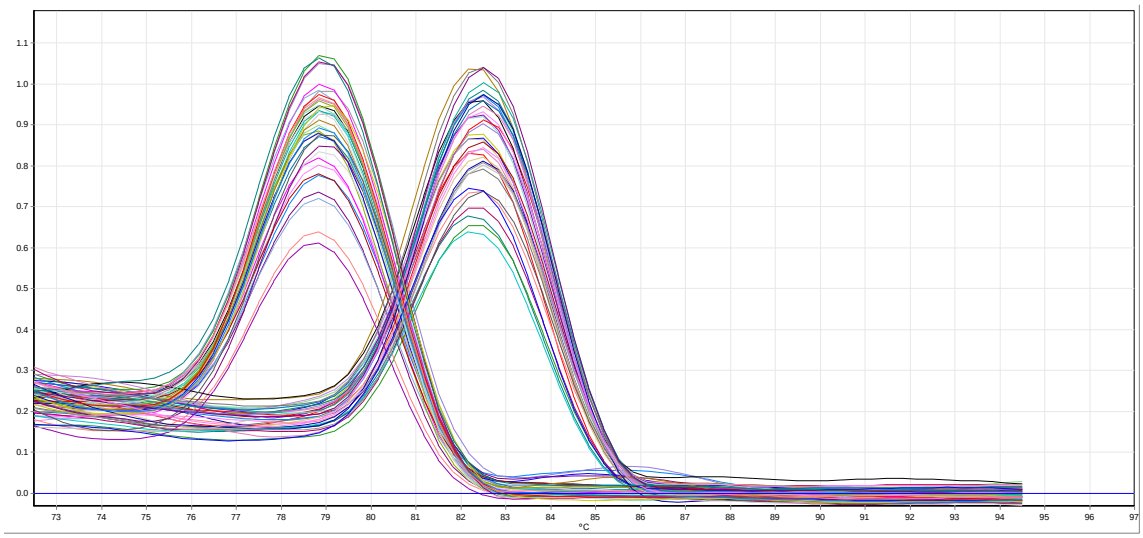

III. HP-CP/siRNA nanoparticles

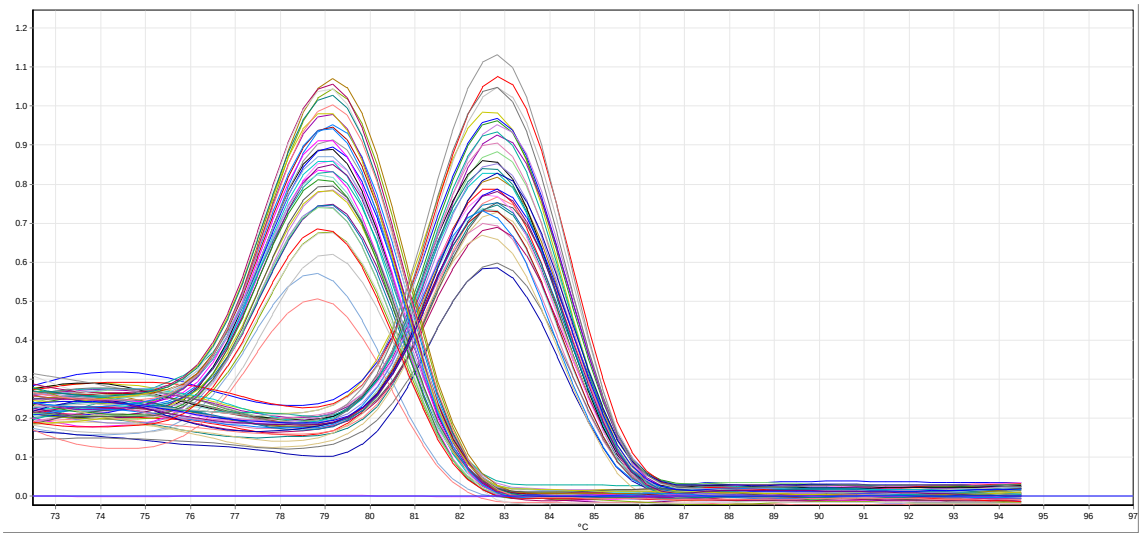

IV. HP-CP/SH-siRNA nanoparticles

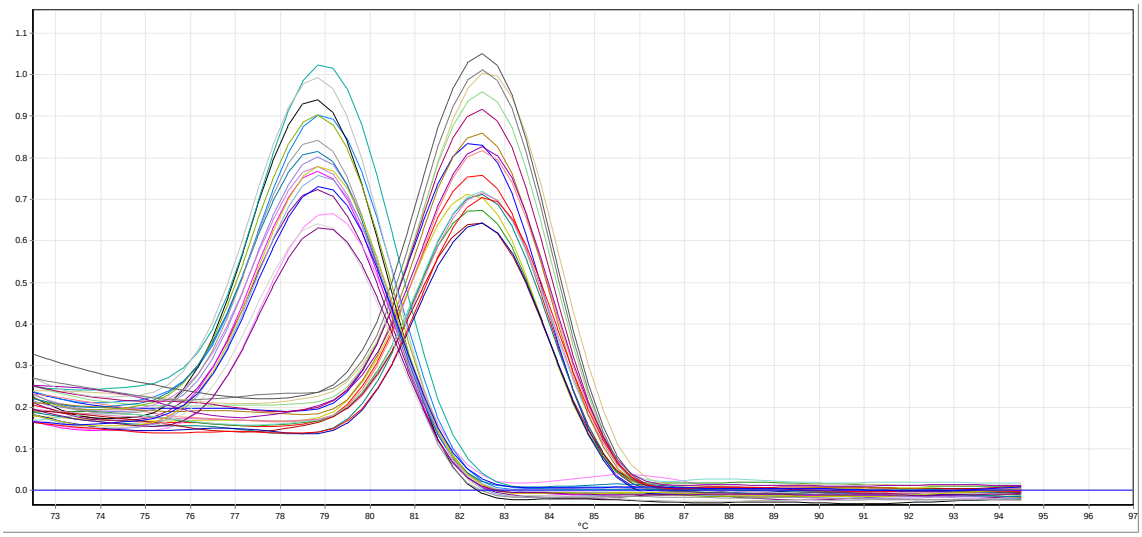

V. Standard curve of absorbance vs protein concentration for cell lysates.